Geological Field Trips

Società Geologica Italiana

ISPRA
Dipartimento per il
SERVIZIO GEOLOGICO D'ITALIA
Organo Cartografico dello Stato (legge n°68 del 2-2-1960)

Sistema Nazionale per la Protezione dell'Ambiente

2017
Vol. 9 (2.2)

INDEXED IN EMERGING SOURCES CITATION INDEX THOMSON REUTERS

ISSN: 2038-4947

From ductile to brittle tectonic evolution of the Aspromonte Massif

Field excursion of the Italian Group of Structural Geology - Catania, 2015

DOI: 10.3301/GFT.2017.03

GFT - *Geological Field Trips*

Periodico semestrale del Servizio Geologico d'Italia - ISPRA e della Società Geologica Italiana
Geol.F.Trips, Vol.**9** No.2.2 (2017), 66 pp., 30 figs. (DOI 10.3301/GFT.2017.03)

From ductile to brittle tectonic evolution of the Aspromonte Massif

Field excursion of the Italian Group of Structural Geology - Catania (CT) 1st – 2nd October 2015

Rosolino Cirrincione[1], Carmelo Monaco[1], Gaetano Ortolano[1], Luigi Ferranti[2], Giovanni Barreca[1], Eugenio Fazio[1], Antonio Pezzino[1], Roberto Visalli[1]

[1] Università degli Studi di Catania - Dipartimento di Scienze Biologiche, Geologiche e Ambientali - Sezione di Scienze della Terra
[2] Università degli Studi di Napoli Federico II - Dipartimento di Scienze della Terra, dell'Ambiente e delle Risorse

Corresponding Author e-mail address: ortolano@unict.it

ISSN: 2038-4947 [online]

http://www.isprambiente.gov.it/it/pubblicazioni/periodici-tecnici/geological-field-trips

DOI: 10.3301/GFT.2017.03

INDEX

Information

Excursion notes

Itinerary

DOI: 10.3301/GFT.2017.03

Riassunto

Questa escursione è stata effettuata in occasione della riunione annuale del Gruppo Italiano di Geologia Strutturale (GIGS 2015) - sezione della Società Geologica Italiana - in collaborazione con il Gruppo Nazionale di Petrografia (GNP). Geologicamente, il Massiccio dell'Aspromonte ricade all'interno dell'Orogene Calabro-Peloritano (OCP), un segmento orogenico nastriforme arcuato localizzato nel più ampio dominio geodinamico del Mediterraneo occidentale, fisiograficamente composto inoltre dal Massiccio Silano, dalla Catena Costiera, dalle Serre e dai Monti Peloritani. L'OCP, comunemente noto col nome di Arco Calabro, è stato recentemente interpretato come la fusione di due microterranes (i.e. settentrionale e meridionale), caratterizzati da una differente evoluzione tettono-metamorfica, oggi separati lungo la stretta di Catanzaro.
La fusione di questi due differenti settori può essere ragionevolmente connessa all'intensa attività tettonica trascorrente che ha accompagnato la geodinamica del Mediterraneo occidentale sin dal Cretacico e che oggi trova riscontro oltre che lungo la stretta di Catanzaro anche dalla presenza di altri allineamenti tettonici, come il complesso delle faglie della linea del Pollino, della linea di Palmi e quella di Taormina. In tale contesto si inserisce l'escursione qui proposta che ha lo scopo di permettere l'osservazione di alcuni elementi chiave utili per capire meglio l'articolata storia geologica di questo settore della catena alpino-appennica a partire già dalla base del Paleozoico.
Il percorso articolato in due giorni, attraversa alcuni tra i luoghi più affascinanti dell'Aspromonte (Calabria meridionale), ha lo scopo di illustrare da un lato l'evoluzione tettono-metamorfica del basamento cristallino sviluppatasi a partire almeno dal passaggio Precambriano-Cambriano, contribuendo così a vincolare diversi aspetti chiave della geodinamica del Mediterraneo occidentale, dall'altro l'evoluzione morfotettonica tardo quaternaria del segmento orogenico calabro in quanto l'Aspromonte ne rappresenta uno dei settori chiave, essendo stato interessato più volte da terremoti distruttivi. Per quest'ultima ragione, alcune delle tappe sono dedicate all'osservazione delle caratteristiche morfologiche, strutturali e sedimentarie di due delle strutture tettoniche più attive dell'Italia meridionale: le faglie normali di Scilla e Armo. Il percorso permette infine di visitare, lungo la costa tirrenica e ionica, due siti controllati da queste grandi faglie normali, che mostrano sequenze complete di terrazzi marini di età pleistocenica, generati dal forte sollevamento tettonico, significativamente più veloce rispetto all'innalzamento del livello medio marino nell'Olocene. Tali siti, spesso

DOI: 10.3301/GFT.2017.03

ben conservati, sono caratterizzati dalla presenza di paleolinee di costa oloceniche sollevate, elementi importanti per ricostruire la paleosismicità di questo settore e, in generale, utili anche per la valutazione del rischio sismico dell'area.

Parole chiave: *Aspromonte, Orogene Calabro-Peloritano, zone di taglio, Orogenesi Alpina, Neotettonica, Calabria*

Abstract

The two-days field trip in the Aspromonte Massif (Calabria – Southern Italy) was carried out for the annual meeting of the Italian Group of Structural Geology (GIGS, 2015) - Section of the Italian Geological Society (SGI) - in collaboration with the National Group of Petrography (GNP). It is planned to illustrate the tectono-metamorphic history of the metamorphic basement cropping out in this sector of the Southern Apennine. Attention will be focused on the complex poly-orogenic and poly-phase evolution that, since the Precambrian-Cambrian boundary, has driven the petrogenetic evolution as well as the structural features of its crystalline basements, permitting also to constrain some key aspects of the Western Mediterranean geodynamics.
Moreover, since the Aspromonte area was repeatedly struck by strong earthquakes and represents one of the key sectors for the reconstruction of the late Quaternary morphotectonic evolution of the Southern Italy, some of the stops will be devoted to the observation of the morphological, structural and sedimentary features of two of the most active structures of this sector of the belt, the Scilla and the Armo normal faults. Finally, the field trip allows to visit two coastal sites controlled by these major normal faults, respectively in the Tyrrhenian and in the Ionian sector of the Messina Strait, which display complete sequences of Pleistocene marine terraces. Due to the tectonic uplift faster than the Holocene sea level rise, these sites also show well preserved raised Holocene paleoshorelines that represent important proxies for reconstructing the paleoseismicity of this area and, in general, for the risk assessment.
From a geological point of view, the Aspromonte Massif belongs to the Calabrian Peloritani Orogen (CPO), including the Sila Massif, the Coastal Chain, the Serre Massif and the Peloritani Mountains. This sector chain, also known in literature as Calabrian Arc, has been recently interpreted as a merged ribbon-like continental crustal section constituted by two main microterranes (i.e. the northern- and southern-CPO separated by the Catanzaro line, CL), which are characterized by different tectono-metamorphic evolutions.

DOI: 10.3301/GFT.2017.03

The amalgamation of these two different sectors can be ascribed to the intense strike-slip tectonics which accompanied the evolution of the Western Mediterranean area from Cretaceous age, presently testified, in addition to the Catanzaro line, also by the tectonic alignment of the Pollino fault zone (PFZ), Palmi line (PL) and Taormina line (TL). In particular, the Aspromonte Massif is a nappe edifice, constituting the Oligocene-Miocene accrectionary wedge of the European-Africa plate boundary. This is originated by the breakup of the earlier Southern European Variscan chain during the Mesozoic-Cenozoic Alpine orogeny. Afterwards, during Eocene-Quaternary times, it has also been involved in the subduction of the Ionian slab and in extensional and uplifting processes that make this area one of the most seismically active of the entire Mediterranean realm.

Key words: *Aspromonte, Calabrian Peloritani Orogen, shear zones, Alpine Orogeny, Neotectonics, Calabria*

Field Trip programme

Duration: 2 days; difficulty level: low, intermediate.
Departure and arrival: Villa San Giovanni (RC) - Railway station.
Route:
1st day: Villa San Giovanni (RC), Santa Trada (RC), Scilla (RC), Palmi (RC), Oliveto (RC), Brancaleone (RC) - night accommodation.

2nd day: Samo (RC), Chorio (RC) and San Lorenzo (RC), Villa S. Giovanni (RC).

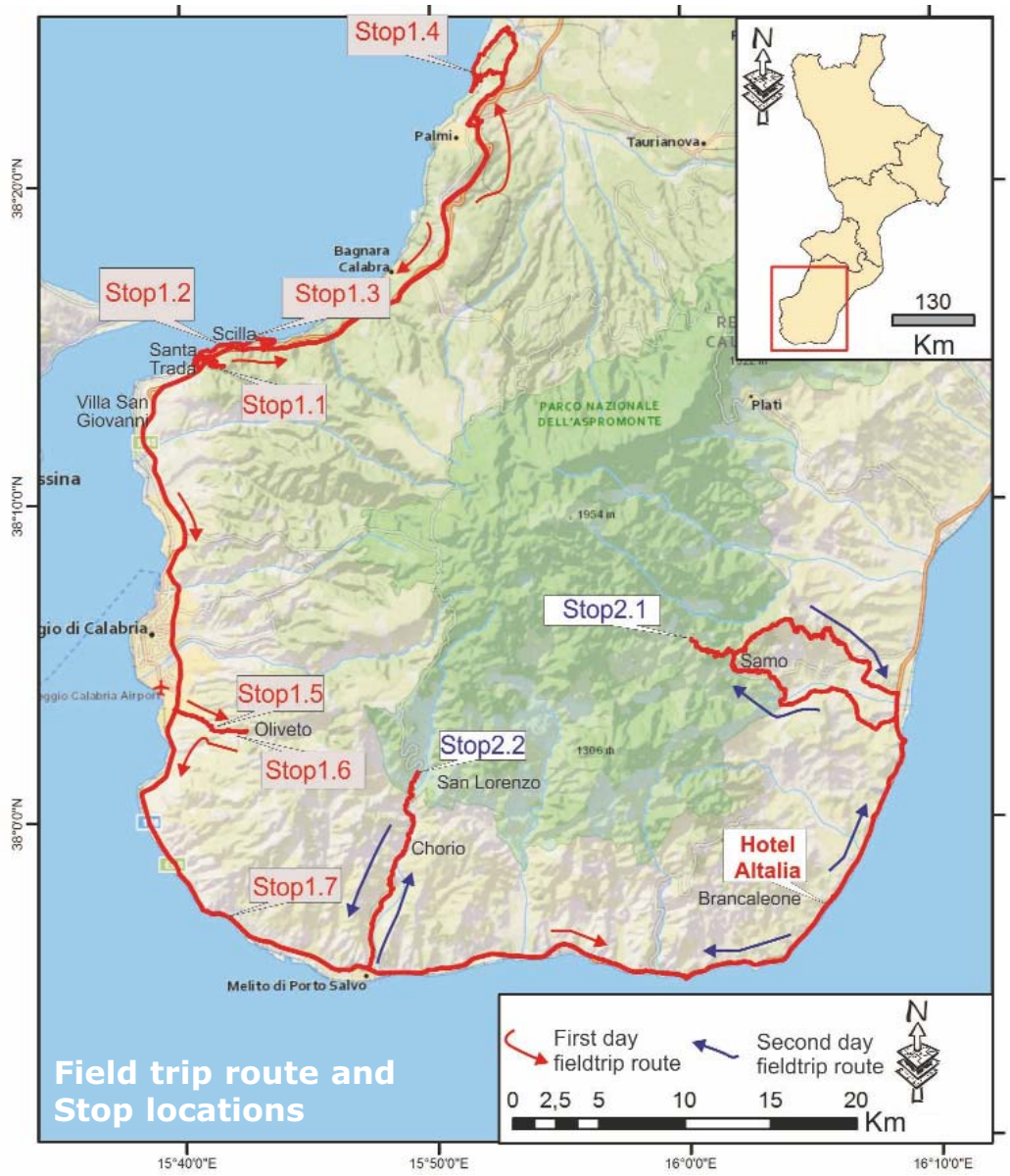

DOI: 10.3301/GFT.2017.03

Emergency Services

In case of emergency please contact the following numbers (valid all over Italy)
- Medical Emergency/Ambulance: **118**
- Police: **113** or **112**
- Firemen: **115**

Useful contacts

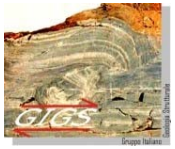

Gruppo Italiano di Geologia Strutturale (GIGS)
Dipartimento di Scienze – Sez. di Scienze Geologiche (Univ. Roma TRE), Largo San L. Murialdo 1, pal. A, Roma, Italia. Tel. +39 06 57338027.
E-mail: gigs@socgeol.it
Website: www.socgeol.it/816/gigs_sezione_geologia_strutturale.html
Twitter: @GigsItalia

Ente Parco Nazionale dell'Aspromonte
Via Aurora, 1 – 89050 - Gambarie di S.Stefano in Aspromonte (RC).
Tel. +39 0965 743 060; Fax +39 0965 743 026.
E-mail: info.posta@parcoaspromonte.gov.it
Website: www.parcoaspromonte.gov.it

CAI Club Alpino Italiano - Sezione Aspromonte
Via S. Francesco da Paola, 106 – 89127 - Reggio Calabria (RC). Tel/Fax: +39 0965 898295
E-mail: info@caireggio.it
Website: www.caireggio.it

Front cover

Flow perturbation folds evolving to sheath folds in the mylonitic skarns of the Palmi shear zone, Scoglio dell'Ulivarella, Palmi (RC).
Photo by Ortolano G.

DOI: 10.3301/GFT.2017.03

1 - Regional tectonic setting

The evolution of the Calabrian Peloritani Orogen (CPO) basement rocks (Fig. 1a) is the result of Palaeozoic orogenic processes, reworked during the Alpine orogenic cycle and lastly variably disarticulated by the nappe-piling activity and strike-slip tectonics of the Apennine orogenic stage. The CPO can be then considered nowadays as a composite terrane consisting of basement rocks

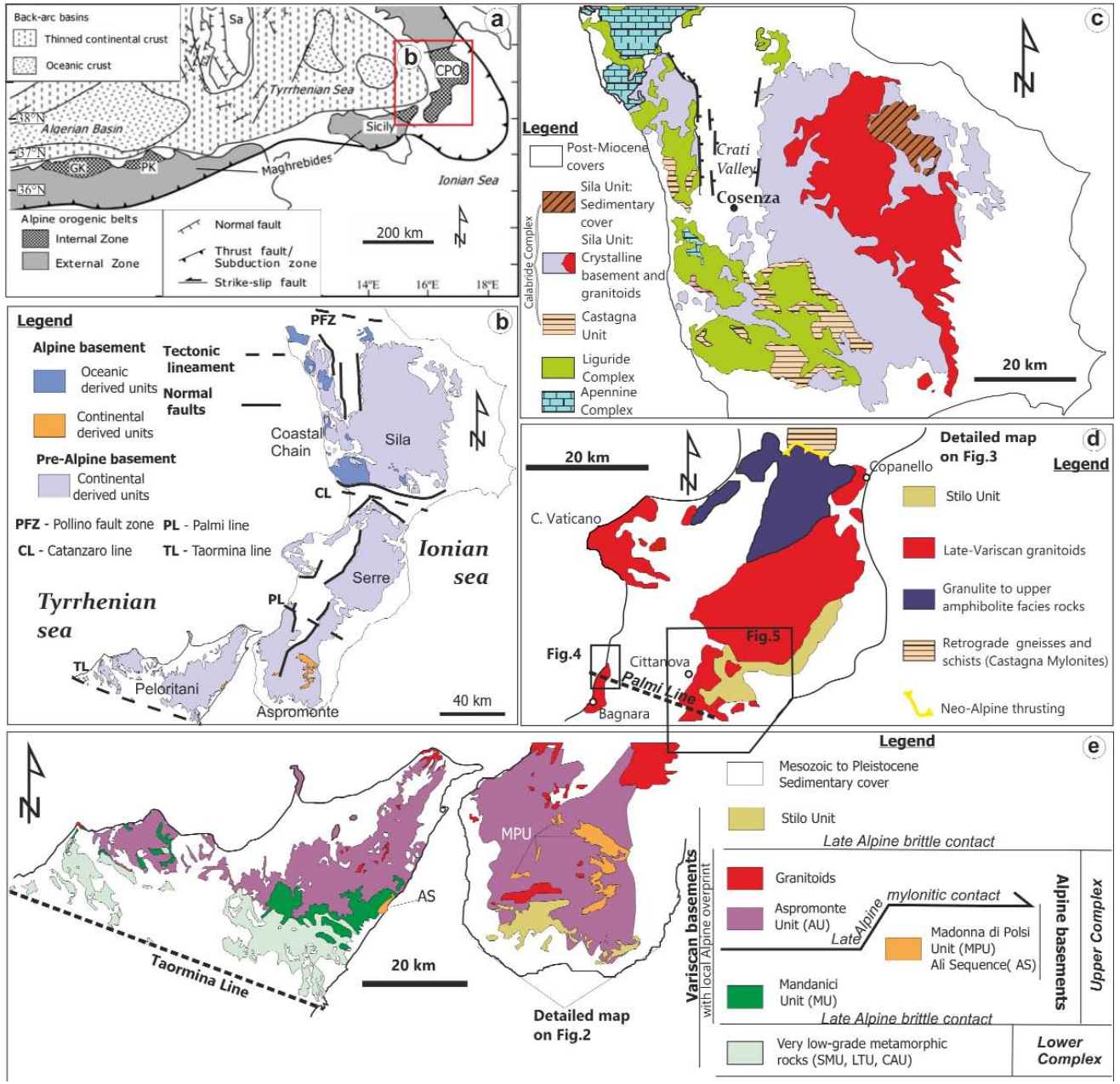

Fig. 1 - Geological sketch map of the Calabria-Peloritani Orogen (after Cirrincione et al., 2015, modified): **a)** Schematic map of the Alpine belt in the southern Mediterranean area (CPO – Calabrian Peloritani Orogen; GK – Grande Kabylie; PK – Petit Kabylie; Sa – Sardinia), modified after Carminati et al., 1998; **b)** geological sketch map of the Calabria-Peloritani Orogen with distribution of its massifs and related Alpine and pre-Alpine basement rocks (modified after Angì et al., 2010); **c)** geological sketch map of the Sila and Coastal Chain Massifs; **d)** geological sketch map of the Serre Massif; **e)** Geological sketch map of the Aspromonte Massif and Peloritani Mountain Belt.

DOI: 10.3301/GFT.2017.03

deriving from a poly-orogenic multi-stage history, currently merged in several sub-terranes, mainly formed during the Variscan orogeny (Pezzino, 1982; Atzori et al., 1984; Bonardi et al., 2004; Cirrincione et al., 2015). In this scenario, the CPO can be separated in different orographic domains known as Coastal Chain and Sila Massifs in northern Calabria (Fig. 1b,c), Serre (Fig. 1b, d) and Aspromonte Massifs (Fig.1b, e) in southern Calabria, and the Peloritani Mountains in Sicily (Fig. 1b, e) (e.g., Cirrincione et al., 2015).

Local evidences of older tectono-metamorphic evolution has been recognized (Ferla, 2000; Micheletti et al., 2007; Williams et al., 2012). These rocks were locally overprinted during the different stages of the Alpine metamorphic events, which also affected part of the Mesozoic oceanic-derived units and sedimentary sequences (Fazio et al., 2008; Cirrincione et al., 2008). During the Oligocene-Miocene boundary, these basements were definitively stacked by the Alpine-Apennine thin-skinned thrusting events, which involved in the southern sector also the syn-collisional turbiditic sequence of the Stilo-Capo d'Orlando formation (SCOF), locally followed by the backthrusting of the varicolori clays (VC) (Cavazza et al., 1997; Ortolano et al., 2005; Pezzino et al., 2008).

In this scenario, the Aspromonte Massif, bounded to North by the crustal-scale strike-slip fault system known as Palmi line (Fig. 1b, d) (Ortolano et al., 2013), can be interpreted as a south-east verging nappe edifice (Ortolano et al., 2015), where the two uppermost tectonic slices are composed of middle-upper crust basement rocks (i.e. the Stilo unit - SU and Aspromonte unit - AU) (Fig. 2). These two units are characterized by a multi-stage Variscan metamorphism, locally involving only the deeper unit during the latest stages of the Alpine metamorphic cycle (Ortolano et al., 2005; Pezzino et al., 2008). The deepest tectonic unit, separated by the intermediate Aspromonte unit by a thick mylonitic horizon, formed during the Oligocene. This unit is characterized by medium grade metapelites, exclusively registered a complete Alpine metamorphic cycle, known in literature as Madonna di Polsi unit (MPU) (Pezzino et al., 1990; 2008; Ortolano et al., 2005; Cirrincione et al., 2008; Fazio et al., 2008) (Fig. 2).

DOI: 10.3301/GFT.2017.03

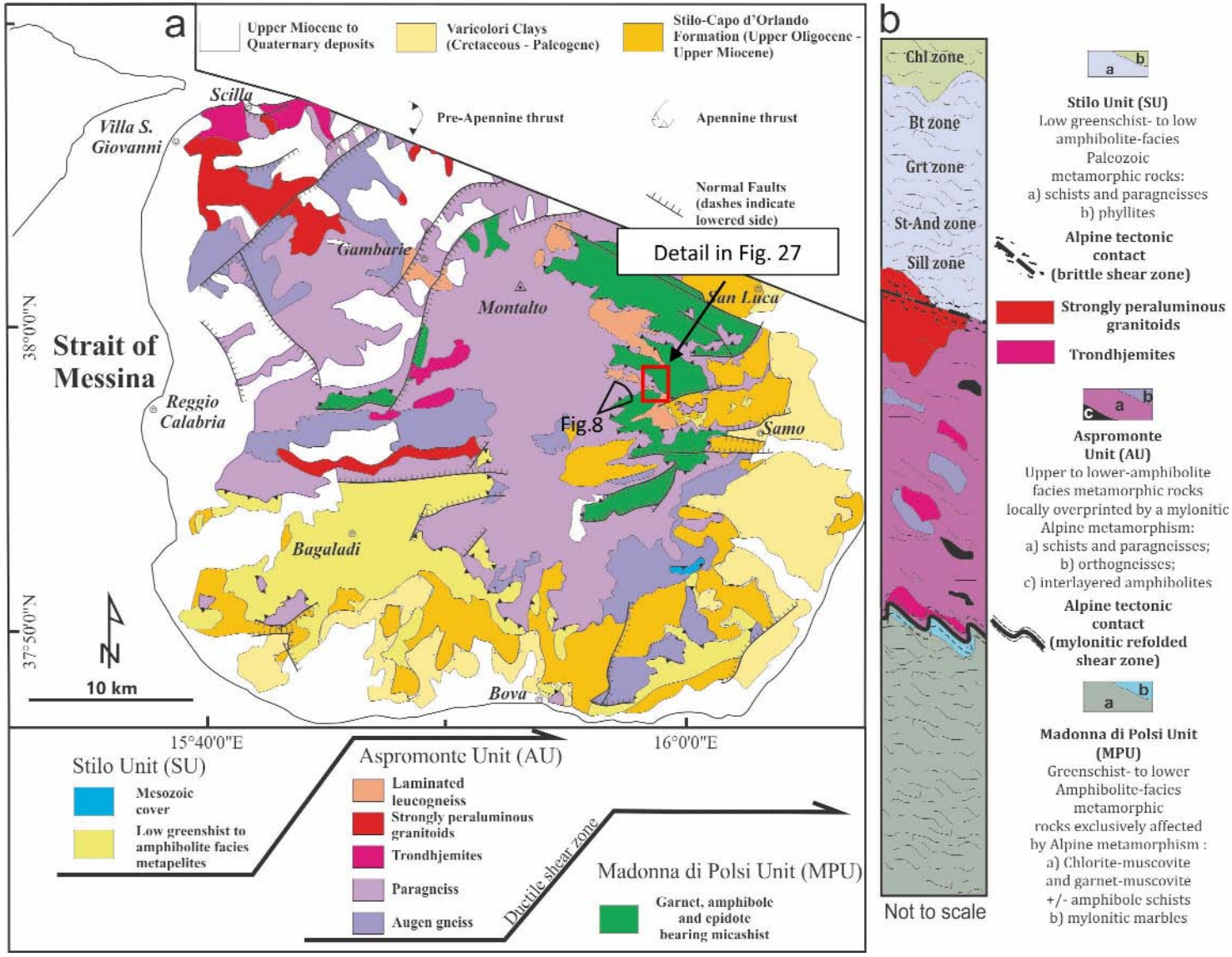

Fig. 2 - **a)** Geological sketch map of the Aspromonte Massif nappe-like edifice. **SU**: Basement rocks are of Palaeozoic age and the cover is Mesozoic. **AU**: Palaeozoic. **MPU**: Mesozoic; **b)** schematic tectono-stratigraphic column of the tectono-metamorphic units (see Fig. 1 for location - modified after Ortolano et al., 2015 and Fazio et al., 2015). Detail of the inset is reported in Fig. 27. Panoramic field of view of Fig. 8 are indicated.

The Upper Oligocene to Upper Miocene turbiditic siliciclastic succession, the "Stilo-Capo d'Orlando formation" covers, with angular unconformity, the nappe edifice, sealing at times the tectonic contact between SU and AU. This succession includes flysch deposits mainly composed of siltstones, subordinate fine to medium-grained sandstones and fairly cemented conglomerates (Ortolano et al., 2015). The back-thrusting of the varicolori clays marks the final stage of the syn-sedimentary tectonic activity (Cavazza et al., 1997).

At the end of the nappe emplacement, the pile of nappes was unconformably covered by Upper Miocene to Pleistocene terrigenous sediments that can be schematically grouped in two major successions. The older one is made up of Upper Miocene-Lower Pliocene deposits that were

DOI: 10.3301/GFT.2017.03

sedimented within a series of perched basins developed on top of crystalline thrust sheets (Monaco et al., 1996a). Sediments related to the infilling of perched basins are also represented by the youngest Upper Pliocene-Pleistocene successions cropping out on the eastern margin of the Sila Massif and on the Ionian offshore (e.g. Crotone basin) along the frontal portion of the arc (Monaco et al., 1996b). Upper Pliocene-Pleistocene sediments also crop out along the Tyrrhenian side of the arc where they fill extensional basins (Fig. 1). In particular, since Late Pliocene, and more markedly in the Quaternary, concurrently with back-arc extension in the Tyrrhenian Sea, the inner side of the Calabrian Arc has experienced extensional deformation accommodated by normal faulting (Ghisetti, 1984, 1992; Tortorici et al., 1995; Monaco & Tortorici, 2000; Jacques et al., 2001). A prominent system of normal fault runs more or less continuously along the Tyrrhenian side of Calabrian terrane, as far as the Strait of Messina area. Extensional tectonics has accompanied a strong regional uplift which caused the development of spectacular flights of marine terraces along the coast and, on land, a deep entrenchment of rivers with the deposition of alluvial and/or transitional coarse grained sediments along the major depressions on top of marine sequences (Dumas et al., 1982; Ghisetti, 1992; Valensise & Pantosti, 1992; Westaway, 1993; Miyauchi et al., 1994; Cucci & Tertulliani, 2006; Bianca et al., 2011). Various mechanisms have been claimed to explain the uplift of the Calabrian Arc. Within one class of models, uplift is viewed as an isostatic response to removal of a high-density deep root, either through break-off of the Ionian-Adriatic slab (Westaway, 1993; Wortel & Spakman, 2000) or through decoupling of the upper crust from the underlying slab and convective flow in the mantle wedge (Locardi & Nicolich, 1988; Miyauchi et al., 1994; Gvirtzman & Nur, 1999; Doglioni et al., 2001). Alternatively, uplift may have been induced by slowing of the slab roll-back and trapping of Calabria between the buoyant continental landmasses of Adria and northern Africa (Goes et al., 2004).

DOI: 10.3301/GFT.2017.03

2 - Tectono-metamorphic evolution

The Oligocene-Miocene back-arc opening of the north-western Mediterranean basins, as a consequence of the roll-back of the Ionian subducting plate, the dismembering of this sector of the original southern European Variscan chain (Fig. 1). This process begin to drive the present-day geodynamic puzzle of the CPO, presently constituted by several crystalline basement sectors characterized by a partially different tectono-metamorphic evolution. One of the result of this geodynamic evolution is, for instance, the lateral juxtaposition of the Aspromonte Massif with the Serre Massif where: **(i)** the former is characterized by a relatively shortened nappe edifice given by the overlap of three main

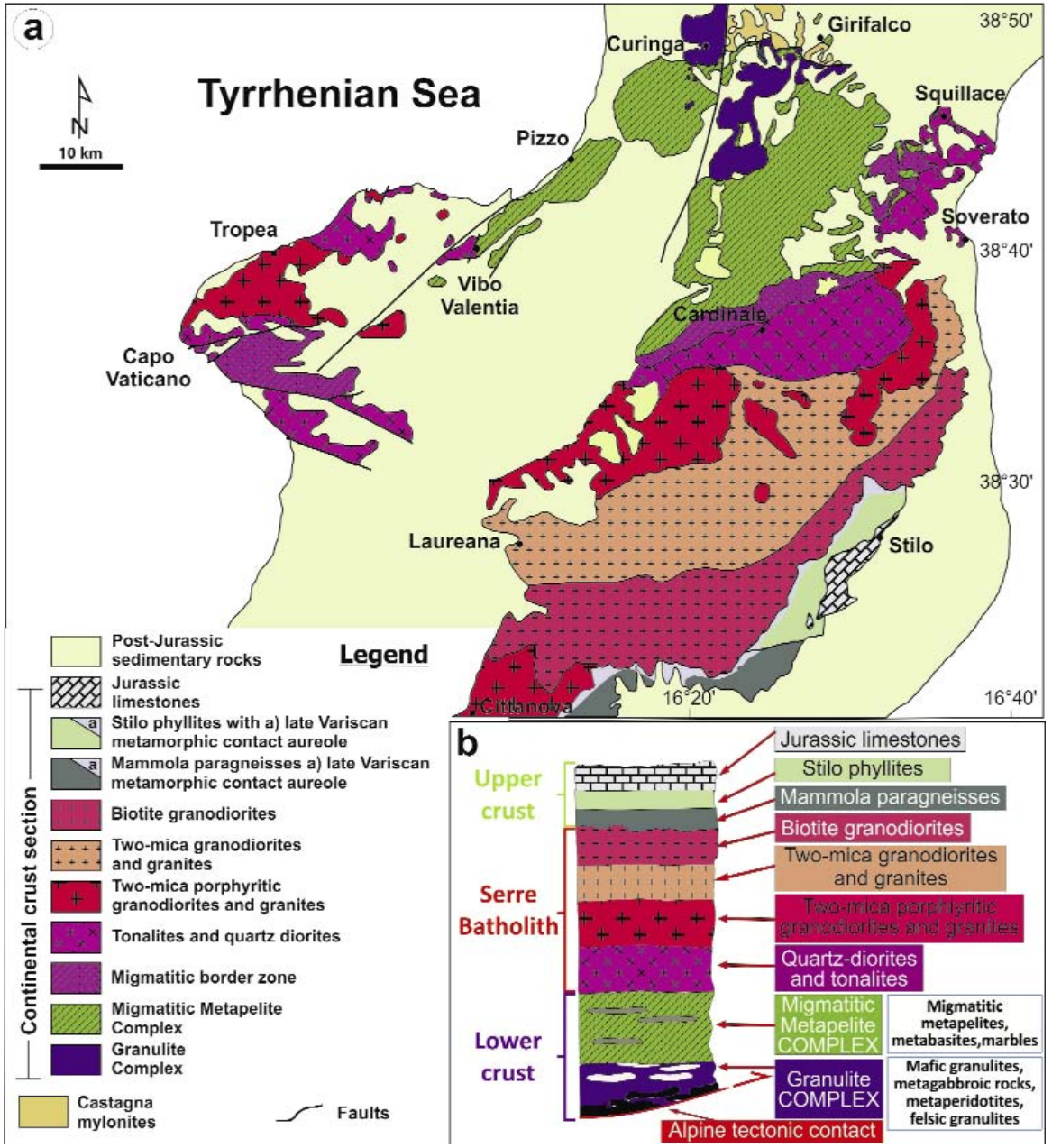

Fig. 3 - **a)** Geological sketch map of the Serre Massif and Capo Vaticano Promontory (after Fiannacca et al., 2015 and references therein); **b)** schematic lithological column for the Serre crustal section (see Fig. 1 for location - modified after Festa et al., 2004).

DOI: 10.3301/GFT.2017.03

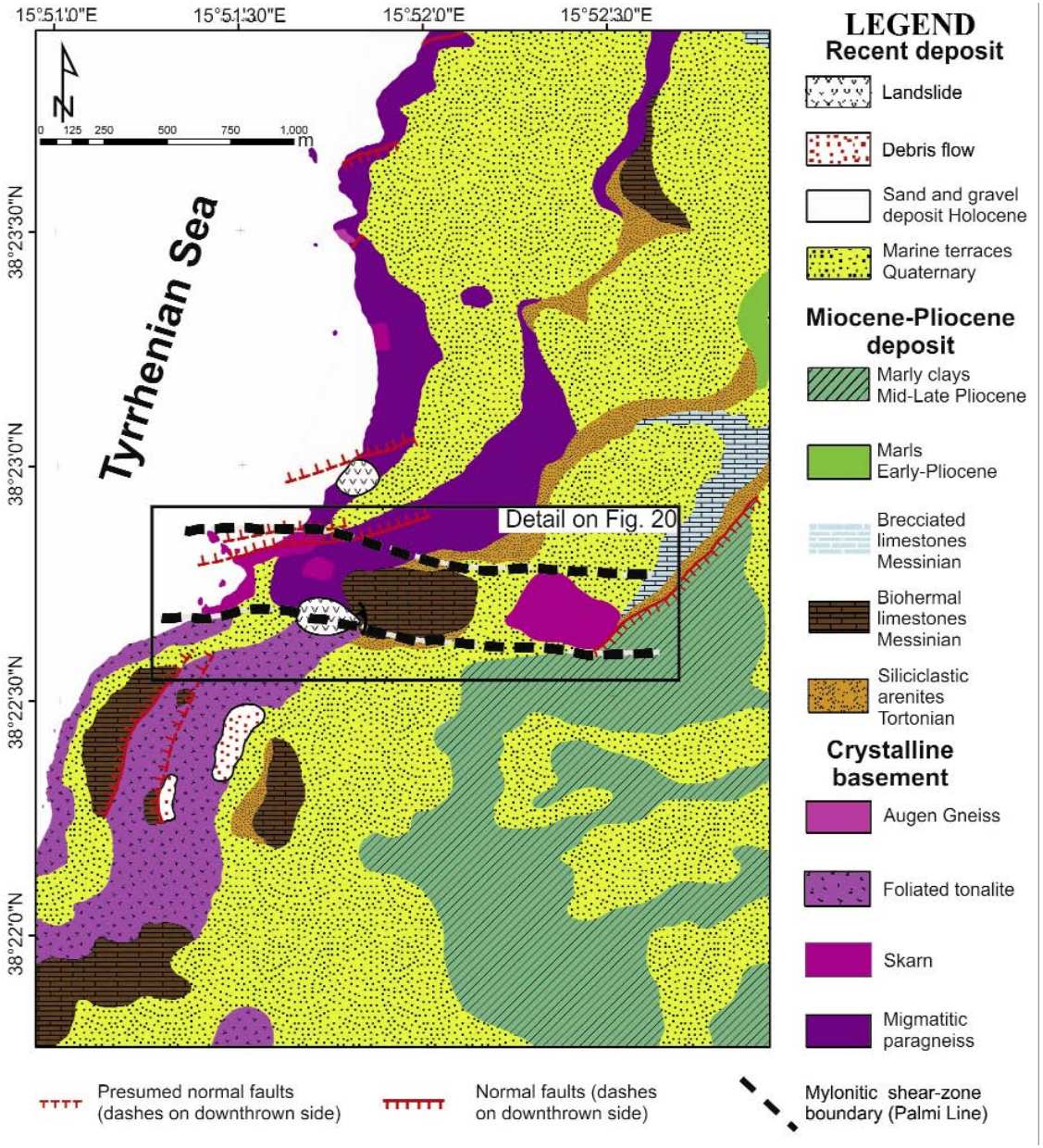

Fig. 4 - Geological sketch map of the Palmi area with location of the mylonitic Palmi shear zone (see Fig. 1 for location - modified after Ortolano et al., 2013). Details of the inset are reported in Fig. 20.

tectonic basement units locally interested by an Oligocene weak to pervasive mylonitic overprint (Pezzino et al., 2008) (Fig. 2); **(ii)** the latter constitutes an entire crustal section, where on a transect roughly oriented NW-SE rocks from lower to upper crustal levels are exposed (Fig. 3). Deep Variscan crustal rocks, exposed at the northern edge of the Massif, passing through late Palaeozoic granodiorite plutons towards southeast to low-medium grade metamorphic rocks covered by unmetamorphosed Mesozoic sediments (Angì et al., 2010). The boundary between these two sectors of the southern CPO can be traced along a complex polyphase strike-slip system (i.e. the Palmi line - Fig. 2), operating since the Early Eocene (51±1 Ma and 56±1 Ma, Rb-Sr biotite ages on mylonitic granitoids; after Prosser et al., 2003) up to the Tortonian age, as testified by the occurrence of a relic mylonitic deep-seated shearing activity recognizable along the Palmi shear zone (PSZ), characterized by a quasi-vertical average WNW-ESE attitude which can be followed in outcrop for about 1200 m inland before disappearing below a Tortonian siliciclastic formation (Tripodi et al., 2013) (Fig. 4), as well as by the extension of the shearing activity in brittle regime along the strike slip system of the Molochio Antonimina line (Fig. 5) (Ortolano et al., 2013; Cirrincione et al., 2015).

DOI: 10.3301/GFT.2017.03

More in detail, the Aspromonte Massif crystalline basement complex can be then described as a nappe pile consisting of three polyphase metamorphic unit. The uppermost one (i.e. the Stilo unit) is made up of low greenschist- to low amphibolite-facies Palaeozoic metamorphic rocks (Crisci et al., 1982; Bonardi et al., 1984, Graessner & Schenk, 1999), locally intruded by Late Variscan magmatic bodies producing a well developed contact aureole with biotite, muscovite and andalusite.

The PTd evolution of this unit consists of a mono-orogenic Variscan metamorphic cycle, characterized by an isoclinal folding, showing a pervasive axial plane schistosity, followed by a crenulation cleavage associated with prograde PT conditions ranging in pressure from ~0.35 to ~0.7 GPa for a temperature spanning from ~480 to ~550 °C. (Fig. 6), Fazio et al., 2012. Pressure of 0.7 GPa and temperature of 570°C values were obtained for the peak metamorphic conditions reached in this area, successively followed by a retrograde evolution caused by the development of a deep-seated shearing activity locally producing a pervasive mylonitic foliation, which is often obliterated by the static effects ascribable to the emplacement of the late-Variscan granitoids (Fig. 6). The ductile deformational phase has been recognized only within metre-tick biotite-paragneisses outcrops occurring in the south-western part of the investigated area. On the basis of the available

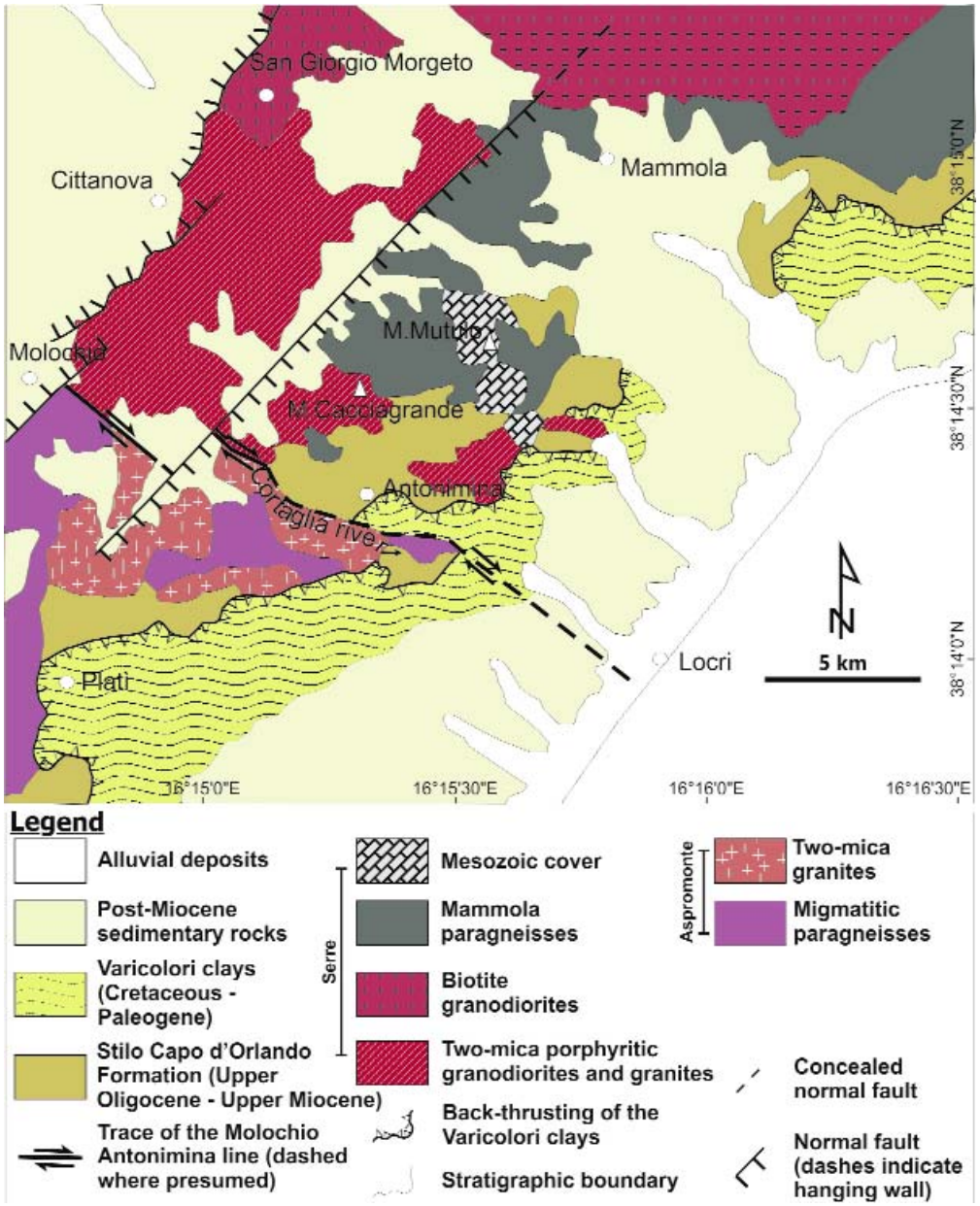

Fig. 5 – Geological sketch map of the boundary between Serre and Aspromonte Massifs along the Molochio Antonimina line (see Fig. 1 for location - modified after Cirrincione et al., 2015).

DOI: 10.3301/GFT.2017.03

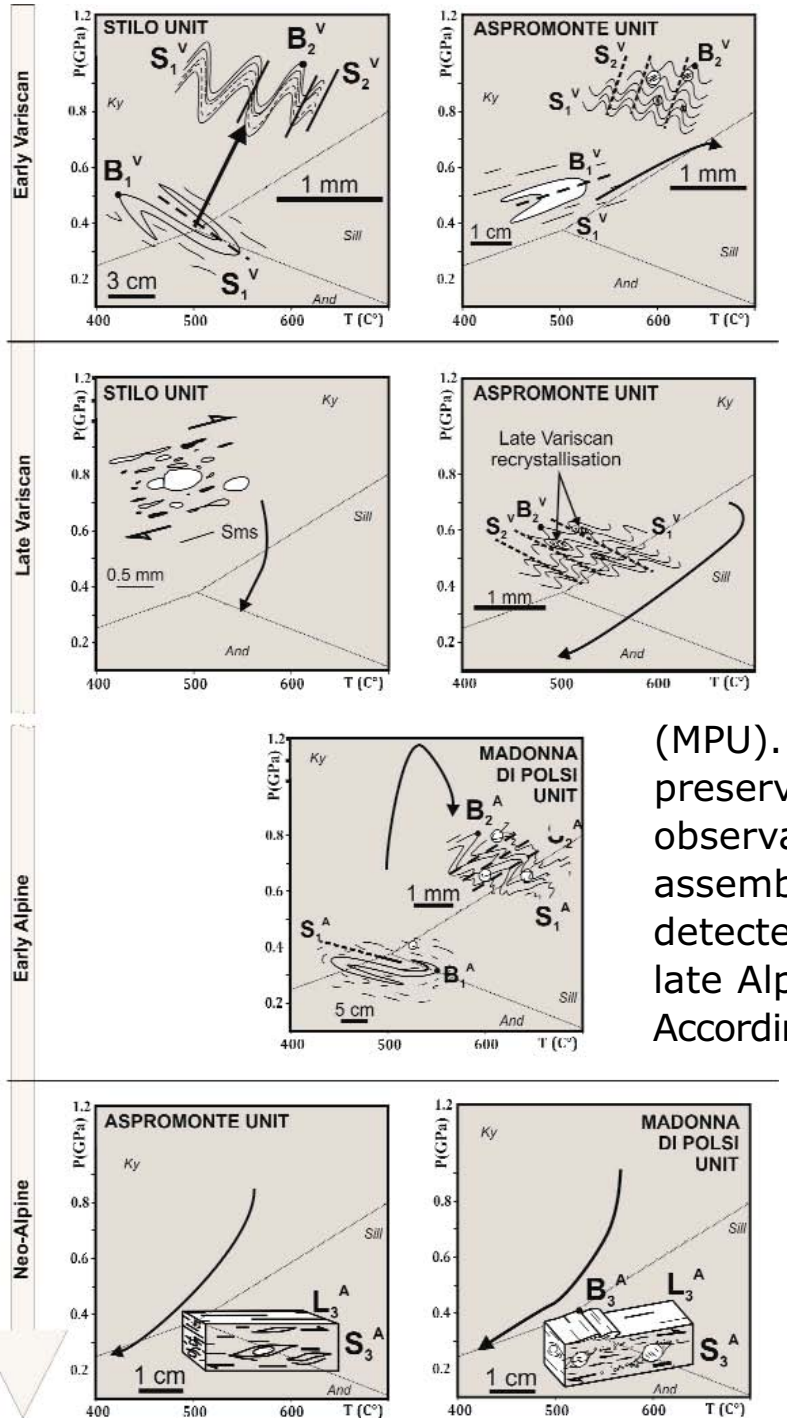

geological data, the exhumation of the SU can be attributed to the effects of a thin-skinned tectonics, coeval with the development of the south-eastward thrusting activity testified by tectonic contacts exclusively marked by cataclastic horizons, with no evidence of post-Variscan mylonitic activity (Cirrincione et al., 2015).

The intermediate Aspromonte unit is made up of amphibolite-facies Palaeozoic rocks characterized by a relatively HT-LP Variscan clockwise PT path, locally replaced by a late Variscan strongly peraluminous plutonic emplacement (ca. 303-300 Ma; Graessner et al., 2000; Fiannacca et al., 2008) with weak evidence of HT re-equilibration. A strong Alpine age mylonitic replacement developed at about 25-30 Ma (Bonardi et al., 1987), produced a thick mylonitic horizon marking the tectonic contact between the Aspromonte unit with the underlying low- to medium- grade metamorphic rocks of Madonna di Polsi unit (MPU). The pervasive mylonitic deformation stage did not permit the preservation of the pre-mylonitic structures. These are indeed only rarely observable at the micro-scale in the AU, as survived inclusion trails assemblages in Variscan garnet (Cirrincione et al., 2008), or rarely detected at the outcrop scale in the MPU rocks as isoclinal fold relic within late Alpine mylonitic foliation.

According to Cirrincione et al. (2008) the pre-mylonitic prograde PT paths of these two units indicate two different evolutions: **a)** the MPU prograde path is characterized by a HP-LT trajectory ranging from 0.95 to 1.25

Fig. 6 – Pressure Temperature deformation (PTd) path of the crystalline basement units of the Aspromonte Massif subdivided into prograde and retrograde paths along the temporal scale of the Variscan and Alpine orogenic stages: **A**=Alpine; **B**=fold axis; **S**=foliation; **V**=Variscan; (after Cirrincione et al., 2015 modified).

DOI: 10.3301/GFT.2017.03

GPa at temperature ranging from 400° to 600 °C (Fig. 6), related to crustal thickening occurred during an early Alpine deformational episode: **b)** a Barrovian-type prograde path is instead characteristic of the AU rock-types, with temperature estimates ranging from 650 to 675°C at relatively low pressure conditions of 0.4–0.5 GPa (Ortolano et al., 2005; Cirrincione et al., 2008) ascribable to an early Variscan tectono-metamorphic evolution, followed by a final widespread episode of hydration under decreasing temperatures (480°C), probably caused by the massive emplacement of the late-Variscan granitoids at about 300 Ma (Fig. 6) (Rottura et al., 1990; Graessner et al., 2000; Fiannacca et al., 2008).

The subsequent pervasive mylonitic stage (top to NE sense of shear; Pezzino et al., 2008) produced a pervasive foliation and a stretching lineation (averagely trending SW-NE) in both AU and MPU rocks. Recent findings of flow-perturbation folds and sheath ones (Alsop & Carreras, 2007) suggest, that such structures are related to the same deep-seated shearing phase which affected both units before they were exhumed during the final compressive stages of the nappe-pile formation (Ortolano et al., 2005). During this last stage MPU and AU rocks were indeed involved in the formation of cm to dam up to hm sized SSE-SE asymmetric folds before being finally exhumed along a joint brittle tectonic contact (Fig. 7). This compressional tectonic activity was often accompanied by the activation of a brittle strike-slip tectonics which locally re-activated relics of the early Alpine deep-seated strike-slip tectonics, which are only rarely preserved (e.g. Palmi shear zone; Ortolano et al., 2013).

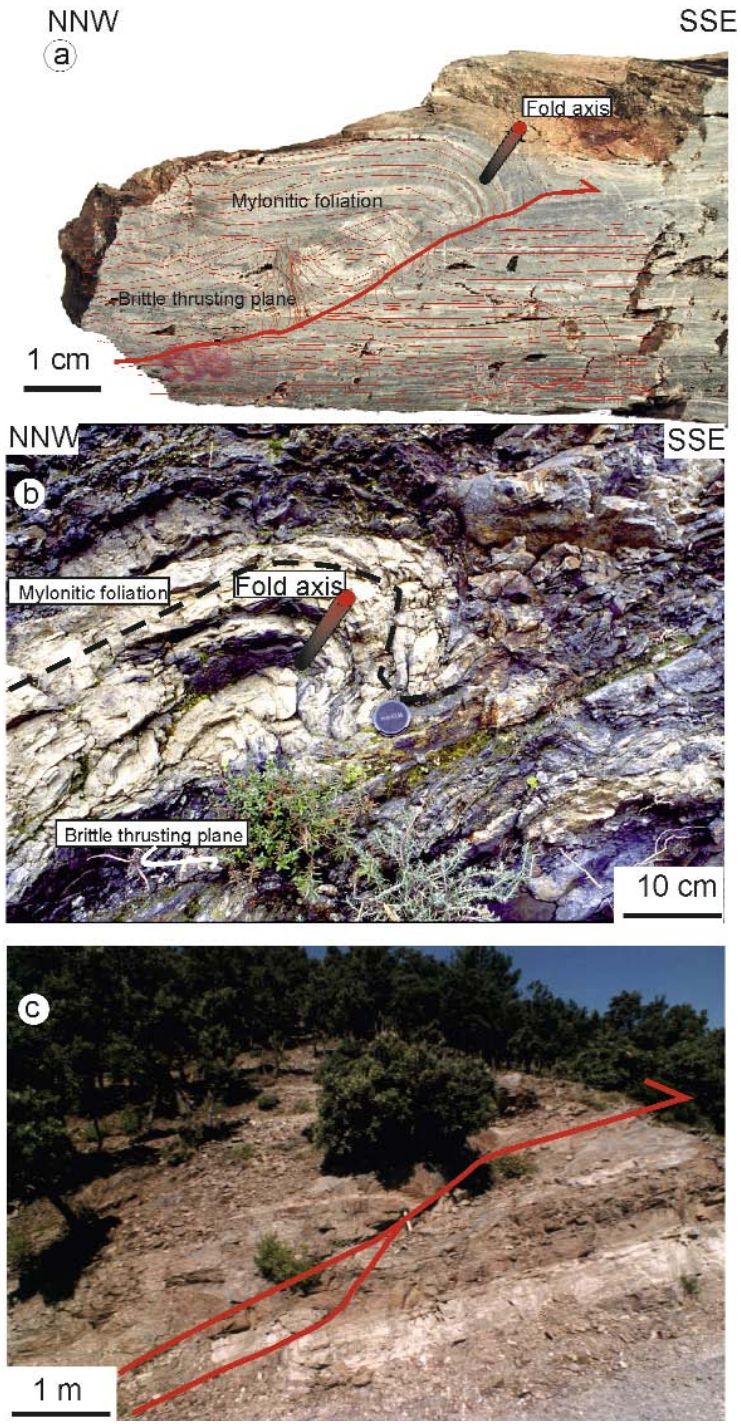

Fig. 7 – **a, b, c)** Fractal distribution of thrusting activity from cm to m sized ramp and flat structures developed during the final exhumation stage of the Apennine orogeny.

DOI: 10.3301/GFT.2017.03

Finally the switch from a compressional to an extensional tectonic regime starts with the activation of a normal fault system evidenced by the presence of widespread high-angle joint network, spanning from microscopically sized structures, passing from dm-sized fracture cleavage up to km-sized horst and graben structures averagely oriented WNW-ESE and WSW-ENE, linked to the main present-day seismogenic structural systems (Fig. 8) (Catalano et al., 2008; Morelli et al., 2011).

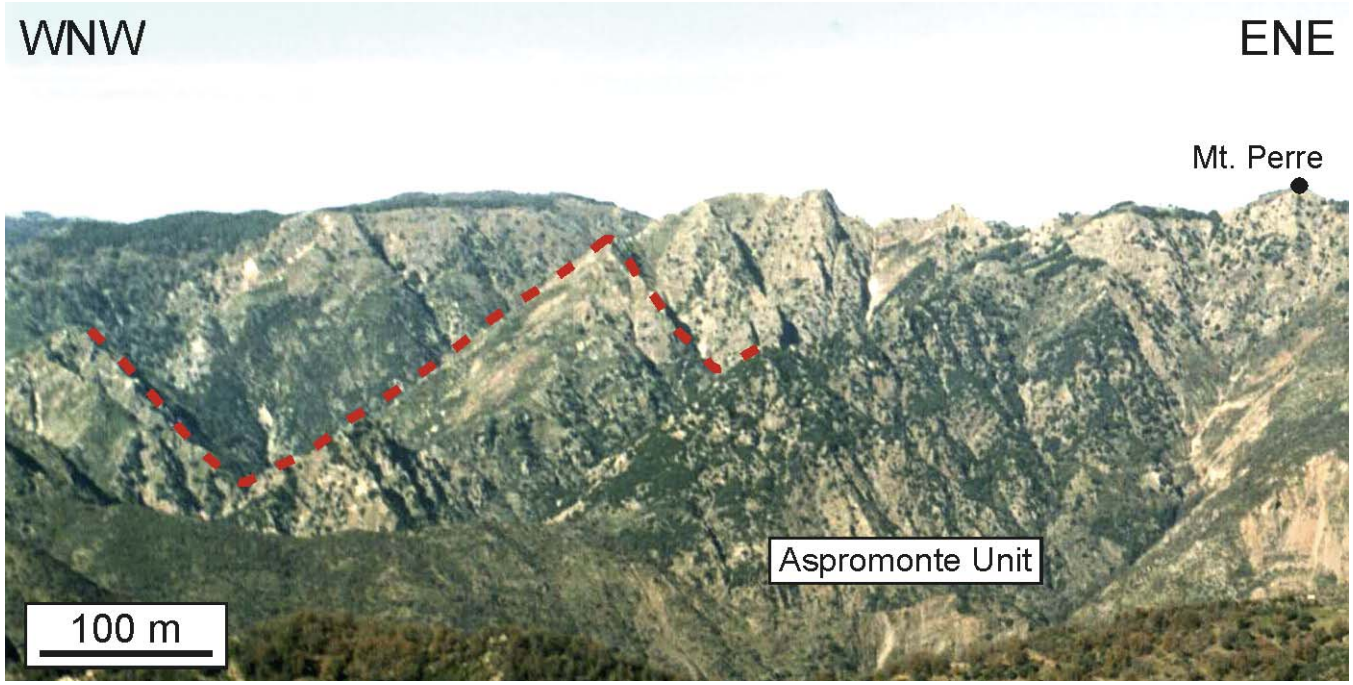

Fig. 8 - Normal fault system highlighted by the presence of triangular facets in the para- and ortho-gneisses of the Aspromonte unit.

DOI: 10.3301/GFT.2017.03

3 - Recent and active tectonics

Geophysical data

The Calabrian Arc is one of the most active tectonic domains in the Central Mediterranean, as shown by the number of disastrous historical earthquakes (Boschi et al., 1995) and the large geodetic displacements (Palano et al., 2012). In particular, south-western Calabria was hit by the 1783 seismic sequence, while the Strait of Messina region has been shaked by the 1908 earthquake and hit by the ensuing tsunami. The present-day tectonic framework of the Calabrian Arc (Figs 9, 10) is the result of the Neogene-Quaternary geodynamic processes related to the ca. N-S Africa-

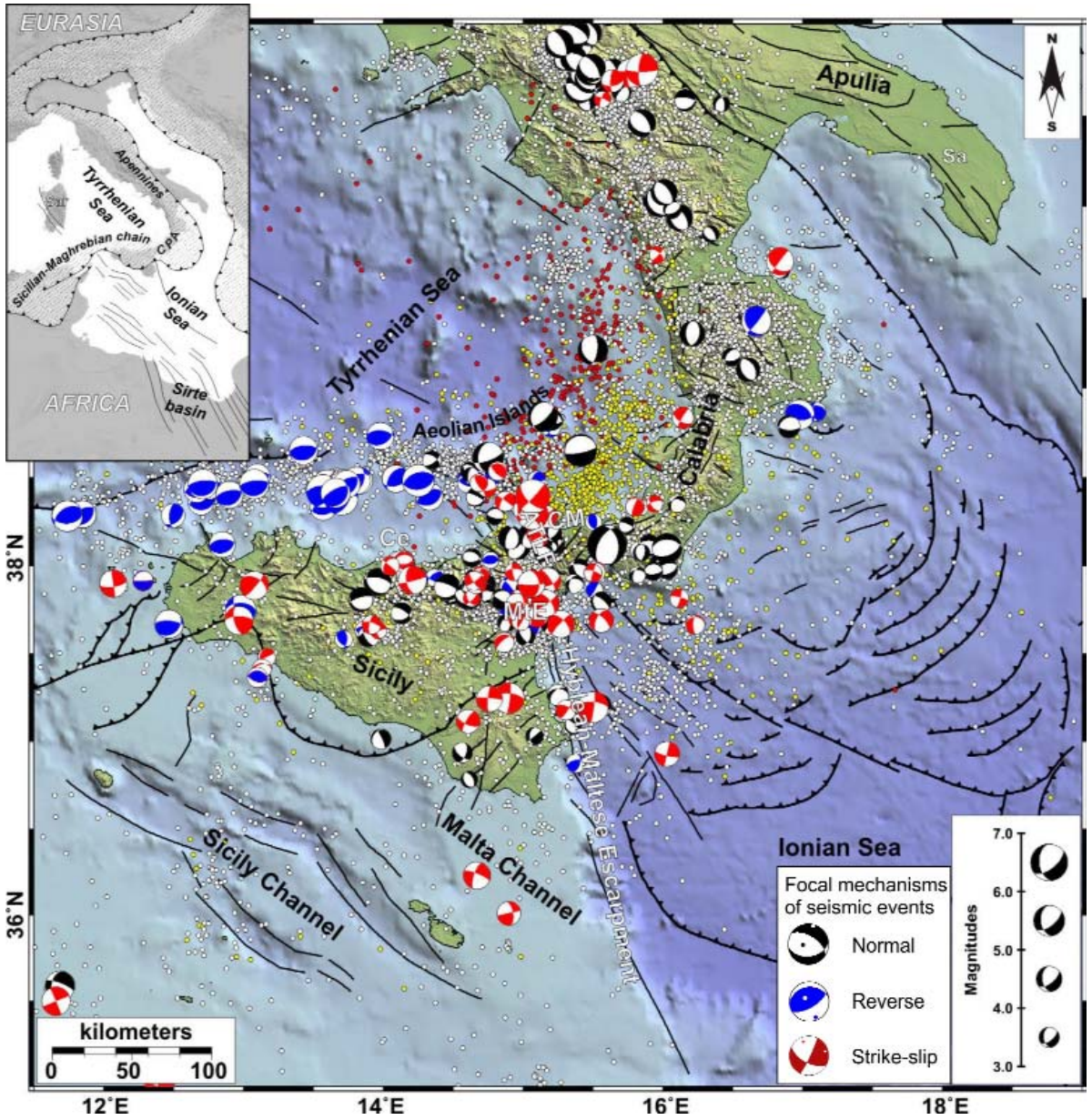

Fig. 9 - Simplified tectonic map of the Sicilian-Calabrian area (from Palano et al., 2012). Tectonic structures in the Ionian Sea redrawn from Polonia et al. (2011). Instrumental seismicity since 1983 with magnitude ≥2.5 (http://iside. rm.ingv.it): white for events occurring at depth h <30 km; yellow for those occurring at depth ranging between 30 and 200 km; red for those at depth >200 km. Focal mechanisms (FM) of events with magnitude >3.0 are also reported: red for strike-slip, blue for thrust faulting and black for normal faulting. Abbreviations are as follows: **ATLF**, Aeolian-Tindari-Letojanni fault system; **Ce**, Cefalù; **MtE**, Mount Etna; **CM**, Capo Milazzo; **Sa**, Salina Island; **Vu**, Vulcano Island; **Us**, Ustica Island; **HP**, Hyblean Plateau. The Africa-Eurasia plate configuration is shown in the inset; **CPA**, Calabro-Peloritan Arc.

DOI: 10.3301/GFT.2017.03

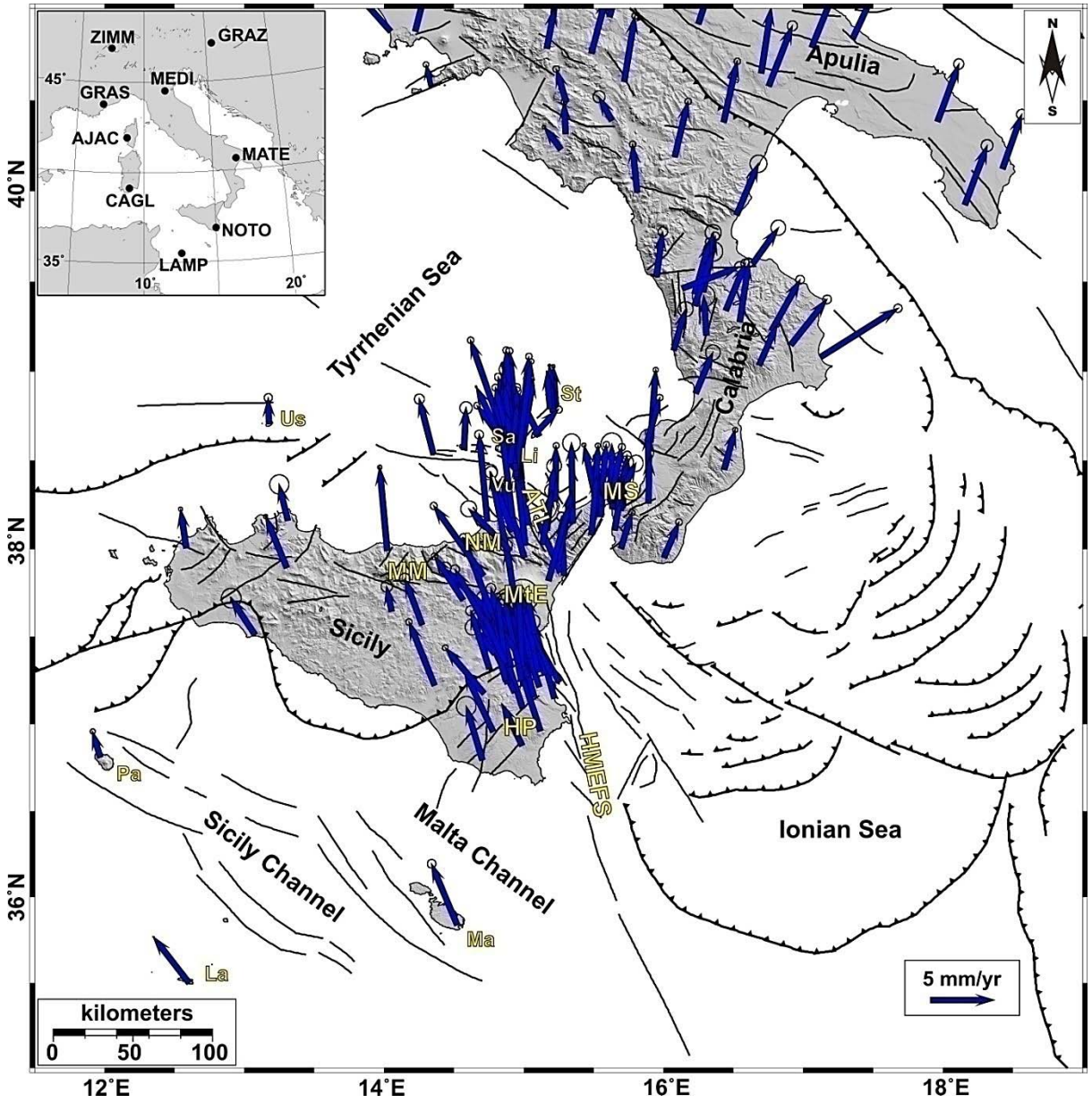

Fig. 10 - GPS velocities and 95% confidence ellipses in a fixed Central Europe frame (from Palano et al., 2012). **ATL**, Aeolian-Tindari-Letojanni fault system; **HMEFS**, Malta Escarpment fault system; **HP**, Hyblean Plateau; **La**, Lampedusa Island; **Li**, Lipari Island; **Ma**, Malta Island; **MM**, Madonie; **MS**, Messina Strait; **MtE**, Etna; **NM**, Nebrodi; **Pa**, Pantelleria; **Sa**, Salina Island; **St**, Stromboli Island; **Us**, Ustica Island; **Vu**, Vulcano Island. Inset shows the location of the IGS stations used to process GPS data from Palano et al., 2012, modified.

Eurasia convergence (e.g., Barberi et al., 1973; Dewey et al., 1989; Patacca et al., 1990).

Despite the convergence process occurred at a rate of 1-2 cm/a, since the last 8-10 Ma the region experienced a rapid E to SE roll-back of the Ionian oceanic crust subducted below the Calabrian Arc at a rate of 5-6 cm/a (Faccenna et al., 2004 and references therein) leading to back-arc extension and sea-floor spreading of the Tyrrhenian Sea basin. However, during the Late Pleistocene, rollback and subduction slowed at less than 1 cm/a (Faccenna et al., 2001). GPS data (D'Agostino et al., 2011) suggest that the south eastward motion of the Ionian margin of Calabria toward the trench, measured relative to Apulia, is still active at 2 mm/a and might reflect movement of the Ionian accretionary complex (Polonia et al., 2011).

DOI: 10.3301/GFT.2017.03

The presence of a ca. 70° NW-dipping Benioff-Wadati slab beneath the Calabrian Arc has been inferred since the early 1970s (Chiarabba et al., 2008, and references therein). The slab geometry is defined by deep earthquakes, which occur down to 600 km depth between Western Calabria and the Southern Tyrrhenian Sea (Frepoli et al., 1996). Laterally, the seismically active portion of the slab is no longer than 250 km (from southern Calabria to the western Aeolian Islands), less than its vertical extent. The absence of the slab underneath Sicily and the southern Apennines supports the idea of slab tears affecting the subducting Ionian crust (e.g., Wortel & Spakman 2000).
According to recent studies, mostly based on geodetic and seismological data (e.g. Goes et al., 2004; Billi et al., 2011), the current tectonic framework of the Calabrian Arc and Southern Tyrrhenian Sea is the result of plate reorganization. Geophysical data indicate that the southern Tyrrhenian area is fragmented into crustal blocks separated by seismically active belts (Palano et al., 2012). Contraction affects mainly the western sector in which focal solutions depicts an E–W oriented compressive belt which extends from the Aeolian Archipelago to the Ustica Island (Pondrelli et al., 2004; Neri et al., 2005; Billi et al., 2006; 2007; 2011). Conversely, the eastern sector (e.g. NE Sicily and western Calabria) is dominated by Late Quaternary extensional deformation (Monaco & Tortorici, 2000; Jacques et al., 2001; D'Agostino & Selvaggi, 2004; D'Agostino et al., 2011; Ferranti et al., 2008a, b; Scarfì et al., 2009). The transition between these two belts is inferred to occur along a transversal NNW–SSE oriented tectonic boundary (the Aeolian–Tindari–Letojanni fault system, Palano et al., 2012) which extends from the Lipari–Vulcano complex, in the central part of the archipelago, southwards to the Gulf of Patti and, across the Peloritani Mountains, to the Ionian coast of NE Sicily.

The **W-E oriented contractional belt offshore Northern Sicily** is characterized by a NNW-SSE geodetic shortening of 1-1.5 mm/a and by frequent, moderate crustal (15-20 km of depth) thrust earthquakes with NW-SE trending, sub-horizontal P-axes (Hollenstein et al., 2003; Neri et al., 2005; Pondrelli et al., 2006; Cuffaro et al., 2011; Devoti et al., 2011). According to Goes et al. (2004), it formed as a consequence of locking of the Sicilian frontal accretion during the last 0.8 Ma and transfer of convergence to the north, probably favoured by the presence of crust thinned by back-arc extension in the Tyrrhenian Sea. In addition, the presence of pre-existing normal faults cutting and weakening the crust may have helped tectonic inversion (Pepe et al., 2004). The absence of deep seismicity below Northern Sicily and Southern Tyrrhenian Sea, as well as of subducted lithosphere material, as suggested by tomography studies (Wortel & Spakman, 2000;

DOI: 10.3301/GFT.2017.03

Piromallo & Morelli, 2003), is an indication that the ongoing convergence reflects continental collision processes. According to Billi et al. (2007, 2011), this structural alignment must be framed in the recent tectonic reorganization of the Nubia-Eurasia convergent boundary. In fact, the south-Tyrrhenian margin has been involved in the last 2 Ma in a progressive onset of compression and consequent basin inversion, propagating from west to east in the former back-arc domains of the Western Mediterranean. However, geological, seismological and geodetic data show that NNW-SSE compression is still accommodated by folding and thrusting at the frontal sectors of the Sicilian chain (e.g. Belice earthquake of 15/01/68, M = 5.4, see also Monaco et al., 1996a, 1996b; Lavecchia et al., 2007; Mattia et al., 2012; Barreca et al., 2014a; De Guidi et al., 2015).

The **extensional domain in North-Eastern Sicily and Western Calabria** is documented by normal faulting (Tortorici et al., 1995; Monaco & Tortorici, 2000), by crustal earthquakes (<10-20 km) with normal focal mechanisms related to a general extension perpendicular to the arc (Neri et al., 2004; Pondrelli et al., 2006; Scarfi et al., 2009; D'Amico et al.,2010; 2011) and by a WNW-ESE geodetic extension at ~1.5 mm/a (D'Agostino et al., 2011). Whereas it is widely proposed that the contractional domain is related to convergence between Europe and Sicily-Nubia, the causes for the extension in the Calabrian Arc are still debated. Various alternative processes are suggested, ranging from **(i)** rifting (Tortorici et al., 1995; Monaco & Tortorici, 2000; Jacques et al., 2001), to **(ii)** back-arc stretching in the Tyrrhenian Sea (Neri et al., 2005), to **(iii)** dynamic yet inadequate balance with regional, deep-induced uplift that has affected the Calabrian Arc since the Middle Pleistocene (Ghisetti, 1992; Westaway, 1993), to **(iv)** response to counter clockwise rotation of the Ionian block (D'Agostino & Selvaggi, 2004; Goes et al., 2004).

The distribution of crustal seismicity (Fig. 9) shows that most of the earthquakes, including events with M> 6, are located in the hanging-wall of the distinct segments of Quaternary normal faults (Monaco & Tortorici, 2000). These are characterized by lengths from 10 to 50 km and very young morphology, and control both the fronts of the main mountainous areas (Coastal Chain, Sila, Serre, Aspromonte, Peloritani) and the coastline of Southwestern Calabria (Capo Vaticano, Scilla, Messina Strait). In Southern Calabria and Northeastern Sicily, the active normal faults have reactivated some bounding structures of an ancient Plio-Pleistocene Messina Strait basin. Particularly, in the Calabrian side, the Scilla and Armo faults show evidence of recent movements and are the likely sources of the earthquakes of February 6th, 1783 (M ~ 6) and December 28th, 1908 (M =

DOI: 10.3301/GFT.2017.03

7.2), respectively (Ghisetti & Vezzani, 1982; Ghisetti 1992; Tortorici et al., 1995; Jacques et al., 2001; Ferranti et al., 2008a; b; Aloisi et al., 2012, 2014). The source of the destructive earthquakes of February 4th, 1169 and January 9th, 1693 (M ~ 7) is probably located offshore, in the Western Ionian Sea, where they have also triggered large tsunamis (Bianca et al., 1999; Tinti & Armigliato, 2001; Argnani & Bonazzi, 2005; Monaco & Tortorici, 2007; Scicchitano et al., 2007; Polonia et al., 2011).

The transition between compressive and extensional domains occurs along the NNW-striking Aeolian-Tindari-Letojanni fault system, a main shear zone marked by diffuse seismicity and evidenced by field, multichannel seismic and GPS data (Mazzuoli et al., 1995; De Astis et al., 2003; Favalli et al., 2005; Billi et al., 2006; Argnani et al., 2007; Mattia et al., 2008; Palano et al., 2012). This system has been variously interpreted as: **(i)** a transform fault, 350–400 km long, that extends from the Aeolian volcanic arc to the NW to the Malta Escarpment to the southeast (Lanzafame & Bousquet, 1997); **(ii)** a lithospheric tear fault bounding the western wedge of the underplating Ionian slab (Nicolich et al., 2000, Doglioni et al., 2001; Faccenna et al., 2004; Chiarabba et al., 2008); **(iii)** a crustal transfer zone between the Northern Sicily W-E contractional belt and the Ionian accretionary wedge (Goes et al., 2004; Neri et al., 2004; Billi et al., 2006). Whatever the interpretation, GPS data (Palano et al., 2012) indicate ~3.6 mm/a dextral-oblique extensional motion on this shear zone (Fig. 10), with transtension and minor transpression partitioned between discrete sectors of the fault system. The southern offshore continuation of the Aeolian-Tindari-Letojanni fault system is of course unconstrained by geodesy. However, the presence in the Ionian basin of NNW-SSE to NW-SE trending structures (Nicolich et al., 2000; Argnani & Bonazzi, 2005; Polonia et al., 2011; 2012), to which several earthquakes with prevailing strike-slip focal mechanisms can be associated (Scarfì et al., 2009), suggests the possible offshore extension of the Aeolian-Tindari-Letojanni fault system. These segments could play the role of lithospheric boundary between the Sicilian-Hyblean and Ionian-Apulian blocks (Nicolich et al., 2000; Goes et al., 2004; Rosenbaum & Lister, 2004; Chiarabba et al., 2008), or, alternatively, accommodate differential movements between the Calabria extensional belt and the Northern Sicily contractional belt, and connecting this latter to the frontal arc located on the Ionian basin (Bousquet & Lanzafame, 2004; Wortel & Spakman, 2000; Neri et al., 2012 and references therein; Goes et al., 2004; Billi et al., 2006).

DOI: 10.3301/GFT.2017.03

Morpho-structural data on vertical deformation

In Eastern Sicily and Calabria, contractional processes at the chain front and extension at the back have been followed by deep entrenchment of the river network from the coast to the interior, as a result of high rates of Quaternary uplifting. This process has been recorded by the formation of raised marine and coastal-alluvial terraces along the Ionian and Tyrrhenian coasts. The occurrence of a sequence of marine terraces represents, in fact, the result of the interaction between long-term tectonic uplift and Quaternary cyclic sea-level changes (Lajoie, 1986; Bosi et al., 1996) which are represented in the global eustatic curve derived from the Oxygen Isotope Time (OIT) scale. This curve (Waelbroeck et al., 2002 and references therein) shows a cyclic trend characterized by peaks corresponding to distinct marine high-stands and low-stands, represented by the odd- and even-numbered Marine Isotope Stages (MIS), respectively. The uplift rates are estimated by subtracting the elevation of each terrace from the sea level of the assigned Marine Isotopic Stage (MIS) and then dividing this value by the age assigned to the terrace (Fig. 11). Uplift rates of about 0.5 mm/a from about 400 ka along the southeastern coast of Sicily, of 1.3 mm/a from about 200 ka in the Catania area and 1.5-2.0/a from 125 ka in the north-east of Sicily and western Calabria have been estimated, values decreasing to about 1.0 mm/a in northeastern Calabria (Ghisetti, 1984; 1992; Stewart et al., 1997; Bordoni & Valensise, 1998; Bianca et al., 1999; 2011; Monaco et al., 2002; Catalano & De Guidi, 2003; Antonioli et al., 2006; Ferranti et al., 2006; 2009).

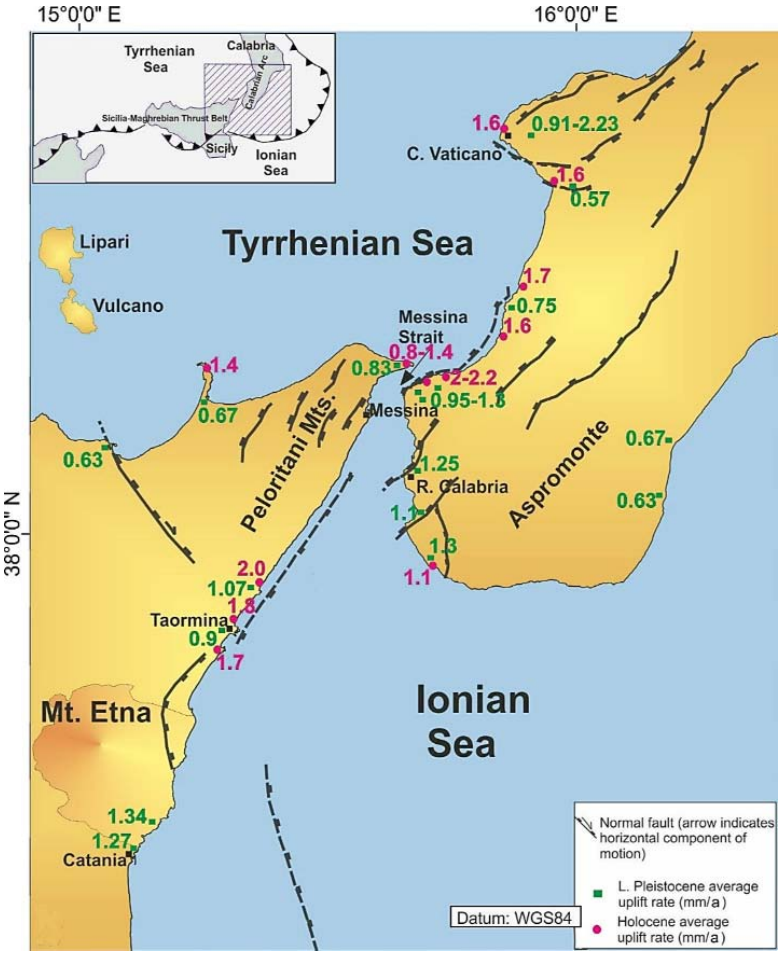

Fig. 11 - Late Pleistocene uplift rates in Southern Calabria and Northeastern Sicily from Spampinato et al., 2014.

The elevation of marine terraces and their offset across the main faults has been used to establish the relative contribution of regional and fault-related sources to uplift. According to Westaway (1993), 1.7 mm/a of post-Middle Pleistocene uplift of Southern Calabria was partitioned into 1 mm/a due to regional processes and the residual to displacement on major faults. This was confirmed by estimates of the shorter term rates of uplifting provided by

DOI: 10.3301/GFT.2017.03

raised Holocene beaches, wave-cut platforms and tidal notches compared to the predicted sea level curves (Firth et al., 1996; Stewart et al, 1997; Rust & Kershaw, 2000; De Guidi et al., 2003; Lambeck et al., 2004; 2011; Antonioli et al., 2004; 2006; Ferranti et al., 2007; Scicchitano et al., 2008, 2011a, b; Spampinato et al., 2011; 2012; 2014). For example (Fig. 11), precise leveling of late Holocene (<5 ka) sea level markers raised up to about 5 m above sea level in the Taormina area suggest an important co-seismic contribution to the total uplift rate of 1.7-1.8 mm/a, with at least three paleo-earthquakes attributed to the activity of offshore faults (De Guidi et al., 2003; Spampinato et al., 2012). Similar results were obtained along the eastern shore of the Messina Strait, where the uplift of late Holocene (<5 ka) paleo-shorelines at rates up to ~ 2 mm/a has been partitioned between regional and co-seismic contributions, the latter attributed to the activity of the Scilla fault (Ferranti et al., 2007).

The Messina Strait

Intense Quaternary extensional tectonics, coupled with coastal uplift, is well documented in the Messina Strait (Fig. 12), a highly seismic area that was struck on 1908

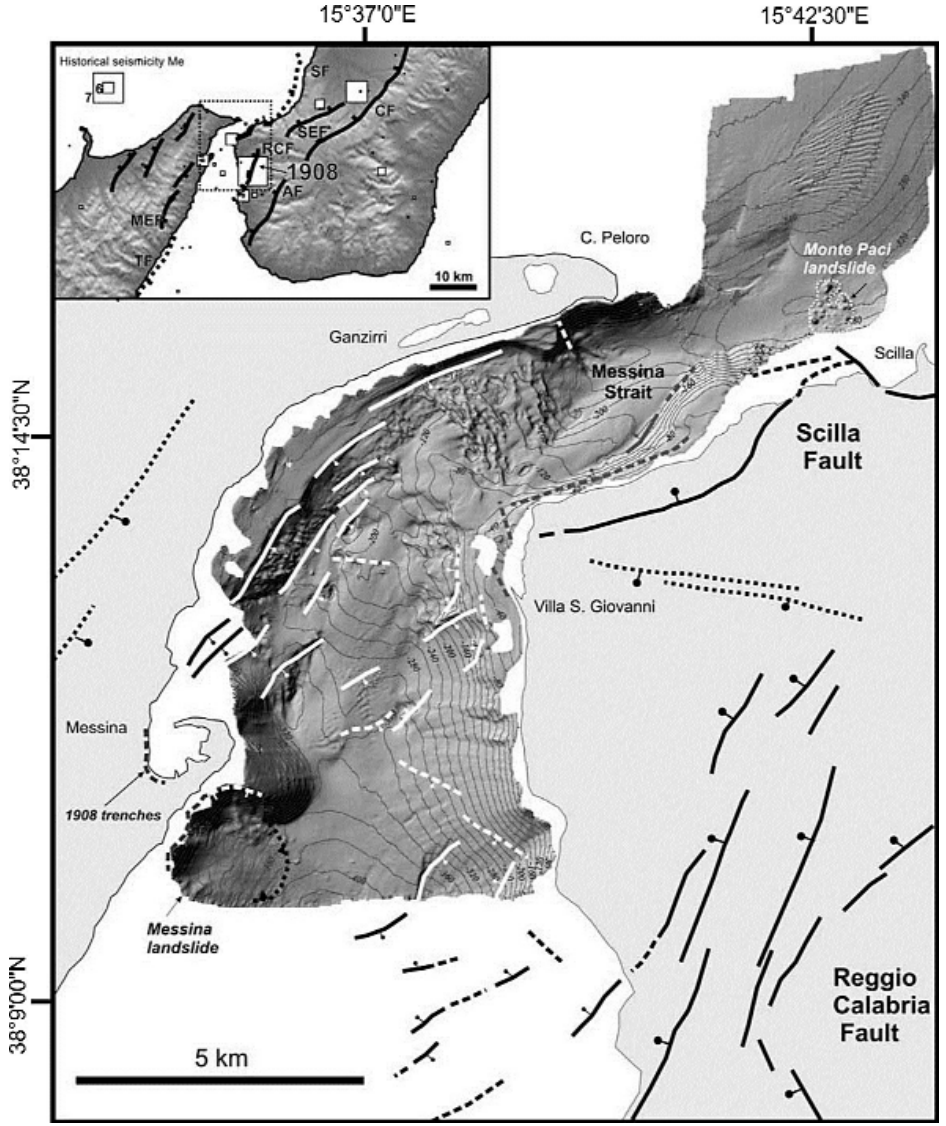

Fig. 12 - Morphostructural setting of the northern sector of the Messina Strait (from Ferranti et al., 2008b). Normal faults with balls on the downthrown side, dashed where inferred. On-land faults slightly modified from Ghisetti (1992), Tortorici et al. (1995), Del Ben et al. (1996), Ferranti et al. (2007); dotted are Early Pleistocene faults. The dotted black line with teeth indicates the trace of the deep toe of the Messina landslide. The white dotted line outlines the extent Punta Paci block landslide. On the Calabrian side raised paleo-shorelines occur at the footwall of the Scilla fault (site a, Marina di San Gregorio; site b, Punta Paci). Inset shows historical seismicity and Quaternary faults: **AF**, Armo fault; **CF**, Cittanova fault; **MEF**, Messina fault; **RCF**, Reggio Calabria fault; **SEF**, Sant'Eufemia fault; **SF**, Scilla fault; **TF**, Taormina fault.

DOI: 10.3301/GFT.2017.03

December 28th by a M 7.1 earthquake and ensuing devastating tsunami (Baratta, 1910; Shick, 1977; Aloisi et al., 2012 and references therein). This structural depression is bounded by active normal faults, marked by well-preserved scarps, which displace Pleistocene marine terraces and Holocene shorelines (Ghisetti, 1981; Valensise & Pantosti, 1992; Catalano et al., 2003; Ferranti et al., 2007; 2008a; Di Stefano & Longhitano, 2009; Scicchitano et al., 2011b).
The WSW-ENE to SSW-NNE striking extensional basin of the Messina Strait formed as a consequence of the Pliocene-Early Pleistocene axial collapse of the inner sectors of the Calabrian Arc. The Late Pliocene-Early Pleistocene deposition was followed by the uplift of the border fault footwalls and subsequent development, during the Lower-Middle Pleistocene, of huge submarine fan-delta systems (Messina gravels and sands). Since the Middle Pleistocene, the strong regional uplift has caused the emersion of these fan-delta systems. In the meantime, the interaction between the uplift process and the eustatic sea-level fluctuations caused the formation of flights of marine terraces on the basin flanks. Uplift rates have been higher in the Calabrian sector where the normal faults show evidence of recent activity. In particular, in the Ganzirri area the MIS 5.5 terrace is located at an altitude of 90 m, while in the Villa San Giovanni area it is uplifted up to 170 m (Ferranti et al., 2006).

Analyses of coastal tectonics have shown that faults located at/or intersecting the coast (Scilla, Reggio Calabria and Armo faults, see inset in Fig. 12) have recent activity. Late Holocene coseismic displacements on the ~30 km long Scilla fault (Westaway, 1993; Jacques et al., 2001) are suggested by Holocene marine platforms and beachrocks which are uplifted above sea level on the fault footwall (sites a and b in Fig. 12, Ferranti et al., 2007; 2008a). The latter authors dated two co-seismic events at ~3.5 and ~1.9 ka BP, with estimated slips ranging between 1.5 and 2.0 m and magnitude of ~6.9–7.0 (see Stop 2). The Reggio Calabria fault (Ghisetti, 1984; 1992) was considered the source of the 1908 earthquake by Tortorici et al. (1995) on the basis of morphotectonic, macroseismic and seismological observations, but evidence of active deformation is scarce. In contrast, the Armo fault shows clearer evidence of Pleistocene activity (Ghisetti, 1984; 1992; Aloisi et al., 2014), and coastal studies suggest a possible reactivation during the Holocene (Scicchitano et al., 2011b). Marine geophysical investigations (Del Ben et al., 1996; Guarnieri, 2006; Ferranti et al., 2008b; Argnani et al., 2009) also highlight the prevalence of active faults on the eastern part of the strait.
High resolution swath bathymetry data and multichannel sparker profiles (Fig. 12, Ferranti et al., 2008b) show that recent faults in the northern and narrower sector of the Messina Strait are arranged in two broad ~NE–SW

DOI: 10.3301/GFT.2017.03

trending arrays with opposing polarity (Fig. 1). The NW-dipping fault array on the eastern side of the Strait, which represents the offshore extension of the Scilla and Reggio Calabria faults, is wider (~5 km), and large offsets of tens of meters are observed in the Middle Pleistocene–Holocene sedimentary sequence (Ferranti et al., 2008b). By contrast, the fault swarm on the western side has more limited appearance and is made up of discontinuous segments. The arrays are connected by a NW–SE trending transfer zone located between Messina and Reggio Calabria (Fig. 13), which seems to control the current release of low seismicity (Scarfì et al., 2009).
Similarly, multichannel seismic profiles collected by Argnani et al. (2009) within the southern, broader part of the Messina Strait place the master faults on the Calabrian side. Specifically, a 30-km long, NW-striking and west-dipping listric fault located at the SW tip of Calabria cuts the seafloor (SCF, Fig. 13). On the other hand, offshore seismic profiles (Monaco et al., 1996a; b; Del Ben et al., 1996; Argnani et al., 2009) do not show evidence of low-angle faults and of their effects underneath the Messina Strait. According to Argnani et al., (2009), the lack of evidence of extensional faults large enough to cause an M ~ 7 earthquake within the northern and western sector of the Strait support the contention that the 1908 seismogenic fault is located along the South Calabria offshore. The lack of clear evidence of surface faulting, however, made it difficult to determine the source of the 1908 earthquake (see below).

The few seismological recordings of 1908 coupled with co-seismic vertical displacements documented by levelling data of Loperfido (1909) have been predominantly interpreted to support a blind low angle (30° to 40°) normal fault dipping towards the SE nearly parallel to the Messina Strait and located along the Sicilian coastline (e.g. Valensise & Pantosti, 1992; Amoruso et al., 2002 DISS Working Group, 2015; De Natale & Pino, 2014 and references therein). However, high-resolution swath bathymetry and seismic profiles (Argnani et al., 2009; Doglioni et al., 2012; Ridente et al., 2014) show that the modeled through-going ~N-S striking faults below the Strait are not present. Conversely, another set of models considers NW-dipping, high-angle normal faults on mainland Calabria as causative sources of the seism (Schick, 1977; Mulargia & Boschi, 1983; Ghisetti, 1984, 1992; Bottari et al., 1986; Westaway, 1992; Tortorici et al., 1995; Bottari, 2008). In particular, the macroseismic picture (Fig. 13) and the youthfulness and fresh bathymetric expression of many of the faults in the eastern array indicates that these faults may be activated during large or moderate earthquakes. This interpretation is consistent with the regional structure of the Messina Strait area, characterized by master faults on the Calabrian side and associated antithetic faults on the Sicilian side (Ghisetti, 1984; Montenat et

DOI: 10.3301/GFT.2017.03

al., 1991; Tortorici et al., 1995). Recently, new field evidence along with a re-evaluation of the levelling and seismic data have been used by Aloisi et al., 2012; 2014, to identify the Armo fault, a NW-dipping normal fault exposed in SW Calabria, as a possible source of the 1908 event (Fig. 13).

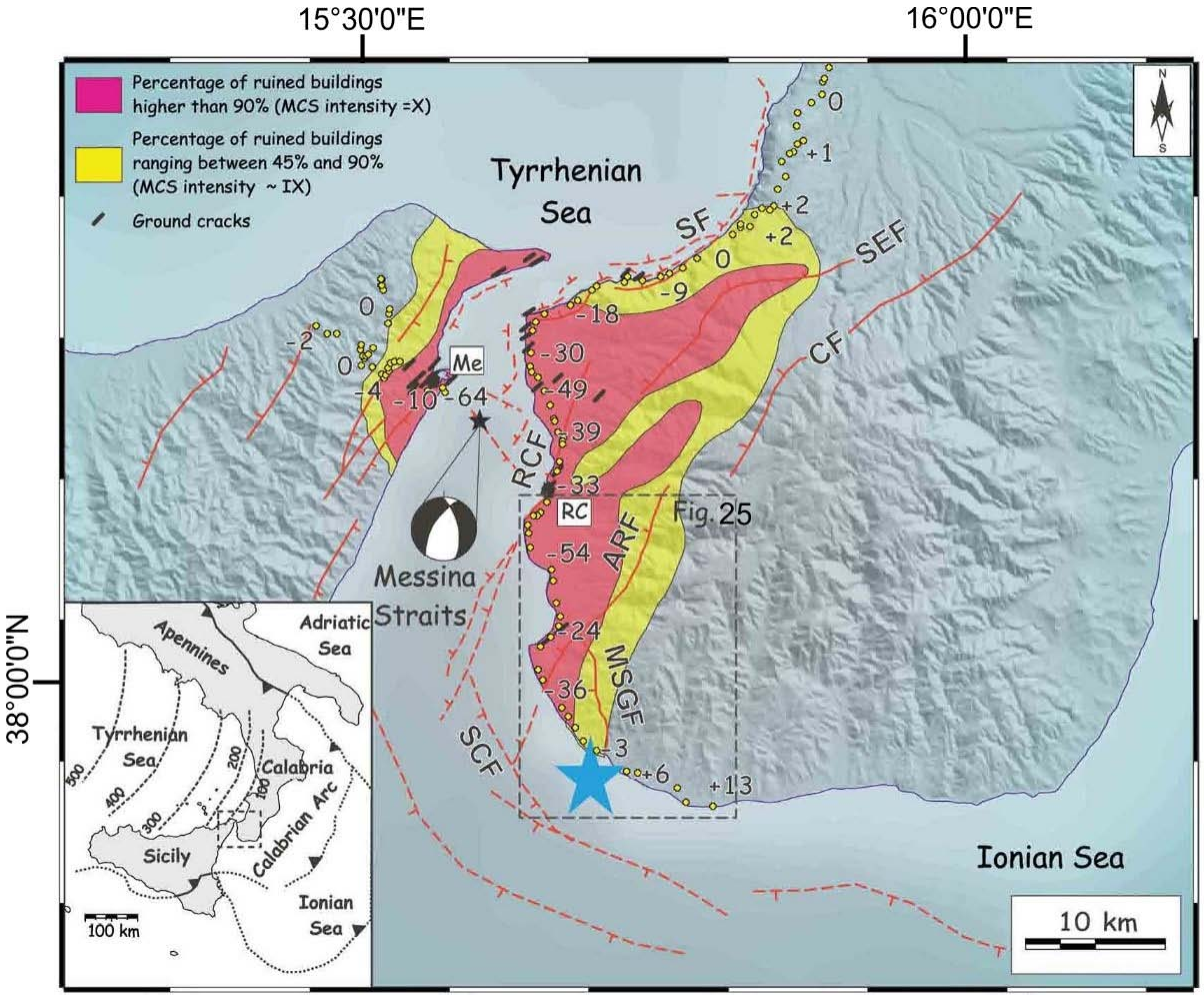

Fig. 13 - Seismotectonic setting of the Messina Strait region. Faults (thick solid lines barbed on the downthrown side, dashed where inferred or submerged) after Ghisetti (1992), Monaco & Tortorici (2000), Jacques et al. (2001), Ferranti et al. (2007), Argnani et al. (2009): **ARF**, Armo fault; **CF**, Cittanova fault; **MSGF**, Motta San Giovanni fault; **RCF**, Reggio Calabria fault; **SCF**, Southern Calabria fault; **SEF**, S. Eufemia fault; **SF**, Scilla fault. The focal mechanism (after Gasparini et al., 1985) and damage distribution of the December 1908 earthquake (data from Baratta, 1910; Boschi et al., 1995; Monaco & Tortorici, 2007) are indicated. Towns are labeled in white boxes: RC, Reggio Calabria; Me, Messina. The projection is WGS84. The levelling data of Loperfido (1909) are reported as yellow circles with average vertical change values. The blue star shows the macroseismic location of Michelini et al. (2005). Inset shows the location of the study area in the tectonic setting of the Central Mediterranean from Aloisi et al., 2012.

DOI: 10.3301/GFT.2017.03

Field Trip

The planned route, that will cross the most fascinating places of the Aspromonte Massif region, is aimed to illustrate a variety of issues ranging from the geology, geomorphology and sedimentary features of the Tyrrhenian coast of the Aspromonte Massif focusing attention on the late Quaternary faults representing the most important regional-scale seismogenic structures, as well as on the complex tectono-metamorphic evolution of the crystalline basement outcrops, characterized by overprinting relationships of the Variscan and Alpine orogenesis.

Day 1

Stop 1.1: Recent tectonics of the Messina Strait: view of the Pleistocene terraces on the Campo Piale horst and of the Scilla fault (Barreca G., Ferranti L., Monaco C.)
Stop 1.2: View of the Holocene raised wave-cut platforms along the Scilla coast (Barreca G., Ferranti L., Monaco C.).
Stop 1.3: Migmatitic complex of the Scilla rock, Aspromonte unit (Fazio E., Cirrincione R., Ortolano G.).
Stop 1.4: Mylonitic skarns, tonalite and migmatitic paragneiss of the Palmi area (Ortolano G., Cirrincione R.).
Stop 1.5: View of the Armo fault (Ferranti L., Monaco C.).
Stop 1.6: Contact between the Pleistocene deposits and the Palaeozoic crystalline basement along the Armo fault (Ferranti L., Cirrincione R.).
Stop 1.7: Holocene raised beachrock near Capo dell'Armi (Ferranti L., Monaco C.).

Day 2

Stop 2.1: Tectono-stratigraphy of the Aspromonte Massif basement complex (Ortolano G., Fazio E.).
Stop 2.2: Relics of late Variscan mylonitic structures in the Stilo unit (Fazio E., Ortolano G.).

DOI: 10.3301/GFT.2017.03

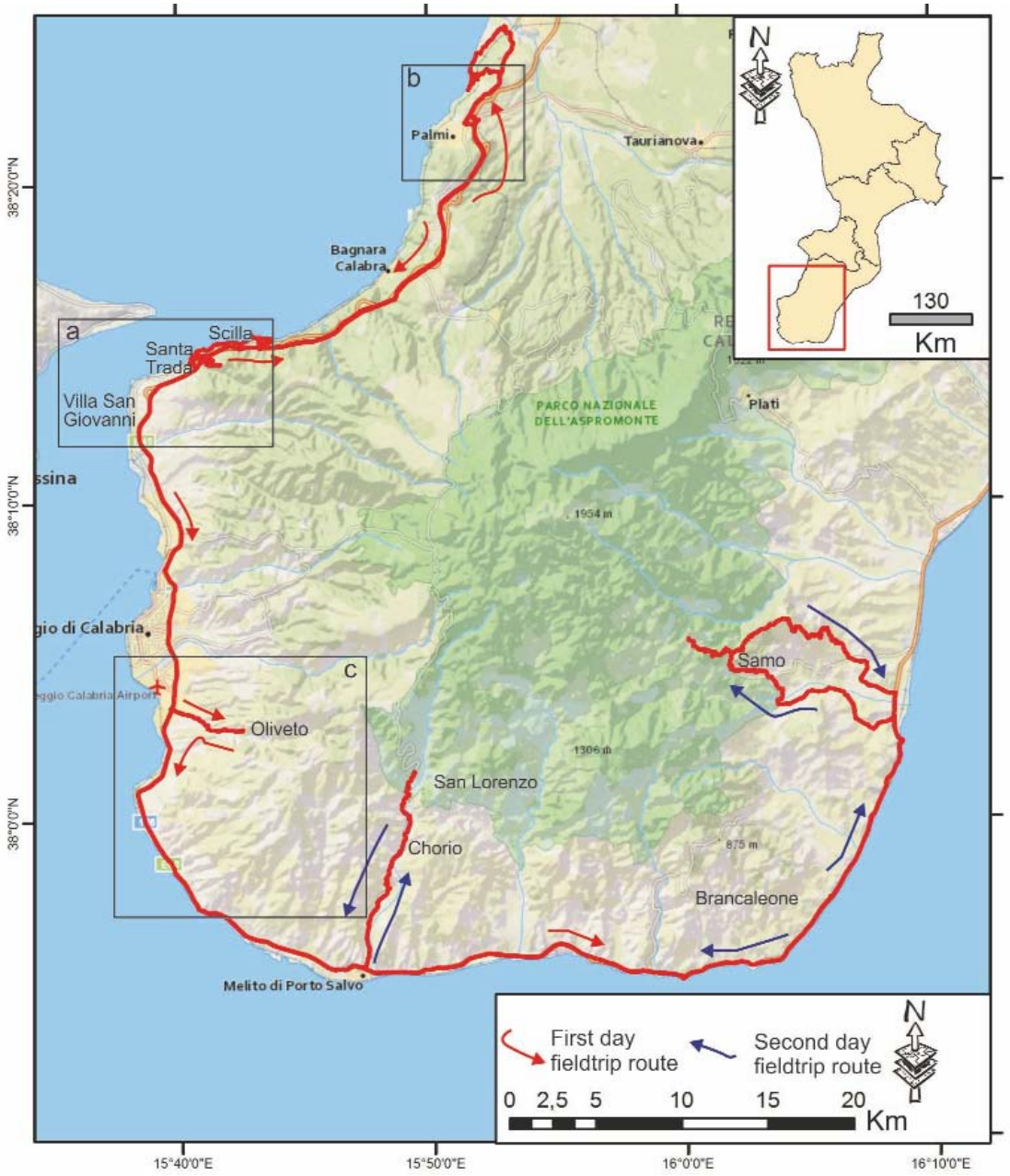

Field trip route sub-areas of the first day. **a)** Specific location of the 1.1, 1.2 and 1.3 stops; **b)** Specific location of the 1.4 stop; **c)** Specific location of the 1.5, 1.6 and 1.7 stops.

Day 1

DOI: 10.3301/GFT.2017.03

The first day's excursion addresses the issue of Late Quaternary faulting and related uplift along some segments of the Calabrian Arc. The planned stops are on the southwestern Calabria edge along the footwall of the Scilla fault where a series of terraces ranging in age from 125 to 60 ka has been preserved.

STOP 1.1: Recent tectonics of the Messina Strait: view of the Pleistocene terraces on the Campo Piale horst and of the Scilla fault (38°14'40"N; 15°41'00"E)

Along the Calabrian side of the Messina Strait, between Villa S. Giovanni and Piano di Matiniti, a complete sequence of ten Late-Quaternary fluvial-coastal terraces is observable at elevations ranging from 40 to 520 m (Fig. 14). The terraced deposits are formed by calcarenites, marine sands and conglomerates, more or less cemented, directly lying on the crystalline basement or on the middle upper (Trubi Fm.), Pleistocene (Vinco calcarenites) or middle-late Pleistocene (Messina gravels and

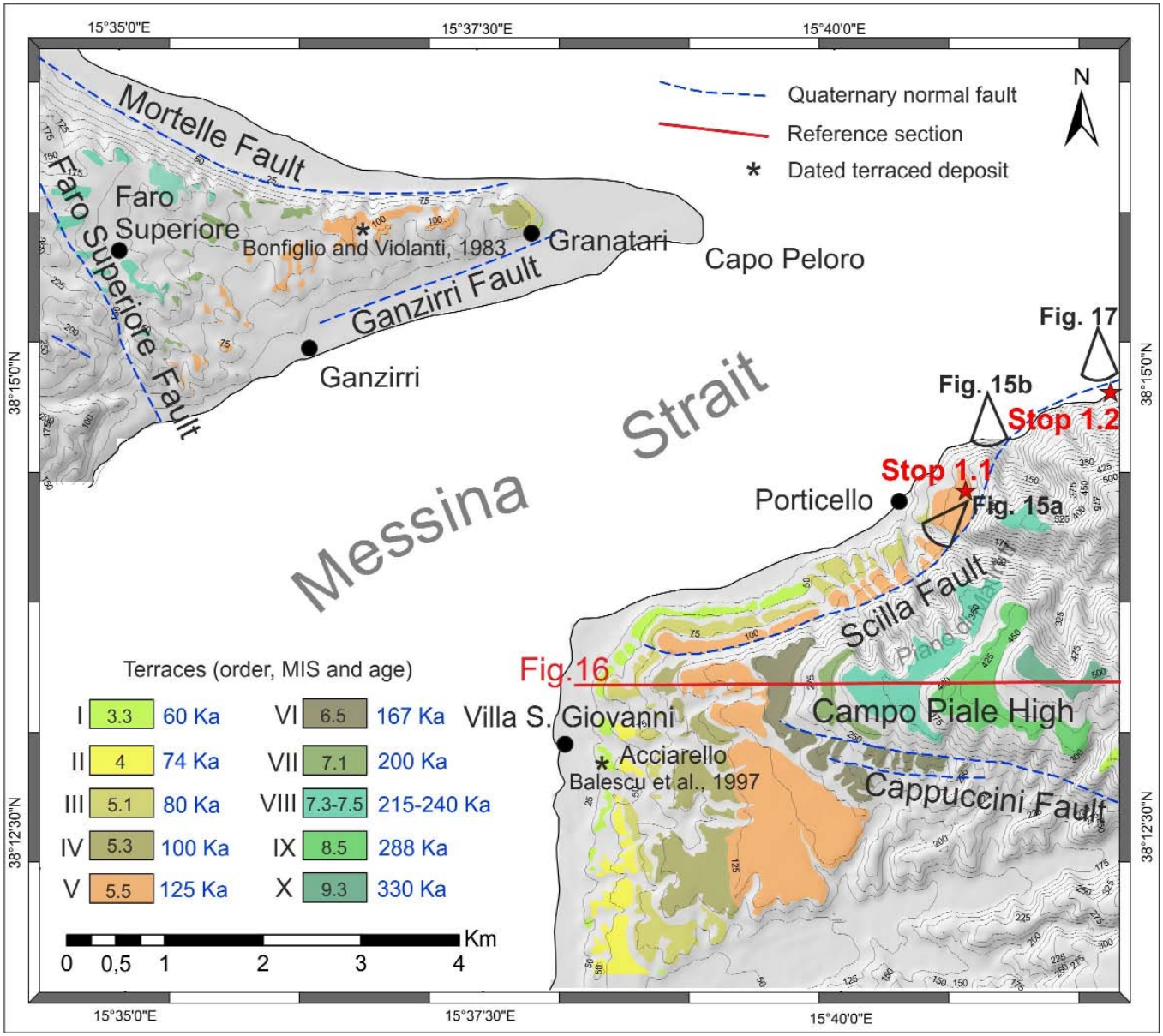

Fig. 14 - Morphotectonic map of the northern sector of the Messina Strait area showing the major Quaternary faults, the distribution of Quaternary terraces and the location of dated deposits. Location of Stops 1.1 and 1.2 and panoramic field of views are indicated (after Monaco et al., 2017).

DOI: 10.3301/GFT.2017.03

sands fm.) sedimentary covers (Ghisetti, 1981; Miyauchi et al., 1994). The marine deposits generally pass upwards to continental reddish silt with sands and gravels layers, thick up to 20 meters.
The terraced series is partly displaced by the Scilla fault that borders the Campo Piale horst to the north. The scarp of the onland western segment of the Scilla fault is characterized by up to 70-m-high triangular facets, suggesting recent activity, and by a cataclastic zone in the crystalline bedrock, including NW-dipping fault planes (Fig. 15). The lowest (I order) terrace extends along to the coast, with inner edge around at 40 meters. It's worth noting that it seals the Scilla fault north of Villa San Giovanni (Fig. 14). Terraces II, III, IV, V and VI extend around the Campo Piale Horst, extensively outcropping along the south-west side, with inner edges at elevations of 60, 95, 120, 175 and 200 m, respectively. The complete terraced sequence of the remaining orders outcrops only along the Campo Piale horst, where the terraces VII, VIII and IX show inner edges at elevations of 285 m, 345 m and 415 meters. Terrace X, the oldest and highest of the whole series, extends at elevations ranging from ~ 480 m to ~ 520 meters. North of the Campo Piale horst, on the hangingwall of the Scilla fault, the assignment of terraces to distinct orders is more complex. In this area only three terraced surfaces have been recognized: the terrace I shows a clear continuity parallel to the coastline; a second surface, with inner edges at elevations between 70 m and 90 m, has

Fig. 15 - **a)** View of the onland western segment of the Scilla fault, bordering to the north the Campo Piale horst. The fault trace and the up to 70-m-high triangular facets marking the fault scarp are outlined with dashed lines. **b)** Detail of the cataclastic zone in the crystalline bedrock associated to the Scilla fault, including NW-dipping fault planes (from Ferranti et al., 2007).

DOI: 10.3301/GFT.2017.03

been attributed to the terrace III outcropping on the Villa S. Giovanni area, suturing the western end of the Scilla fault; a third surface, with inner edges at elevations between 100 m and 140 m, has been attributed to the V order (MIS 5.5, 125 ka) by geomorphological correlations (see Miyauchi et al., 1994; Jacques et al., 2001).
As regards the age attribution, the finding of *Strombus bubonius* in the Reggio Calabria area (Bonfiglio, 1972; Dumas et al., 1987) and the absolute dating obtained by thermoluminescence (TL) and optically stimulated luminescence (OSL) methods (Balescu et al., 1997), perfectly constraint the age of the terraced deposits between 60 and 330 ka. In particular, an age of around 60 ka has been attributed to the sandy deposits of the lowest terrace (I order), outcropping in the Acciarello place near Villa S. Giovanni (Balescu et al., 1997, see Fig. 14), while the morphological correlation of the terrace V with the *Strombus bubonius* deposits (see also Miyauchi et al., 1994; Dumas & Raffy, 2004), has allowed to correlate this last to the MIS 5.5 (125 ka). This allowed us to correlate the other orders of terrace with the other positive peaks of the eustatic curve occurred between the MIS 3.3 and the MIS 9.3 (Fig. 16). Terraces of II and VI order cannot be correlated with

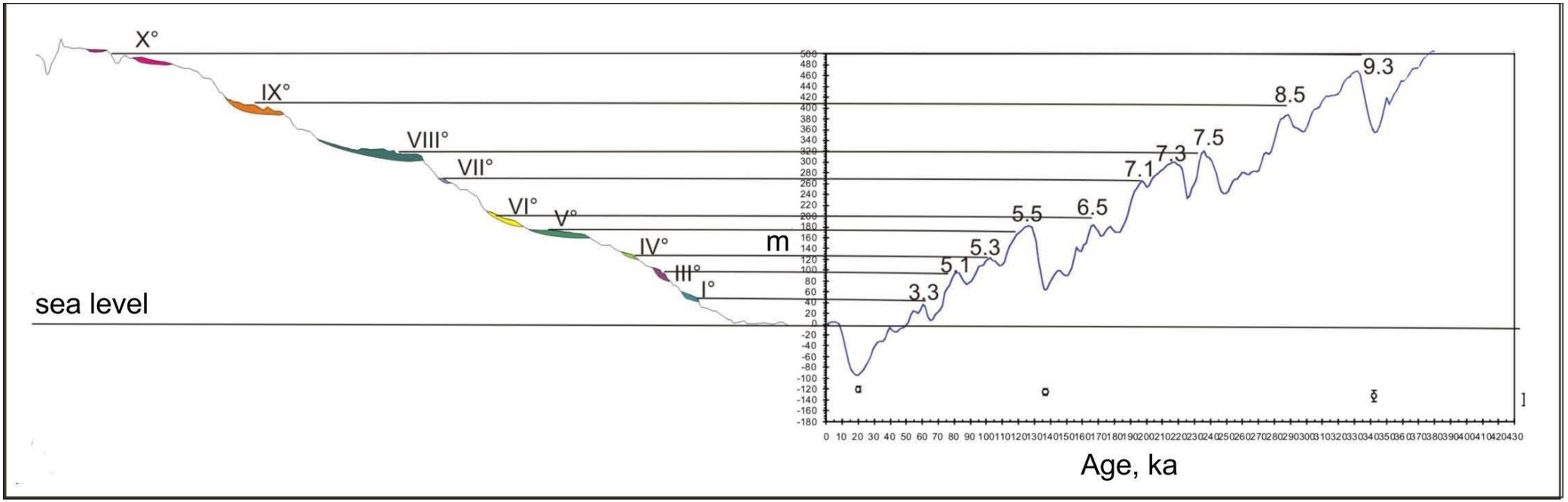

Fig. 16 – Correlation between the altimetric position of the inner edges of marine terraces in the Calabrian side of the Messina Strait (see trace in Fig. 14) and the high stands of the eustatic curve of Waelbroek et al. (2002), modified for uplift rate of 1.4 mm/a.

DOI: 10.3301/GFT.2017.03

positive peaks (see also Dumas & Raffy, 2004) and for this reason they have been tentatively attributed to the MIS 4 (74 ka) and to the MIS 6.5 (167 ka), respectively.
The uplift rates change in time and space and represent the sum of the regional signal, homogeneous in the last 700 ka (Westaway, 1993) and the co-seismic vertical deformation induced by the fault activity around the main Quaternary faults. These two components are added on footwall of the seismogenic faults, while on the hanging wall the co-seismic vertical movements are removed from the regional rate. The estimated uplift rates range from 0.8 mm/a for the period 330-60 ka, on the downthrown block of the Scilla fault, to 2.0 mm/a (twice the regional component of 1.0 mm/a estimated by Westaway (1993) for the period 330-200 ka, on the Campo Piale high. The constant elevation of the I order terrace suggests a uniform uplift rate of 1.4 mm/a along the entire coastal area, and, consequently, a deactivation of the western sector of the Scilla fault in the last 60 ka, even though the offshore activity of segments belonging to the same system is not excluded (see Selli et al., 1979; Ferranti et al., 2008a). However, it is considered still active in its eastern sector (see Stop 1.2), since it is considered responsible of one of the sequence earthquakes on February-March 1783 (Monaco & Tortorici, 2000; Jacques et al., 2001) and of the co-seismic uplifts of the coastal area between Scilla and Palmi area, situated on the footwall of the structure, in the last 5000 years (Ferranti et al., 2007, 2008a). In general, the Calabrian side of the Messina Strait was uplifted more quickly than the Sicilian side, where the elevation of the MIS 5.5 (125 ka) terrace (Bonfiglio & Violanti, 1983) suggests an uplift rate slightly smaller than the regional component.

STOP 1.2: View of the Holocene raised wave-cut platforms along the Scilla coast (38°15’09”N; 15°42’07”E)

Along the Scilla coast two Holocene uplifted shorelines have been identified (Marina di San Gregorio and Punta Paci, see Fig. 12 for location; Antonioli et al., 2004; Ferranti et al., 2007; 2008a). Morphological and sedimentary constraints allow an elevation estimate at ~3.0 m for the upper shoreline at Punta Paci, where a large wave-cut platform outcrops, clearly visible from the national road (Fig. 17). Age constraints for the shoreline range between ~5-3.5 ka. The lower shoreline is characterized by a prominent barnacle band, lying at elevations ranging between ~0.8 and ~1.9 m, and an algal rim bored by *Lithophaga* holes is found at ~1.4 m below the denser patch of the barnacle band. Duration of the lower shoreline is tightly constrained by radiocarbon ages of barnacles between 3.5 and 1.9 ka, and its inception is in good agreement with cessation of the older shoreline (Ferranti et al., 2007; 2008a).

DOI: 10.3301/GFT.2017.03

Fig. 17 - **a)** Uplifted Holocene marine platform at Punta Paci (Scilla, see Fig. 14 for location); **b)** View from the sea of the upper shoreline (red dotted line).

Integration of on-land and offshore geomorphological and structural investigations coupled to mapping and extensive radiometric dating of the raised Holocene beaches reveals that these are located at the footwall of the western segment of the Scilla fault (see Stop 1.1) and that uplift has both steady and abrupt components (Ferranti et al., 2007; 2008a). Radiometric dating of the shorelines indicates that rapid co-seismic displacements occurred at ~1.9 and ~3.5 ka, and possibly at ~5 ka (Fig. 18). Co-seismic displacement shows a consistent site value and pattern of along-strike variation, suggestive of characteristic-type behaviour for the fault. The ~1.5-2.0 m average footwall uplift during co-seismic slips documents Me ~6.9-7.0 earthquakes with ~1.6-1.7 ka recurrence time. The palaeo-seismological record based on the palaeo-shorelines suggests that the last rupture on the Scilla fault on

DOI: 10.3301/GFT.2017.03

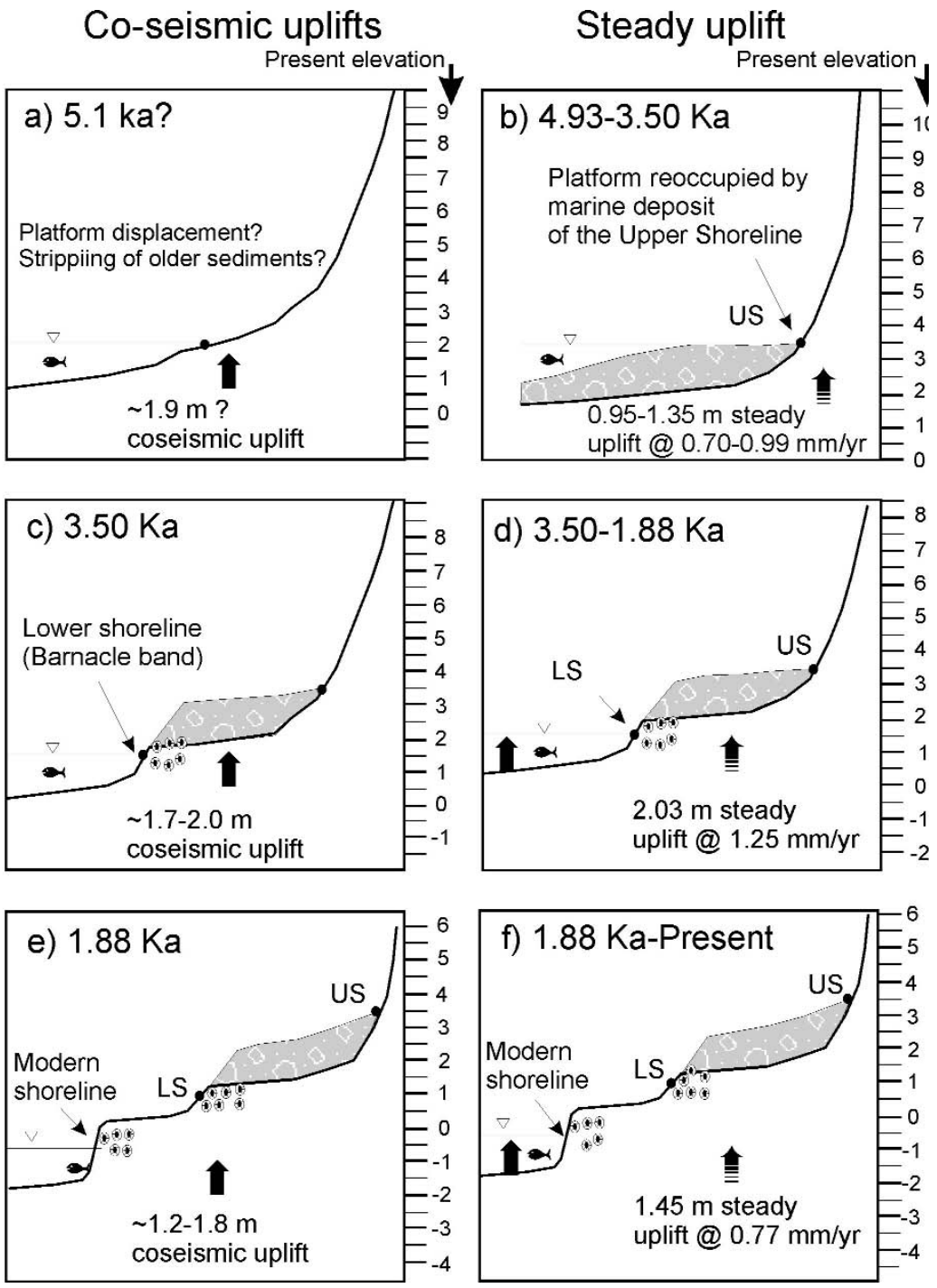

Fig. 18 – Uplift history of the Scilla coast during six distinct episodes of steady and abrupt displacement based on the relations between morphological features of the upper and lower palaeo-shorelines, their elevation above the present sea-level, and the radiometric ages (after Ferranti et al., 2007). **US**, upper shoreline; **LS**, lower shoreline. Elevation in meters (y axis).

February 6th, 1783 Mw = 5.9-6.3 earthquake (Jacques et al., 2001) was at the expected time but it may have not entirely released the loaded stress since the last great event at ~1.9 ka. Precise compensation for sea level changes constrains late Holocene steady uplift during the interseismic intervals at ~1 mm/a, a value consistent with long-term (0.1-1 Ma) estimates of regional uplift (Westaway, 1993). Thus, late Holocene total uplift of ~1.6-2.1 mm/a is nearly equally balanced between regional and co-seismic components.

STOP 1.3: Migmatitic complex of Scilla, Aspromonte unit (38°15'22.28"N; 15°42'50.18"E)

The Scilla promontory consists essentially of high grade metamorphic rocks belonging to the Aspromonte unit, it is separated from the remaining part of the Aspromonte Massif by a normal west-dipping fault oriented N 55°E (dip direction is towards the Tyrrhenian Sea) with an amount of dip of 70°. The prevailing lithotype consists of migmatitic gneiss showing a flebitic-stromatitic texture. It is commonly

DOI: 10.3301/GFT.2017.03

characterized by coarse-medium grainsize and by a layering of biotite-rich and quartz-feldspar-rich levels (Fig. 19a). Fine grained paragneiss with a massive grano-xenoblastic structure is subordinate.

Isoclinal to tight folds show steeply dipping axial surfaces (avg. 70°) with wavelength ranging from cm to m scale. Two main generations of aplite-pegmatite leucogranitic dykes were recognized: dykes of the first generation are from moderately dipping to subvertical, with thickness ranging from 1 to 25 cm; whereas dykes of second generation are usually sub-horizontal with larger thickness (up to 60 cm). They have orientations forming three main clusters: a E-W direction is the dominant one, whereas NE-SW and NW-SE orientations are subordinate (Atzori et al., 1975).

The dark-gray coloured portion (melanosome) is fine grained with an omeoblastic microstructures. The paragenetic minerals of this intensively folded gneiss are biotite, garnet, staurolite, andalusite, muscovite, plagioclase and quartz. Reaction microstructure like staurolite inclusions in andalusite imply the reaction St+Ms+Qtz = Bt+And±Grt+V; sometimes amphibole occurs. Titanite, apatite e iron oxides are accessory minerals. Monazite occurs as inclusions within biotite, muscovite and plagioclase grains. The light-coloured portion (leucosome) is made of quartz and plagioclase magablasts (An_{25-30}) arranged into eterogranular millimetre to centimetre thick layers.

Amphibolite layers from centimetre to metric thickness are often interbedded with two main lithotypes (Fig. 19b). Usually are dark-green coloured rocks characterized by an omeoblastic or eteroblastic structure. Green amphibole, plagioclase and quartz are the main constituent minerals, bitotite and cummingtonite are also present in the mineralogical assemblage. Apatite, zircon, rutile and sporadic garnet represent accessory phases. A network of leucocratic granodioritic dykes and pegmatites often pervasively crosscut the main foliation. Dykes usually have an ipidiomorphic omeogranular structure. Oligoclase, quartz, biotite, sillimanite, and muscovite constitute the most common assemblage. Pegmatites are exceptionally coarse grained with crystals of quartz, K-feldspar and biotite up to a decimetre in length (Fig. 19c, d). The age of this magmatism is 300±4 Ma (Fiannacca et al., 2008).

Atzori et al. (1990) indicated a common metamorphic history for augen gneisses and associated biotitic paragneisses from the north-eastern Peloritani with Rb/Sr ages on micas of 280–292 Ma, interpreted as cooling ages after the Variscan metamorphism. U–Pb monazite ages (Graessner et al., 2000) for similar paragneisses (amphibolite facies) of the Aspromonte Massif indicated a metamorphic peak at 295 to 293 ± 4 Ma (with P–T conditions of 620 °C at ca. 0.25 GPa).

DOI: 10.3301/GFT.2017.03

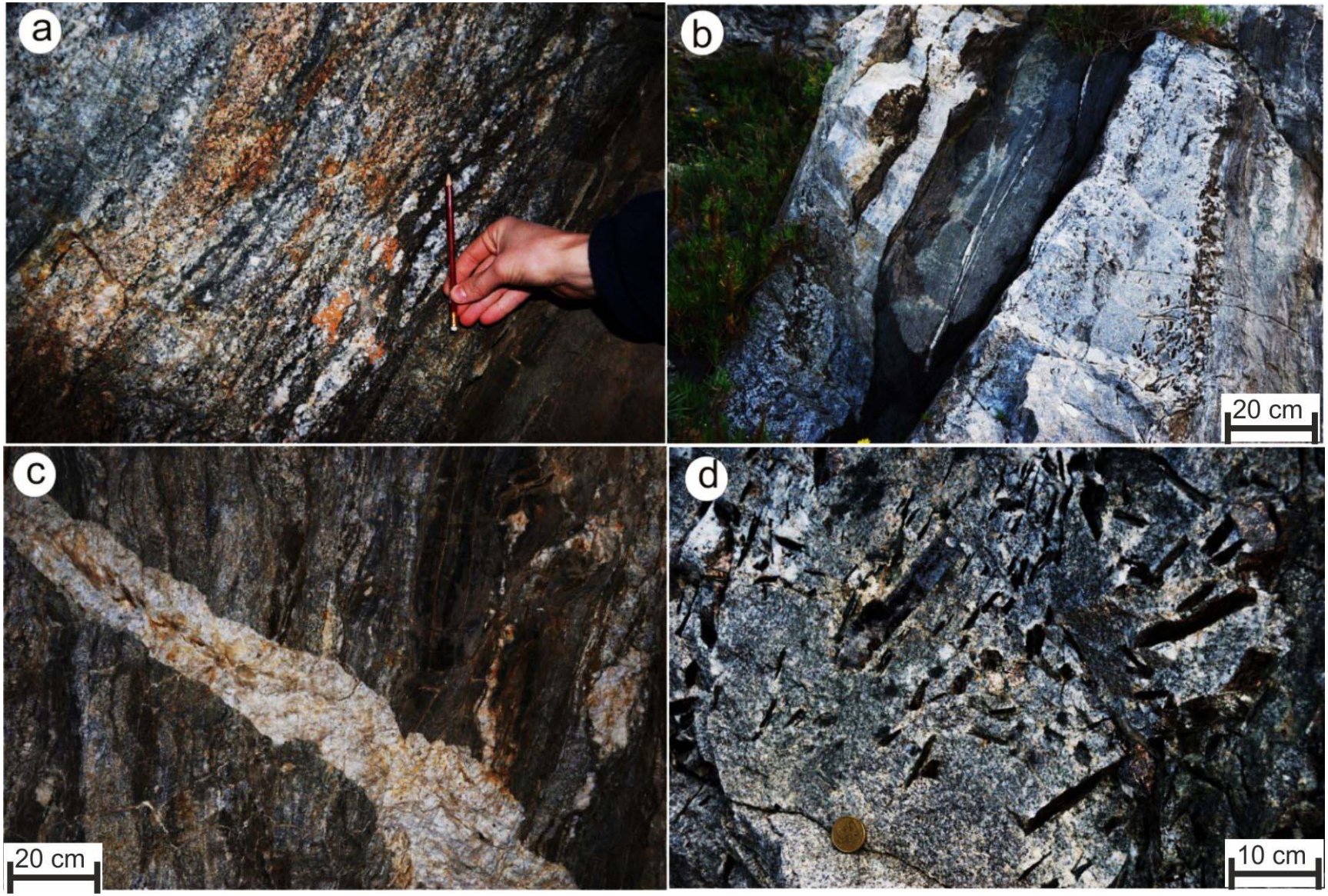

Fig. 19 - **a)** alternance leucosome/melanosome layering in the migmatitic complex of Scilla; **b)** meter sized amphibolite layers interbedded within migmatitic leocosome; **c)** example of a pegmatitic dyke intrusion postdating the migmatitic layering of the host rocks; **d)** biotite megacryst within a pegmatite.

Clockwise P–T–(t) paths inferred for the medium-to high-grade rocks of the Aspromonte Massif and Peloritani Mountains have been considered to be consistent with processes of crustal thickening during early- and middle-Hercynian collisional stages, followed by crustal thinning, granitoid intrusion and unroofing during the late Variscan extension (Festa et al., 2004; Caggianelli et al., 2007).

DOI: 10.3301/GFT.2017.03

STOP 1.4: Mylonitic skarns, tonalite and migmatitic paragneiss of the Palmi area (38°22'50.80"N; 15°51'31.41"E)

The mylonitic rocks of the Palmi shear zone crop out along the Southern Tyrrhenian coast of Calabria at the northern margin of the Aspromonte Massif, in a transitional zone with respect to the Serre Massif (Fig. 4). It is characterized by a tabular structure with predominantly sub-vertical foliation (Fig. 20a). The shear zone involves essentially skarns and to a lesser extent migmatitic paragneiss and tonalite. Most of the deformation is accommodated by skarns which act as a weakening layer between the more competent domains of the foliated tonalites and of the migmatititic paragneisses (Figs 4, 20a).

Migmatitic paragneisses cropping out northward with respect to the mylonitic shear zone show a layering due to migmatitization processes averagely dipping toward SE with a dip ranging from 20° to 45° (Fig. 21a, b). Tonalitic gneisses ascribable to the former stages of late Variscan plutonic magmatism show textures variable from relatively massive to well foliated, with average attitude dipping toward SE.

Structural analysis of mylonitic rocks highlighted as the average attitude of the subvertical foliation as well as the stretching lineation ranges from W-E, to NW-SE suggesting an anostomosing character of the shear zone (Fig. 20b). The mylonitic foliation involves particularly the carbonaceous matrix of the skarn reaching the plastic rheological behaviour before tonalities and paragneiss that often act as undeformed rigid blocks within mylonitized carbonaceous matrix.

Nevertheless, the whole rock rheology resulted strongly influenced by the different relative abundance of the rock-types involved throughout the extension of the shear zone that controlled in turn the deformational behaviour and then the final mylonitic structural features. The trend of the mylonitic foliation in the skarns, for instance, resulted strongly perturbed by the presence of the widespread rigid metamorphic and plutonic inclusions, passively rotated within the deformational flow within the mylonitized skarns (Fig. 22a, b). By contrast, the increase of migmatitic paragneiss and of tonalite involved in the mylonitic process, observed in the middle part of the outcropping shear zone, strongly influenced the rheological behaviour of the strain partioning, producing widespread inclusions characterized by the developement of a pervasive mylonitic foliation (Fig. 22c, d).

The occurrence of isoclinal fold sections with axis often parallel to the local stretching lineation, subordinately rotating to a quasi-vertical plunge (Figs 20b; 22e; 23), highlights the formation of sheath-folds, confirmed by the presence of cat eye sections (Fig. 22f) accompanied by local evidence of highly curvilinear fold hinges (Fig. 23). Sheath folds formation indicates that as the PSZ was characterized by a unique shearing event, probably already

DOI: 10.3301/GFT.2017.03

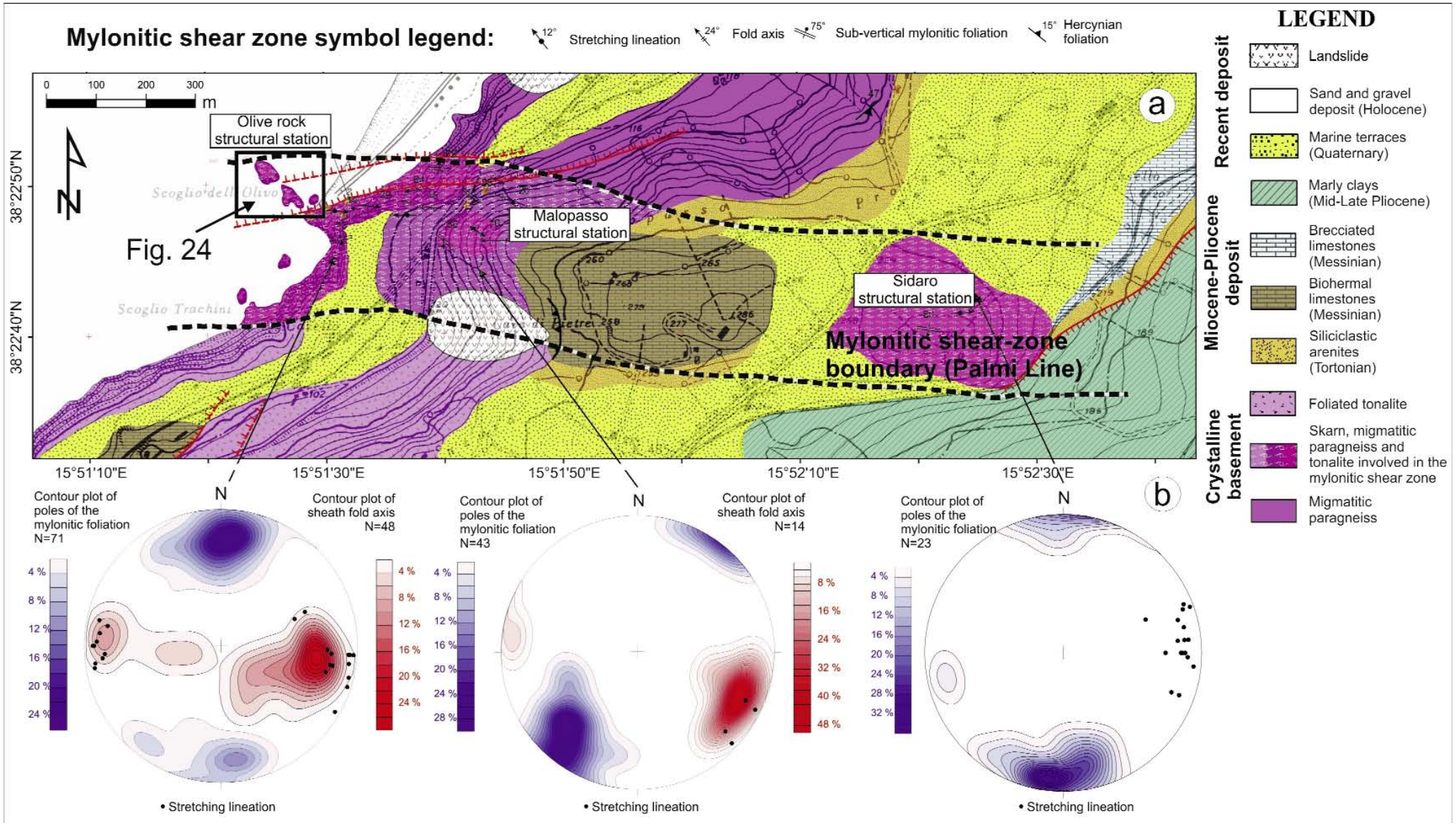

Fig. 20 - **a)** Geological map of the Palmi shear zone; **b)** Contour plot of the mylonitic structural features (Schmidt net, lower hemisphere): blue contouring – poles of the mylonitic foliation, red contouring – sheath fold axes, black circles –mylonitic stretching lineation (modified after Ortolano et al., 2013).

DOI: 10.3301/GFT.2017.03

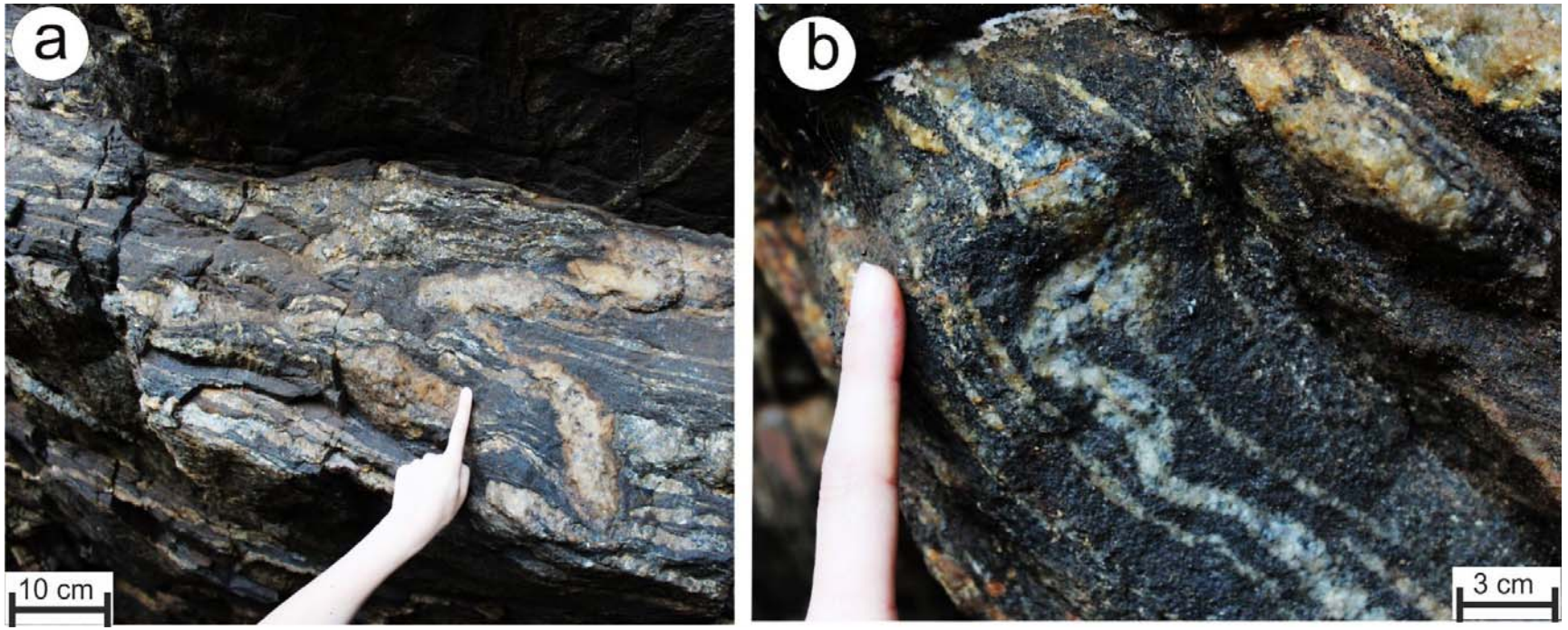

Fig. 21 - **a)** Alternance of leucosome/melanosome depicting the layering of the migmatitic complex of the Pietre Nere area (Palmi RC); **b)** particular of migmatitic leucosome with ptygmatic folds.

active during the former stage of the deep-seated Alpine tectonics of this area (i.e. Cretaceous-Paleocene boundary) and still active up to 56 to 51 Ma ago as constrained by the Rb-Sr age obtained from whole mica analysis of mylonitic tonalite (Prosser et al., 2003), which can be interpreted as a minimum age constraint.

Microstructural investigations, also highlight that the mylonitic skarns are characterized by a dominant calcite, K-feldspar, quartz assemblage, subordinately accompanied by the presence of humite, olivine, clinopiroxene, scapolite, clinozoisite, amphibole and talc. This last assemblage can be considered the result of the metasomatic exchange activity between Variscan impure marbles with the fluid released by the emplacement of the late-Variscan tonalite magma. Within the mylonitic skarns are indeed observable, also in thin sections, widespread clasts of felsic olocystalline rocks with isotropic texture principally constituted by plagioclase, clinopiroxene, K-feldspar and olivine, which can be interpreted as a high temperature relic assemblage linked with the well-known quasi-static late Variscan thermal increase (Prosser et al., 2003). These inclusions are spared by the mylonitic deformation, almost totally accommodated by calcite that controls the whole rock rheology of this sector of the outcropping shear zone.

Mylonitic paragneiss as well as mylonitic tonalite are differently controlled by quartz dominated rock rheology as

DOI: 10.3301/GFT.2017.03

evidenced by the formation of dynamically recrystallized quartz-rich layers surrounding widespread plagioclase and k-feldspar porphyroclasts. Quartz-rich layer microstructural observations highlighted the presence of dominant sub-grain rotation re-crystallization (SR), subordinately accompanied by grain boundary migration (GBM), consistently with a relatively intermediate temperature during shearing.

Analysis of the widespread kinematic indicators such as δ-type porphyroclasts of plagioclase, K-feldspar and tonalite fragments, mica fish, book shelf sliding structures and shear bands, testify to a top-to-E, SE sense of shear in the present-day geographic coordinates.

Microstructural investigations have been integrated by the study of the quartz c-axis pattern, aiming to obtain constraints on both the kinematics and the temperature operating during shearing deformation (see Cirrincione et al., 2009 and reference therein for further details on the applied procedure).

Inferred quartz c-axis patterns, carried out on 14 quartz-rich domains of two migmatitic-paragneiss and one tonalitic-gneiss samples involved in the mylonitic process, show the main activation of two different slip systems: the

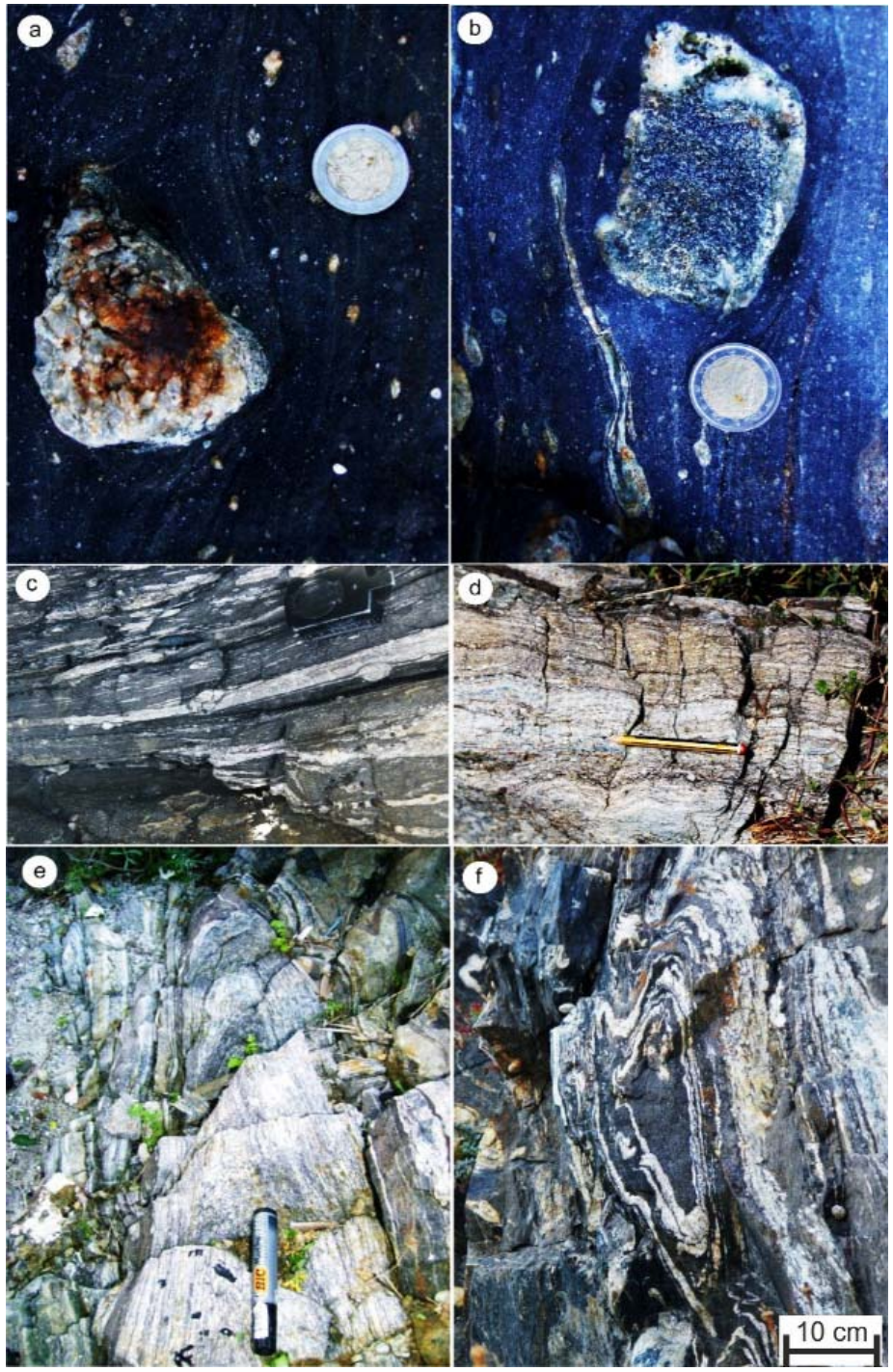

Fig. 22 **a)**, **b)** Example of low strained tonalite porphyroclasts within microcrystalline calcite of mylonitic skarns (Olive rock area); **c)** alternance of mylonitic tonalite layers with feldspar porphyroclasts and mylonitic skarns (Olive rock area); **d)** mylonitic tonalite (Sidaro area); **e)** oblique fold with axis parallel to the E-W stretching lineation (Olive rock area); **f)** cat eye section of sheath fold (Malopasso area), see Fig. 20a for photo area location.

DOI: 10.3301/GFT.2017.03

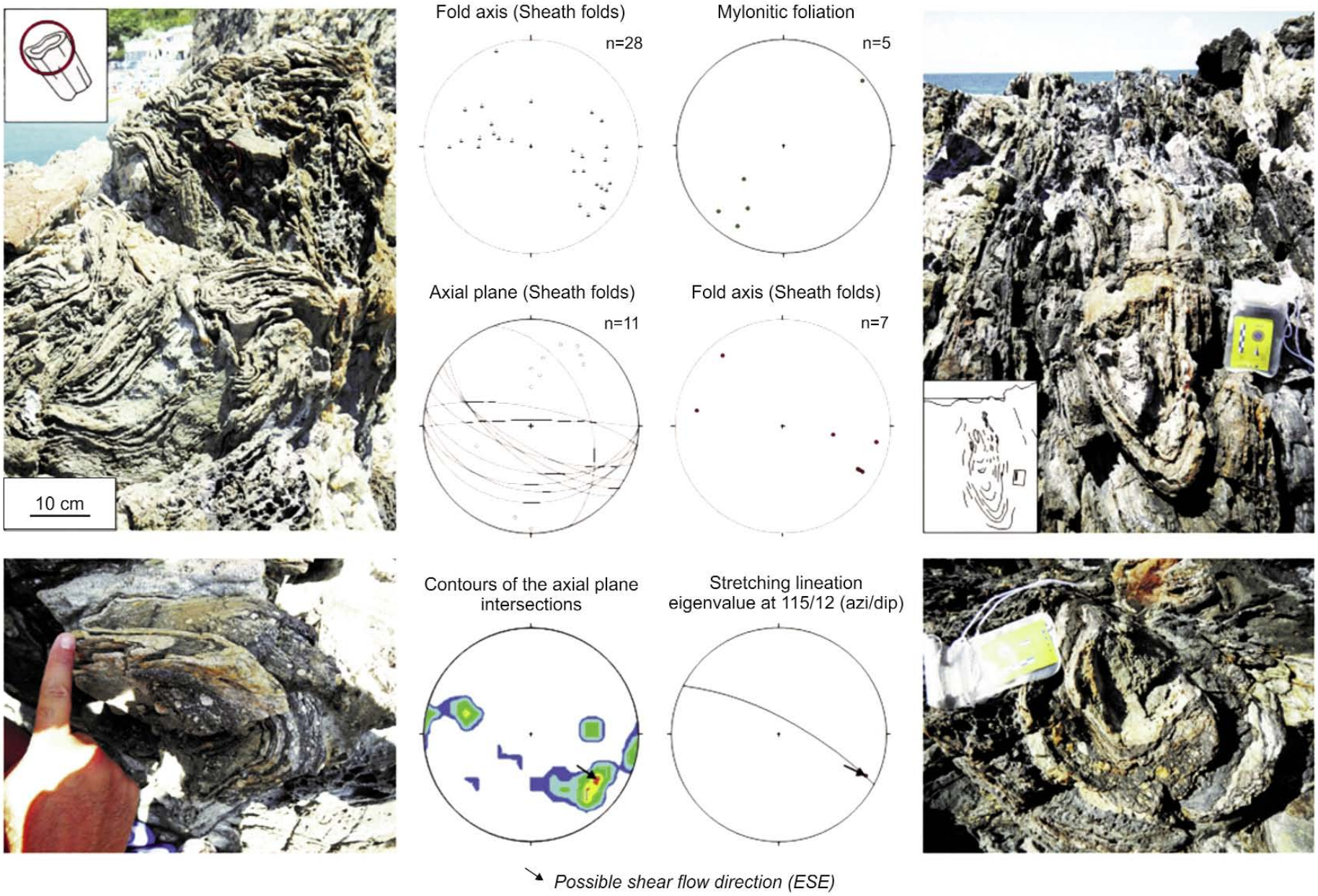

Fig. 23 - Various examples of sheath folds are clearly exposed at this site (four pictures). Curvilinear hinge folding patterns are extremely diffuse throughout the outcrop. A possible shear flow direction has been inferred from sheath fold geometries by means of axial plane intersections method (see stereoplots- lower hemisphere – Schmidt projection), which is also consistent with clustering of stretching lineation, pointing towards a ESE direction (see Fig. 20a for photo area location).

DOI: 10.3301/GFT.2017.03

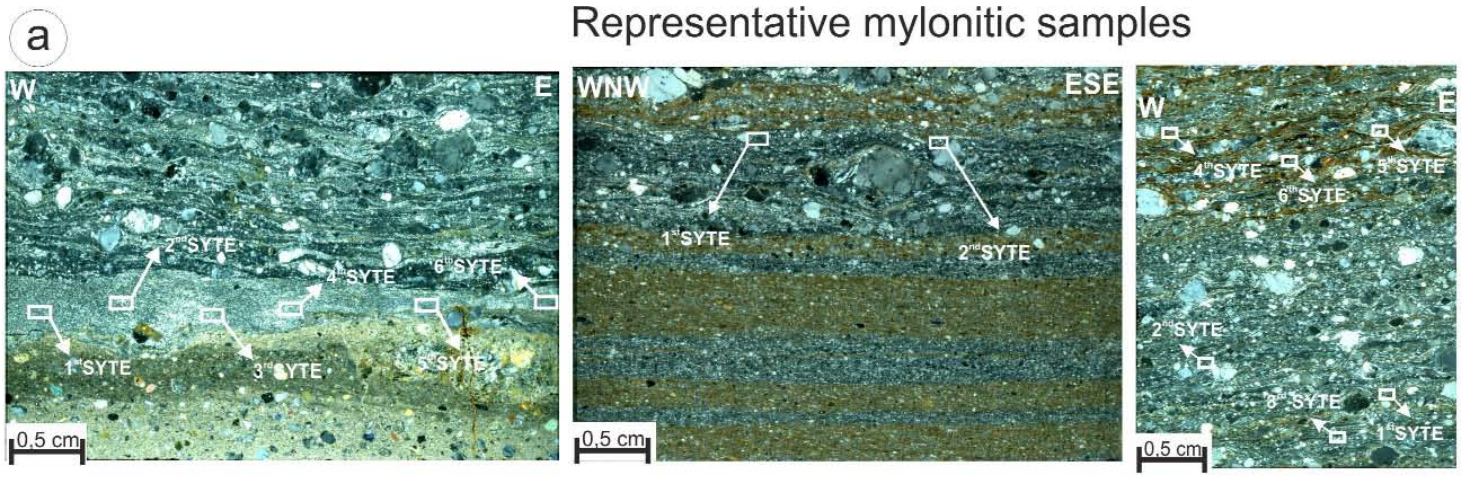

Fig. 24 - **a)** Selection of mylonitic rock samples (high resolution thin section scans - from the left: alternance of mylonitic skarn level and mylonitic tonalite layers, mylonitic paragneiss, mylonitic tonalite) with location of the quartz-rich domains used for the quartz c-axis patterns investigation; **b)** representative quartz c-axis pattern elaboration; **c)** synthesis of quartz c-axis pattern analytical results (modified after Ortolano et al., 2013).

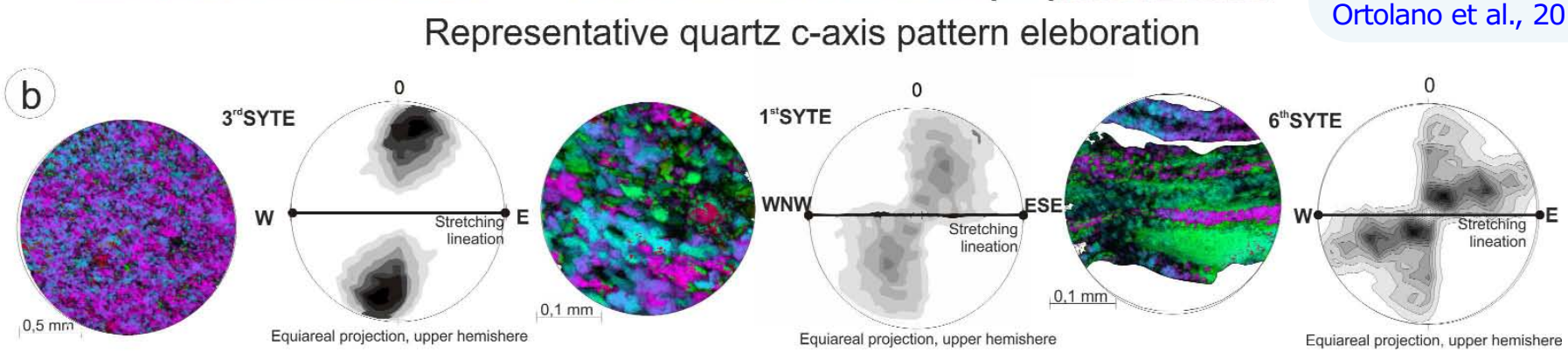

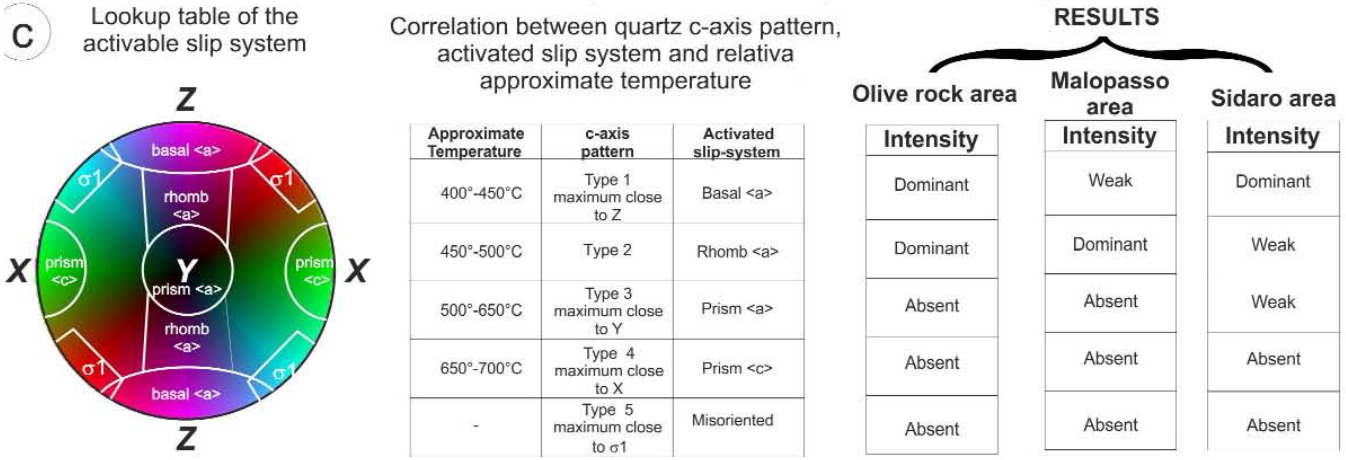

Approximate Temperature	c-axis pattern	Activated slip-system	Olive rock area Intensity	Malopasso area Intensity	Sidaro area Intensity
400°-450°C	Type 1 maximum close to Z	Basal <a>	Dominant	Weak	Dominant
450°-500°C	Type 2	Rhomb <a>	Dominant	Dominant	Weak
500°-650°C	Type 3 maximum close to Y	Prism <a>	Absent	Absent	Weak
650°-700°C	Type 4 maximum close to X	Prism <c>	Absent	Absent	Absent
-	Type 5 maximum close to σ1	Misoriented	Absent	Absent	Absent

rhomb <a> and basal <a>, consistent with a unique deformational event developed in greenschist facies conditions between 400° and 500°C (Fig. 24). The contour plots further shows a relatively marked internal asymmetry with respect to the stretching lineation, confirming the top-to-E-SE sense of shear in the present-day geographic coordinates (Fig. 24b, c).

DOI: 10.3301/GFT.2017.03

STOP 1.5: View of the Armo fault (38°03'12''N; 15°40'47''E)

The 18 km-long on-land section of the SSW-NNE striking (average N30°E) Armo fault separates the south-eastern margin of the Pleistocene Reggio Calabria basin (Ghisetti, 1984) from the upraised basement rocks of the Aspromonte Range (Figs 13, 25). In this Stop, a panoramic view of the ~ 300 m high Quaternary linear scarp is visible (Fig. 26a). The Armo fault was active during lower Pleistocene as testified by syn-sedimentary relationships (Ghisetti, 1984; Barrier, 1987), but large displacements occur since Middle Pleistocene (Barrier, 1987; Monaco et al., 1996a; b). To the south, a NNW-SSE striking splay (Motta San Giovanni fault - MSGF; Figs 13, 25) branches from the major fault.

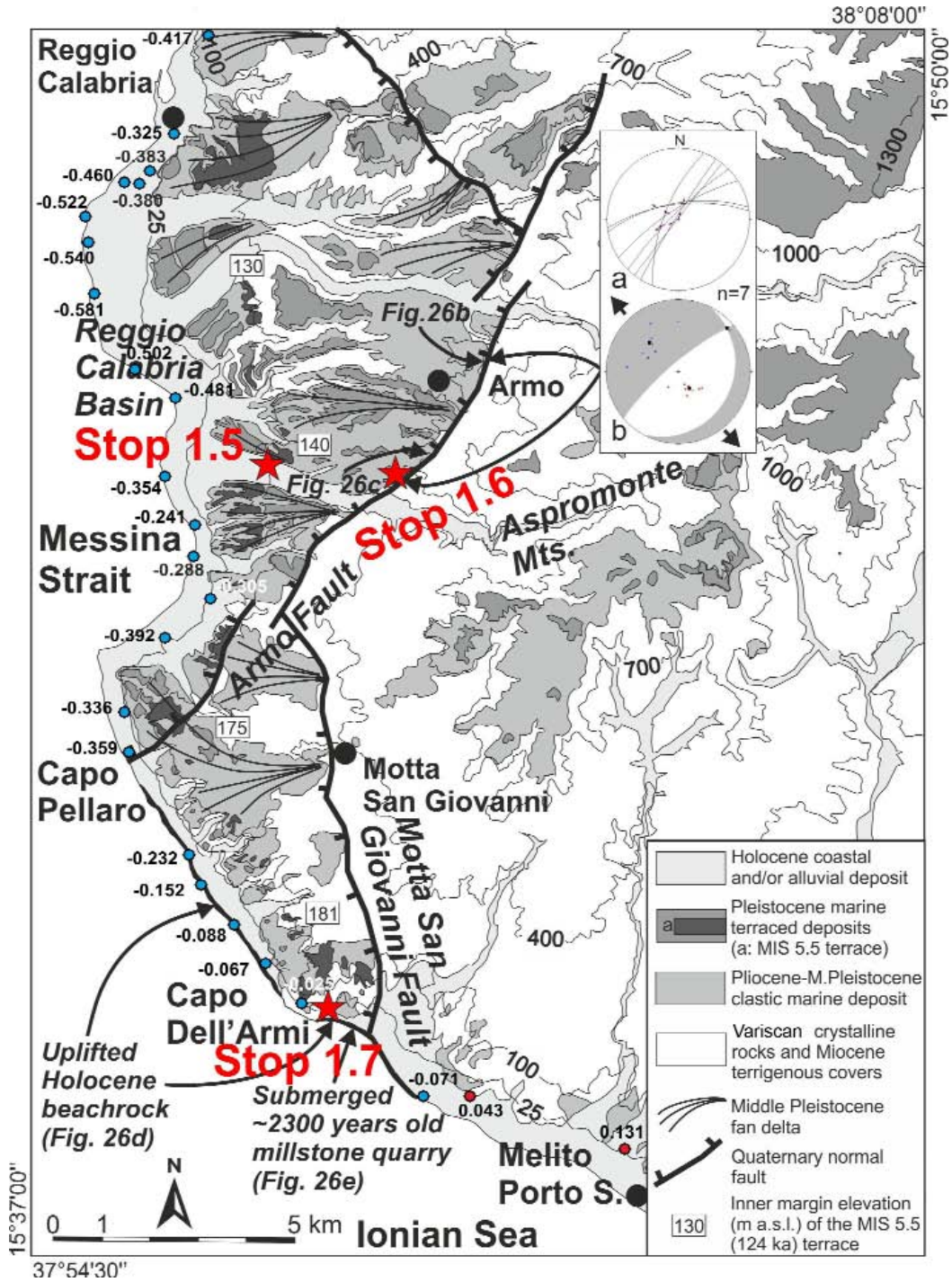

Fig. 25 - Morphotectonic map of the southeastern sector of the Messina Strait (Calabrian side, see Fig. 13 for location). The spatial distribution of elevation changes recorded by Loperfido (1909) are shown (blue for lowering and red circles for uplift). Lower hemisphere Schmidt diagrams in the inset show: **(a)** projections of Armo fault kinematic data. Arrows on fault planes indicate motion of the hanging wall block. **(b)** Composite pseudo-fault plane solutions (FPS) computed from fault-kinematic data using software Faultkin v.1.2 (Marrett & Allmendinger, 1990), available at ftp://www.geo.cornell.edu/pub/rwa/FaultKin/.Filled squares in stereo diagrams are calculated kinematic axes. Black arrows show the horizontal projection of the extensional axis. Location of Stops 1.5, 1.6 and 1.7 is indicated.

DOI: 10.3301/GFT.2017.03

STOP 1.6: Contact between the Pleistocene deposits and the Palaeozoic crystalline basement along the Armo fault (38°03'08"N; 15°42'23"E)

In the central part of the Armo fault near the Armo and Oliveto villages (Fig. 25), we can observe the fault contact between the Lower Pleistocene deposits and the Palaeozoic crystalline basement and collect fault planes and slip lineations data useful to perform kinematic analyses (Aloisi et al., 2012; Figs 25, 26b). In this Stop, near the village of Oliveto, it is possible to observe the nearshore deposits of the margins of the Upper Pliocene-Lower Pleistocene Reggio Calabria Basin (Fig. 25), onlapping the major border fault scarp (Fig. 26c). Next to the fault plane, several lens-shaped gravel beds and slumps containing blocks of basement rocks are frequently embedded within marine deposits that are, in turn, deformed by small normal faults and cataclastic bands, thus suggesting a synsedimentary activity of the Armo fault.

We note that the azimuth of the computed extension axis (Fig. 25; Aloisi et al., 2012) is in good agreement with the GPS-estimated tensile axis for the Messina Strait area (D'Agostino & Selvaggi, 2004; Mattia et al., 2008; Serpelloni et al., 2010), with the extension axis determined from structural analysis on the Scilla fault (Ferranti et al., 2008a), and with the tensile axis of crustal earthquakes in the hanging-wall of the Armo and Reggio Calabria faults (Scarfì et al., 2009).

Although fault-slip analysis in the bedrock yields parameters for the average Quaternary history of the fault or for an unknown time interval of it, activity in more recent times is documented by the deformation of the MIS 5.5 (125 ka BP) marine terrace (Aloisi et al., 2012).

The outcropping crystalline rocks consist of muscovite- and biotite-bearing micaschists and subordinate paragneisses with sporadic lenses of amphibole-bearing schists, belonging to the Stilo unit. The attitude of the main Variscan foliation is 333/32 (dip direction/dip). Relics of isoclinal to asymmetrical fold hinges with centimetre-scale wavelength are diffuse. At places a crenulation cleavage of the main foliation is developed and a crenulation lineation is visible. Approaching the damage zone of the main fault plane a progressively intense cataclastic overprint causing highly fracturing of basement rocks widely occurs.

DOI: 10.3301/GFT.2017.03

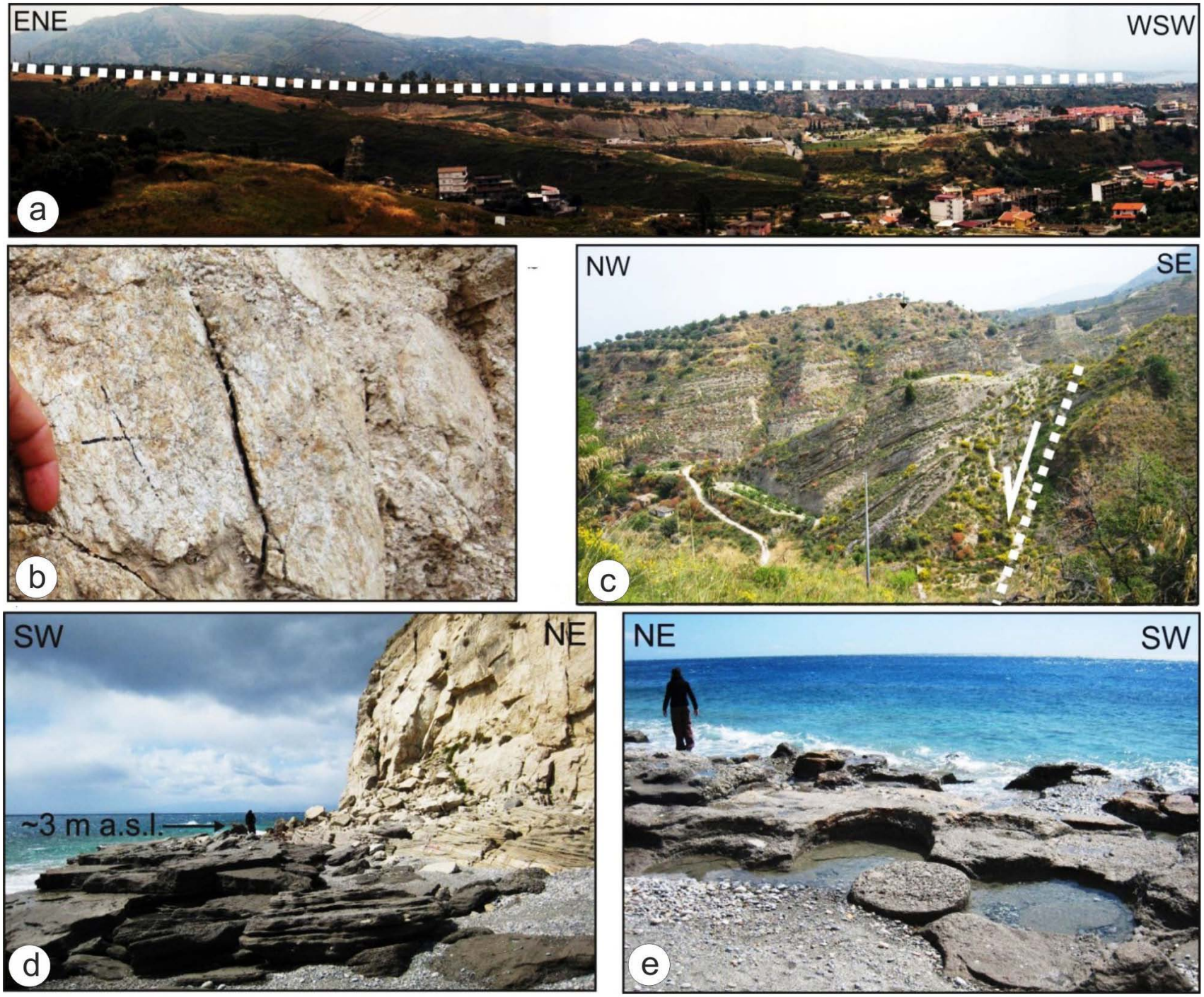

Fig. 26 –
a) Panoramic view of the southern sector of the Armo fault.
b) Slickenlines on crystalline rocks along the shear zone of the Armo fault (see Fig. 25 for location and for data inversion).
c) Upper Pliocene-Lower Pleistocene nearshore deposits deformed by the Armo fault near Oliveto.
d) Uplifted beachrock at Capo dell'Armi (see Fig. 25 for location).
e) Partially submerged Hellenistic millstone quarry at Capo dell'Armi (see Fig. 25 for location).

DOI: 10.3301/GFT.2017.03

STOP 1.7: Holocene raised beachrock near Capo dell'Armi (37°57'06''N; 15°41'11''E)

Shorter-term activity of the Armo fault is suggested by uplifted Holocene coastal deposits outcropping in its footwall along the coast from Capo Pellaro to Melito di Porto Salvo, with a ~10 km linear extension (Fig. 25). Along this coastal stretch, a well preserved beachrock (see also Pirazzoli et al., 1997) is raised up to 3.0 m (Fig. 26d), and was dated by AMS radiocarbon analysis on a shell of *Hinia* sp. at ~5 ka BP (Scicchitano et al., 2011a; 2011b). Correction for the sea-level rise occurring since 5 ka yields an uplift rate of 1.2 mm/a, a value comparable to the long-term footwall uplift rate, and interpreted here as indicating ongoing late Holocene fault activity.
Millstone for oil are also visible at Capo dell'Armi in a partially submerged quarry carved into the beachrock body at elevations of between 0.2 m b.s.l. up to 1 m (Scicchitano et al., 2011a; b; Fig. 26e). Several millstones were never finished or extracted. They are elliptical or sub-circular with the major axis ranging in size between 1.10 m and 1.30 meters. The extraction cuts are up to 0.25 m deep and 0.10 m large. Outcropping millstones are well preserved, whereas the submerged ones are strongly eroded although their shape and dimensions can still be readily measured. The lowest elevation of the base of the extraction cut is located at a depth of -0.2 m below the sea level.
The contrasting indication on vertical motion obtained by geological and archaeological markers at Capo dell'Armi could be explained by an uplift scenario characterized by a cyclical occurrence of co-seismic events related to the activity of the Armo fault. The MIS 5.5 terrace and the 5000 a old beachrock have been probably affected by regional uplifting and fault-related footwall deformation. Taking into account a possible Hellenistic age of the millstone quarry (Scicchitano et al., 2011a; b) and its location at the hangingwall of Motta San Giovanni fault (Fig. 25), the present position of the quarry below the sea level could be explained by local subsidence related to the activity of this splay of the Armo fault (Aloisi et al., 2012). As a matter of fact, displacement related to the1908 earthquake caused a coseismic down-warping of the Capo dell'Armi area of about 10 cm which was documented by the leveling survey of Loperfido (1909).

DOI: 10.3301/GFT.2017.03

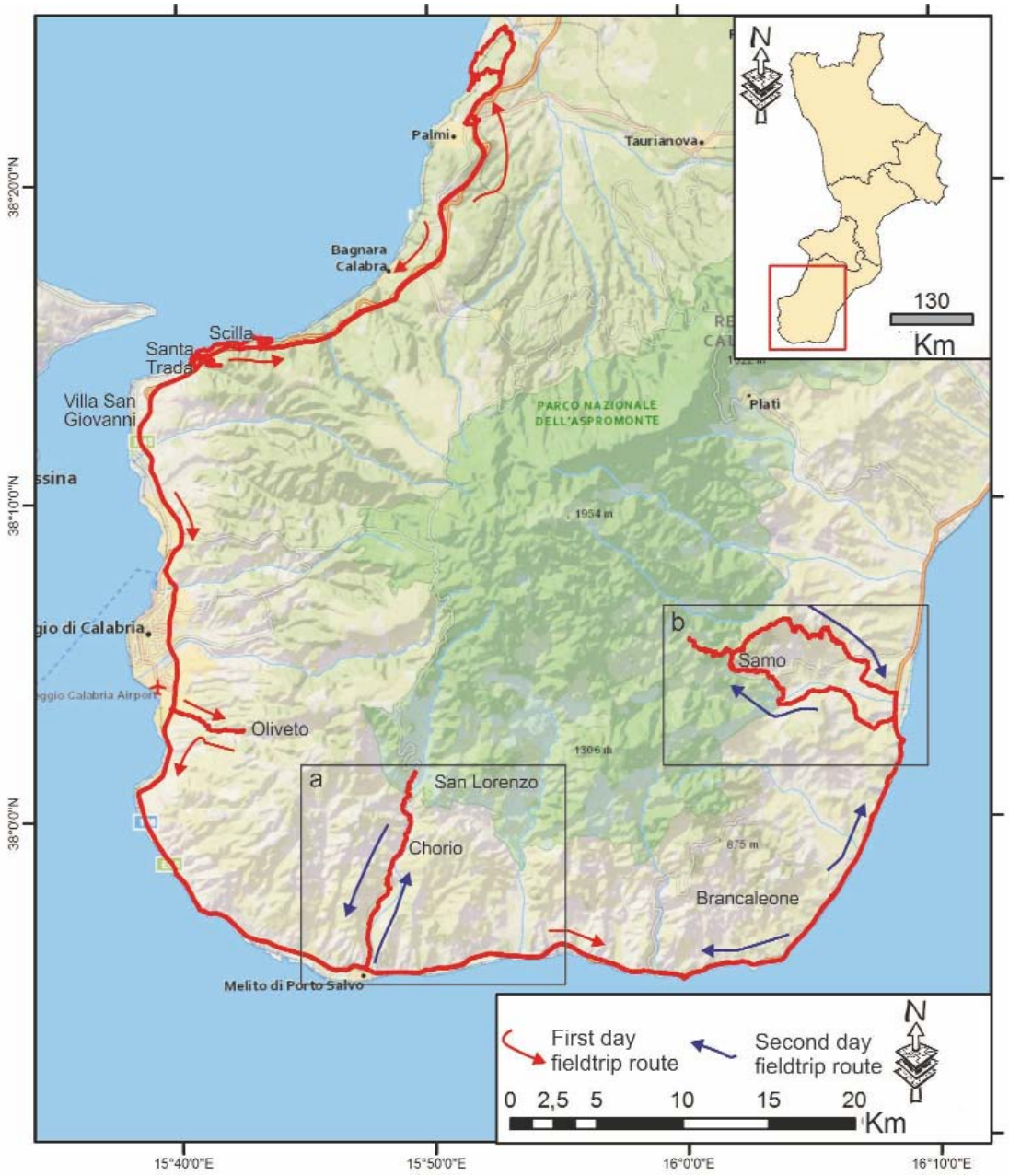

Fieldtrip route sub-areas of the second day. Specific location of the 2.1 and 2.2 Stops in **a)** and **b)** respectively.

DAY 2

The second day's excursion addresses the issue of metamorphic basement rocks cropping out in the southeastern Calabria. The planned stops are focused on the crystalline basement nappe edifice of the Aspromonte Massif.

DOI: 10.3301/GFT.2017.03

STOP 2.1: Tectono-stratigraphy of the Aspromonte Massif nappe edifice (38°05'26.54"N; 16°00'24.59"E)

Arrived to Bianco, it is necessary turn to Samo. After passing the village turn towards Portella D'Orgaro, then follow the indications for the Zillastro spring.
In this Stop it is possible to observe in a relatively small area the entire tectono-stratigraphy of the Aspromonte Massif nappe edifice as evidenced in the detailed geological map of Fig. 27.

Stop 2.1a: Klippe of the Stilo unit phyllite (38°5'26.96"N; 16°00'24.23"E)

In particular along the main road approaching the Stop 2.1 it is possible to recognize the occurrence of a Stilo unit klippe of phyllites, sandwiched at the top by the transgression of the SCOF (Stilo-Capo d'Orlando formation) arenites and, at the bottom by a huge cataclastic horizon separating the SU phyllites from the AU mylonitic paragneisses (Fig. 28).

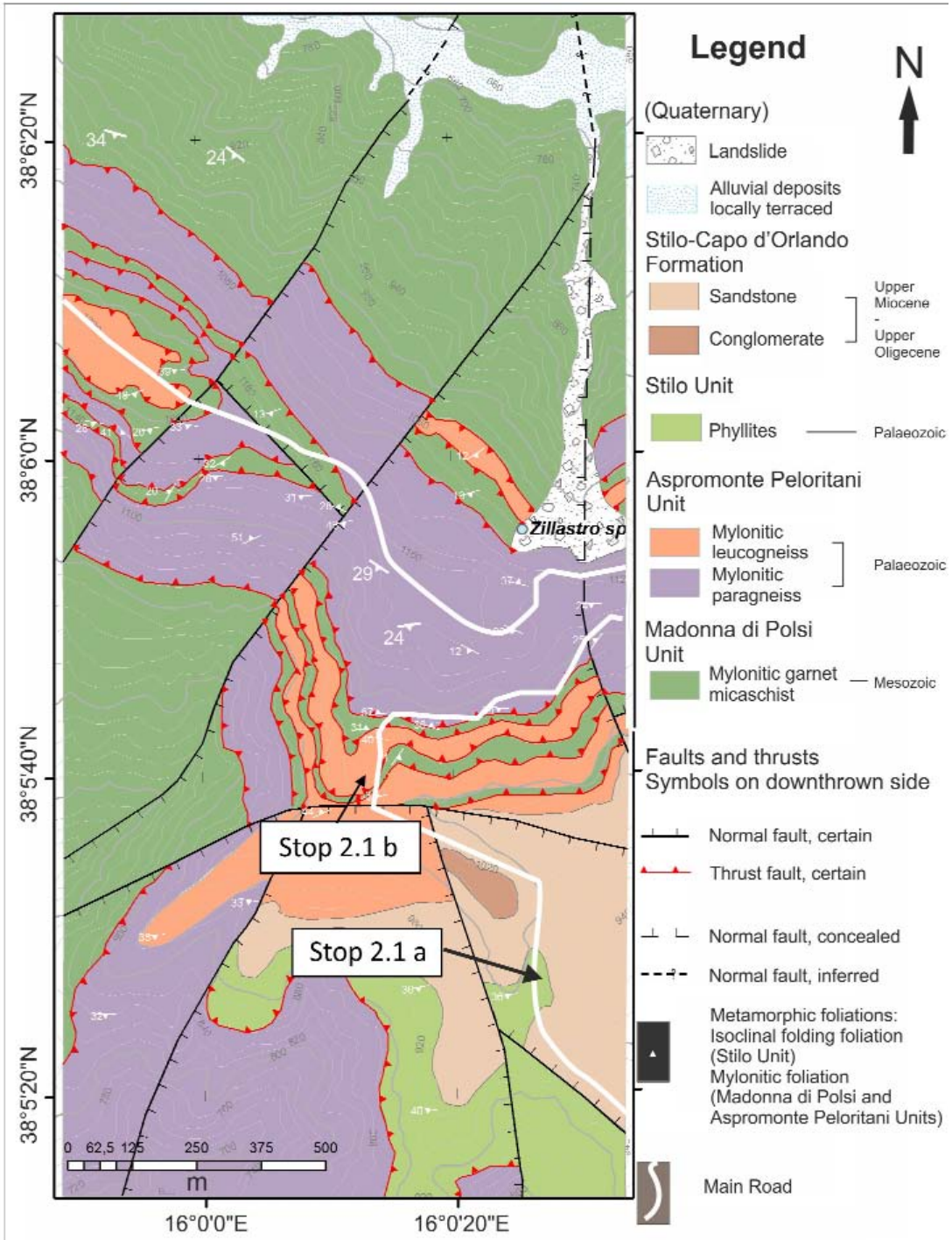

Fig. 27 - Geological map of the Zillastro zone with location of the stop areas (see Fig. 1 for location within the Aspromonte Massif).

DOI: 10.3301/GFT.2017.03

Fig. 28 – Phyllite of the Stilo unit partially covered, in non-conformity, by arenaceous layers of the Stilo-Capo d'Orlando formation (SCOF) with widespread presence of quartz-rich isoclinal folds depicting the main Variscan foliation surface.

Stop 2.1b: Alternance of mylonitic para- and ortho-gneisses of the Aspromonte unit (38°05'39.81"N; 16°00'14.63"E)

At this Stop, it is possible to observe an impressive alternance of leucocratic gneiss, augen gneiss and paragneiss of the AU involved at various extent in a late Alpine mylonitic process (Fig. 29a, b).

Outcropping rocks are highly foliated ultramylonites, mylonites, and cataclasites showing a monotone attitude of the mylonitic foliation (averaging oriented 265° with a dip of 50° towards N). Effects of strain softening are clearly

DOI: 10.3301/GFT.2017.03

recognizable at the outcrop scale, responsible for the development of very narrow shear zones. In most parts of the outcrop a constant alternation from proto- to ultra-mylonite due to the repetition by folding of the mylonitic horizon is shown.

In this area indeed, previously developed metamorphic structures of Variscan (in the AU) and early-Alpine ages (in the MPU) (schematically depicted in Fig. 6), were nearly totally obliterated by the Oligocene-Miocene retrograde mylonitic event, consistent with a deep-seated exhumation of these two basement units in a compressive regime (Ortolano et al., 2005; 2015; Pezzino et al., 2008). At this time, a pronounced mylonitic schistosity is produced (Fig. 29c, d). These surfaces averagely strike ENE-WSW with a variable dip direction spanning from 15° to 85°. Simultaneously, a pervasive stretching lineation predominantly oriented SW-NE is

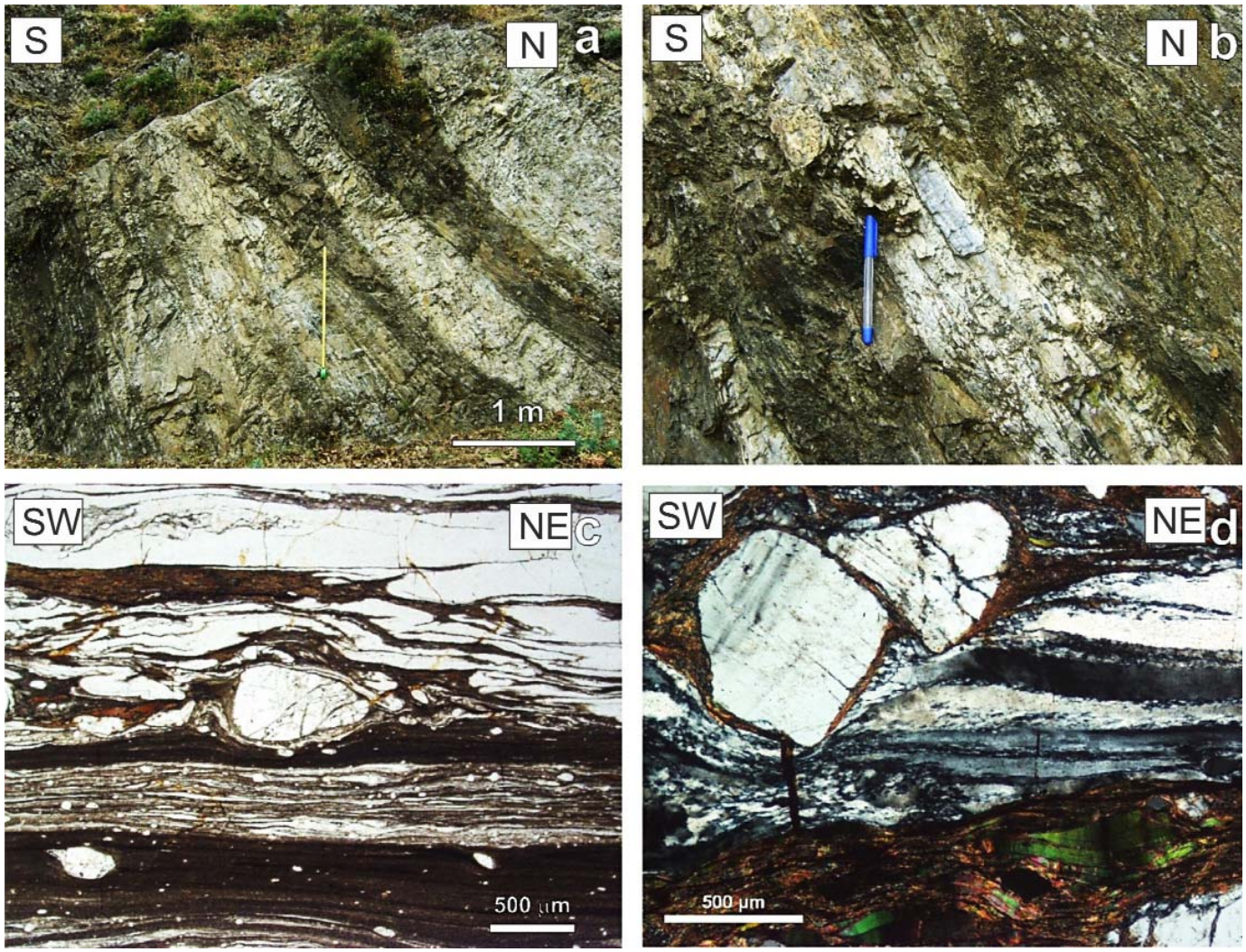

Fig. 29 - **a)** Outcrop view: leucocratic ortogneisses and paragneisses); **b)** detail of the contact between different lithologies where narrow shear zones preferentially developed; **c - d)** microphotos of APU mylonites showing K-feldspar porphyroclasts, ribbon-like quartz, mica fish, and an ultramylonite band parallel to the mylonitic foliation (crossed polars). Sense of shear is top to the NE.

DOI: 10.3301/GFT.2017.03

formed, whose kinematic indicators provide a top-to-NE sense of shear in the current geographic coordinates. Syn- to late- mylonitic folding stage produces very tight folds with the development of a new axial plane foliation accompanied by the generation of an intersection lineation almost perpendicularly oriented to the stretching one. These tight folds can be interpreted as flow perturbation folds locally evolving to sheath folds as evidenced by the observed curvilinear hinge folding patterns ascribable to a fold propagation evolution in a context characterized by the formation of a non-coaxial mylonitic evolution.
Late tectonic phases (Alpine and Apennine) partially displace early structures and it is possible to observe good examples of brittle deformation overprinting earlier ductile fabric.
This repetition brings to the folding of the original mylonitic foliation originally developed during the Oligocene - Miocene tectonic emplacement of the AU upon MPU rocks. This is well evidenced in the area by the repetition of the contact between these last units, which together constitute the two lowermost tectonic slices of the outcropping Aspromonte Massif nappe edifice (Fig. 27).
Finally, during the last part of their exhumation a switch from a ductile behavior, characterized by m-scale SSE-NNW verging asymmetric folds, to a brittle one consisting of NE-SW low angle brittle joints took place (examples are visible on Fig. 7). The final record of the tectonic history is the activation of normal fault systems indicating the beginning of the extensional regime.

The main assemblage of mylonitic rocks outcropping at the Stop 2.1 is given by quartz, plagioclase, K-feldspar, white mica, and biotite sometimes retrogressed into chlorite. Tourmaline, iron-oxides, and garnet are quite sporadic. Microstructural features are typical of sub-simple shear developed under ductile deformation with kinematic indicators (e.g. mica fish) suggesting a top to the NE sense of shear (Fig. 29c, d). Well-preserved eye-type folds (oblique- and sheath-type folds), have also been recognized at the micro-scale. Quartz occurs as ribbons, sometimes showing micro-folds with axial planes sub-parallel to the mylonitic foliation. Quartz subgrains often form an oblique foliation, indicating a dominant subgrain rotation recrystallization (SGR). Bulging (BLG) recrystallization is suggested by smaller quartz grains at the edges of larger sigmoid-shaped quartz grains, which sometimes show effects of intra-crystalline plasticity (chessboard pattern extinction). Mylonitic foliation is widely truncated by a pervasive network of veins. Feldspars, usually forming elliptical smoothed porphyroclasts, testify an intense reworking during shearing. Fragmented augens of K-feldspar show domino-type micro-textures (e.g. book-shelf sliding) with micro-cracks filled by chlorite and sericite. Both biotite cleavage parallel to 001, and albite twins in plagioclase show intense intracrystalline deformation and lattice bending.

DOI: 10.3301/GFT.2017.03

A network of post-shear discordant veins filled by quartz and feldspar crosscut at high angle the mylonitic foliation. Late-fractures showing micron-sized dislocations affecting mylonitic foliation are common.

STOP 2.2: Relics of late Variscan mylonitic structures in the Stilo unit (38°01'30.43"N; 15°49'7.08"E)

Arrived to Melito di Porto Salvo turns toward Bagaladi along the connecting road with Gambarie d'Aspromonte. At this Stop the classical appearance of phyllites, schists and paragneisses belonging to the Stilo unit can be observed. All of these different lithotypes show both gradual and sharp transitions between them. Cataclastic shear zones are visible at various scales. Similar mylonitic rocks are also exposed in the area close to San Lorenzo village (phyllites, metapsammites, quartzites, and muscovite chlorite schists). At times, into micaschist/paragneiss lithotypes, it is possible to observe relics of earlier isoclinal folds (Fig. 30a). Only at

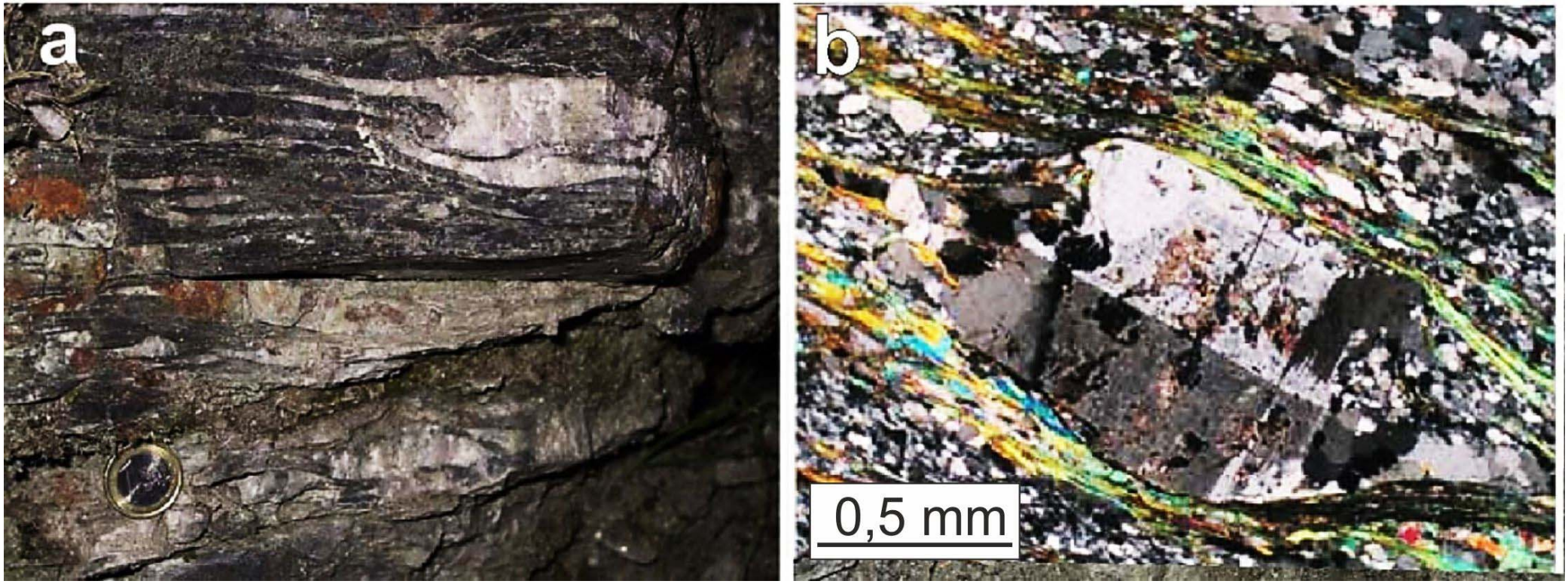

Fig. 30 - **a)** Variscan relic structures; **b)** microphotos of mylonitic paragneisses near Chorio village.

DOI: 10.3301/GFT.2017.03

microscopic scale the mylonitic textures are evident. They show a clear mylonitic foliation marked by syn-kinematic crystals of biotite and quartz, rarely of white mica, which often is characterized by smaller grainsize.

The main mylonitic foliation coincides with the earlier isoclinal axial plane foliation. It is also very common to observe chevron type folds with sub-horizontal axial surfaces and metric wavelength linked to the last deformational episode recognized in the SU rocks. Recovery has also been important for these rocks, which highlight how syn-kinematic minerals are partly obliterated by new crystallized ones. Recovery and associated static crystallization of andalusite (well documented by previous authors; e.g. Crisci et al., 1980) is probably due to the thermal perturbation induced in this area by the emplacement of late Variscan plutonic bodies (Fig. 30b). This feature put into evidence as the shear phase recognized within the SU is to be linked with a pre- to late-Variscan mylonitic phase, which is totally different from the late Alpine mylonitic phase reconstructed for the AU and MPU rocks (Angì et al., 2010).

DOI: 10.3301/GFT.2017.03

DOI: 10.3301/GFT.2017.03

References

Aloisi M., Bruno V., Cannavò F., Ferranti L., Mattia M., Monaco C. & Palano M. (2012) - Are the source models of the M 7.1 1908 Messina Strait earthquake reliable? Insights from a novel inversion and a sensitivity analysis of Loperfido (1909) levelling data. Geophysical Journal International, DOI 10.1093/gji/ggs062.

Aloisi M., Bruno V., Cannavò F., Ferranti L., Mattia, M. & Monaco C. (2014) - Reply to 'Comments on the paper "Are the source models of the M7.1 1908 Messina Strait earthquake reliable? Insights from a novel inversion and sensitivity analysis of levelling data" by Aloisi et al., 2012. Geophysical Journal International, 197 (3), 1403-1409.

Alsop G.I. & Carreras J. (2007) - The structural evolution of sheath folds: A case study from Cap de Creus. J. Struct. Geol. 29, 1915–1930.

Amoruso A., Crescentini & L. Scarpa R. (2002) - Source parameters of the 1908 Messina Strait, Italy, earthquake from geodetic and seismic data. J. Geophys. Res., 107 (B4), 10.1029/2001JB000434.

Angì G., Cirrincione R., Fazio E., Fiannacca P., Ortolano G. & Pezzino A. (2010) - Metamorphic evolution of preserved Hercynian crustal section in the Serre Massif (Calabria-Peloritani Orogen, southern Italy). Lithos, 115, 237–262.

Antonioli F., Dai Pra G., Segre A.G. & Sylos Labini S. (2004) - New data on late Holocene uplift-rate in Calabria and Messina Strait area, Italy. Quaternaria Nova, 8, 71-84.

Antonioli F., Ferranti L., Lambeck K., Kershaw S., Verrubbi V. & Dai Pra G. (2006) - Late Pleistocene to Holocene record of changing uplift-rates in southern Calabria and northeastern Sicily (southern Italy, Central Mediterranean Sea). Tectonophysics, 422, 23–40.

Argnani A. & Bonazzi C. (2005) - Malta Escarpment fault zone offshore eastern Sicily: Pliocene-Quaternary tectonic evolution based on new multichannel seismic data. Tectonics, 24, TC 4009, doi :10.1029/2004TC001656.

Argnani A., Serpelloni E. & Bonazzi C. (2007) - Pattern of deformation around the cen-tral Aeolian Islands: evidence from multichannel seismic and GPS data. TerraNova, 1–7, http://dx.doi.org/10.1111/j.1365-3121.2007.00753.x.

Argnani A., Brancolini G., Bonazzi C., Rovere M., Accaino F., Zgur F. & Lodolo E. (2009) - The result of the Taormina 2006 seismic survey: possible implications for active tectonics in the Messina Strait. Tectonophysics, 476, 159–169.

Atzori P., Messina A. & Pezzino A. (1975) - Indagini strutturali sull'affioramento migmatitico di Scilla (Calabria) - Rivista Mineraria Siciliana N. 154-156.

Atzori P., Ferla P., Paglionico A., Piccarreta G. & Rottura A. (1984) - Remnants of the Variscan Orogen along the Calabrian-Peloritan Arc, southern Italy: a review. J. Geol. Soc. London, 141, 137-145.

Atzori, P., Del Moro, A., Rottura, (1990) - A. Rb/Sr radiometric data from medium- to high-grade metamorphic rocks (Aspromonte nappe) of the north-eastern Peloritani Mountains (Calabrian Arc), Italy European Journal of Mineralogy, 2 (3), pp. 363-371.

Balescu S., Dumas B., Guérémy P., Lamothe M., Lhénaff R. and Raffy J. (1997) - Thermoluminescence dating tests of Pleistocene sediments from uplifted marine shorelines along the southwest coastline of the Calabria Peninsula (southern Italy). Palaeog. Palaeocl. 130, 25-41.

DOI: 10.3301/GFT.2017.03

Baratta M. (1910) - La catastrofe sismica calabro-messinese (28 Dicembre 1908), Relazione alla Soc. Geogr. Ital.

Barberi F., Gasparini P., Innocenti F. & Villari L. (1973) - Volcanism of the soutern Tyrrhenian Sea and its geodynamic implications Journal of Geophysical Research, 78, p. 5221.

Barreca G., Bruno V., Cultrera F., Ferranti L., Guglielmino F., Guzzetta L., Mattia M., Monaco C. & Pepe F. (2014a) - Geodetic and geological evidence of active tectonics in south-western Sicily (Italy). Journal of Geodynamics, 82, 138-149, Doi:10.1016/j.jog.2014.03.004.

Barreca G., Bruno V., Cultrera F., Mattia M., Monaco C. & Scarfì L. (2014b) - New insights in the geodynamics of the Lipari–Vulcano area (Aeolian archipelago, southern Italy) from geological, geodetic and seismological data. Journal of Geodynamics, 82, 150-167, Doi: 10.1016/j.jog.2014.07.003.

Barrier P. (1987) - Stratìgraphie des dépots pliocènes et quaternaires du Détroit de Messine. Doc. et Tiaz,. IGAL, 11:59-81, Paris.

Bianca M., Monaco C., Tortorici L. & Cernobori L. (1999) - Quaternary normal faulting in southeastern Sicily (Italy): a seismic source for the 1693 large earthquake. Geophysical Journal International, 139, 370–394.

Bianca M., Catalano, S. De Guidi, G. Gueli A.M., Monaco C., Ristuccia G.M., Stella, G., Tortorici G., Tortorici L. & Troja S.O. (2011) - Luminescence chronology of Pleis-tocene marine terraces of Capo Vaticano peninsula (Calabria, Southern Italy). Quat. Int. 232, 1–8.

Billi A., Barberi G., Faccenna C., Neri G., Pepe F. & Sulli A. (2006) - Tectonics and seismicity of the Tindari Fault System, southern Italy: crustal deformations at the transition between ongoing contractional and exten-sional domains located above the edge of a subducting slab. Tectonics, 25, http://dx.doi.org/10.1029/2004TC001763.

Billi A., Presti D., Faccenna C., Neri G. & Orecchio B. (2007) - Seismotectonics of the Nubia plate compressive margin in the south-Tyrrhenian region, Italy: clues for subduction inception. J. Geophys. Res. 112, B08302, http://dx.doi.org/10.1029/2006JB004837.

Billi A., Faccenna C., Bellier O., Minelli L., Neri G., Piromallo C., Presti D., Scrocca, D. & Serpelloni E. (2011) - Recent tectonic reorganization of the Nubia-Eurasia convergent boundary heading for the closure of the western Mediterranean. Bull.Soc. Géol. de France 182, 279–303.

Bonardi G., Messina A., Perrone V., Russo S. & Zuppetta A. (1984) - L'unita di Stilo nel settore meridionale dell'Arco Calabro-Peloritano, Boll. Soc. Geol. It., 103, 279-309.

Bonardi G., Compagnoni R., Del Moro A., Messina A. & Perrone V. (1987) - Riequilibrazioni tettonico-metamorfiche alpine dell'Unità dell'Aspromonte, Calabria Meridionale. Rend. SIMP, 42, 301.

Bonardi G., Caggianelli A., Critelli S., Messina A. & Perrone V. (2004) - Geotraverse across the Calabria-Peloritani Terrane (Southern Italy) - Field Trip Guide Book - P66 - 32nd International Geological Congress - Florence - Italy August 20-28, 2004 - Volume n° 6 - from P55 to PW06, 60 pp.

Bonfiglio L. (1972). Il Tirreniano di Bovetto e Ravagnese presso Reggio Calabria. Quaternaria, 16, 137-148.

Bonfiglio L. & Violanti D. (1983) - Prima segnalazione di Tirreniano ed evoluzione pleistocenica di Capo Peloro (Sicilia nord-orientale). Geogr. Fis. Dinam. Quater., 6, 3-15.

Bordoni P. & Valensise G. (1998) - Deformation of the 125 ka marine terrace in Italy: tectonic implications. In: Stewart I.S. & Vita-Finzi C. (Eds) Coastal Tectonics. Geological Society, London, Special Publication, 46, 71-110.

DOI: 10.3301/GFT.2017.03

Boschi E., Ferrari G., Gasperini P., Guidoboni E., Smriglio G. & Valensise G. (1995) - Catalogo dei forti terremoti in Italia dal 461 a.D. al 1980, Istituto Nazionale di Geofisica and S.G.A. Bologna, 970 pp.

Bosi C., Carobene L. & Sposato A. (1996) - Il ruolo dell'eustatismo nella evoluzione geologica nell'area mediterranea, Mem. Soc. Geol. It., 51, 363-382.

Bottari A. (2008) - Osservazioni macrosismiche e studi, in Riassunti estesi del Convegno 1908–2008 Scienza e Società a cento anni dal Grande Terremoto, Reggio Calabria 10–12 dicembre 2008, Miscellanea I.N.G.V.,3, pp. 19–20.

Bottari A., Carapezza E., Carapezza M., Carveni P., Cefali F., Lo Giudice E. & Pandolfo C. (1986) - The 1908 Messina earthquake in the regional geostructural framework. J. Geodynamics, 5, 275-302.

Bousquet J.C. & Lanzafame G. (2004), Compression and Quaternary tectonic inversion on the northern edge of the Hyblean Mountains, foreland of the Apenine-Maghrebian chain in eastern Sicily (Italy): Geodynamic implications for Mt. Etna. GeoActa, 3, 165–177.

Caggianelli A., Liotta D., Prosser G. & Ranalli, G. (2007) - Pressure–temperature evolution of the late Hercynian Calabria continental crust: compatibility with post-collisional extensional tectonics. Terra Nova, 19(6), 502–514.

Carminati E., Wortela M.J.R., Spakmana W., Sabadinib R. (1998) - The role of slab detachment processes in the opening of the western–central Mediterranean basins: some geological and geophysical evidence. Earth and Planetary Science Letters, 160 (3-4), 651-665, https://doi.org/10.1016/S0012-821X(98)00118-6.

Catalano, S., De Guidi, G. (2003) - Late Quaternary uplift of northeastern Sicily: Relation with the active normal faulting deformation. Journal of Geodynamics, 36 (4), pp. 445-467.

Catalano S., De Guidi G., Monaco C., Tortorici G. & Tortorici L. (2003) - Long-term behaviour of the Late Quaternary normal faults in the Strait of Messina area (Calabrian Arc): structural and morphological constraints. Quatern. Int., 101

Catalano S., De Guidi G., Monaco C., Tortorici G. & Tortorici, L. (2008) - Active faulting and seismicity along the Siculo-Calabrian Rift Zone (Southern Italy). Tectonophysics, 453, 177-192.

Cavazza W., Blenkinsop J., Decelles P.G., Patterson R.T. & Reinhardt E.G. (1997) - Stratigrafia e sedimentologia della sequenza sedimentaria oligocenico-quaternaria del bacino calabro-ionico. Boll. Soc.Geol. It., 116, 51-77.

Chiarabba C., De Gori P. & Speranza F. (2008) - The southern Tyrrhenian subduction zone. Deep geometry, magmatism and Plio-Pleistocen evolution, Earth Planet. Sci. Lett., 268, 408–423, doi:10.1016/j.epsl.2008.01.036.

Cirrincione R., Ortolano G., Pezzino A. & Punturo R. (2008) - Poly-orogenic multi-stage metamorphic evolution inferred via P-T pseudosections: An example from Aspromonte Massif basement rocks (Southern Calabria, Italy). Lithos, 103, 466–502.

Cirrincione R., Fazio E., Fiannacca P., Ortolano G. & Punturo R. (2009) - Microstructural investigation of naturally deformed leucogneiss from an alpine shear zone (Southern Calabria - Italy). Pure and Applied Geophysics, 166 (5-7), 995-1010.

Cirrincione R., Fazio E., Fiannacca P., Ortolano G., Pezzino A. & Punturo R. (2015) - The Calabria-Peloritani Orogen, a composite terrane in Central Mediterranean; its overall architecture and geodynamic significance for a pre-Alpine scenario around the Tethyan basin. In: "Progresses in deciphering structures and compositions of basement rocks". Periodico di Mineralogia, 84, 3B (Special Issue), 701-749. DOI: 10.2451/2015PM0446

Crisci G. M., Donati G., Messina A., Russo S. & Perrone V. (1982) - L'Unità superiore dell'Aspromonte. Studio geologico e petrografico. Rend. S.I.M.P., 38(3), 989-1014.

DOI: 10.3301/GFT.2017.03

Cucci L. & Tertulliani A. (2006) - I terrazzi marini nell'area di Capo Vaticano (Arco Calabro): solo un record di sollevamento regionale o anche di deformazionecosismica? Il Quaternario 19, 89–101.

Cuffaro M., Riguzzi F., Scrocca D. & Doglioni C. (2011) - Coexisting tectonic settings: The example of the southern Tyrrhenian Sea, Int. J. Earth Sci., 100(8), 1915–1924, doi:10.1007/s00531-010-0625-z.

D'Agostino N. & Selvaggi G. (2004) - Crustal motion along the Eurasia-Nubia plate boundary In the Calabrian Arc and Sicily and active extension in the Messina Strait from GPS measurements. J. Geophys. Res., 109 (B11402), doi: 10.1029/2004JB002998

D'Agostino N., D'Anastasio E., Gervasi A., Guerra I., Nedimovi´c M.R., See-ber L. & Steckler M. (2011) - Forearc extension and slow rollback of the Calabrian Arc from GPS measurements. Geophys. Res. Lett. 38, L17304, http://dx.doi.org/10.1029/2011GL048270.

D'Amico S., Orecchio B., Presti D., Zhu L., Herrmann R.B. & Neri G. (2010) - Broad-band waveform inversion of moderate earthquakes in the Messina Strait,Southern Italy. Phys. Earth Planet. Int 179, 97–106, .

D'Amico S., Orecchio B., Presti D., Gervasi A., Guerra I., Neri G., Zhu L. & Herrmann R.B. (2011) - Testing the stability of moment tensor solutions for small and mod-erate earthquakes in the Calabrian-Peloritan arc region. Boll. Geo. Teor. Appl. 52,283–298, http://dx.doi.org/10.4430/bgta0009.

De Astis G., Ventura G. & Vilardo G. (2003) - Geodynamic significance of theAeolian volcanism (Southern Tyrrhenian Sea, Italy) in light of structural, seismological and geochemical data. Tectonics 22 (4), 1040, http://dx.doi.org/10.1029/2003TC001506.

De Guidi G., Catalano S., Monaco C. & Tortorici L. (2003) - Morphological evidence of Holocene coseismic deformation in the Taormina region (NE Sicily). Journal of Geodynamics, 36, 193-211.

De Guidi G., Barberi G., Barreca G., Bruno V., Cultrera F., Grassi S, Imposa S., Mattia M., Monaco C., Scarfì L. & Scudero S. (2015) - Geological, seismological and geodetic evidence of active thrusting and folding south of Mt. Etna (eastern Sicily): revaluation of "seismic efficiency" of the Sicilian Basal Thrust. Journal of Geodynamics, 90, 32–41, doi: org/10.1016/j.jog.2015.06.001.

Del Ben A., Gargano C. & Lentini F. (1996) – Ricostruzione strutturale e stratigrafica dell'area dello Stretto di Messina mediante analisi comparata dei dati geologici e sismici. Mem. Soc. Geol. It., 51, 703-717.

De Natale G. & Pino N.A. (2014) - Comment on 'Are the source models of the M 7.1 1908 Messina Strait earthquake reliable? Insights from a novel inversion and sensitivity analysis of levelling data' by M. Aloisi, V. Bruno, F. Cannavò, L. Ferranti, M. Mattia, C. Monaco & M. Palano. Geophys. J. Int., 197, 1399–1402, doi: 10.1093/gji/ggu063.

Devoti R., Esposito A., Pietrantonio G., Pisani A.R. & Riguzzi F. (2011) - Evidence of large scale deformation patterns from GPS data in the Italian subduction boundary, Earth Planet. Sci. Lett., 311, 230–241, doi:10.1016/j.epsl.2011.09.034.

Dewey J.F., Helman M.L., Turco E., Hutton D.H.W. & Knott S.D. (1989) - Kinematics of the western Mediterranean. In: M.P. Coward, D. Dietrich & R.G. Park (Ed.), "Alpine Tectonics", Geological Society London Special publication, 45, 265-283.

Di Stefano A. & Longhitano S.G. (2009) - Tectonics and sedimentation of the Lower and Middle Pleistocene mixed siliciclastic/bioclastic sedimentary successions of the Ionian Peloritani Mts (NE Sicily, Southern Italy): the onset of opening of the Messina Strait, Central European Journal of Geosciences, 1(1), 33–62.

DISS Working Group (2015) - Database of Individual Seismogenic Sources (DISS), Version 3.2.0: A compilation of potential sources for earthquakes larger than M 5.5 in Italy and surrounding areas. http://diss.rm.ingv.it/diss/, © INGV 2015 - Istituto Nazionale di Geofisica e Vulcanologia - All rights reserved; Doi:10.6092/INGV.IT-DISS3.2.0

DOI: 10.3301/GFT.2017.03

Doglioni C., Innocenti F. & Mariotti G. (2001) - Why Mt. Etna? Terra Nova 13, 25–31.

Doglioni C., Ligi M., Scrocca D., Bigi S., Bortoluzzi G., Carminati E., Cuffaro M., D'Oriano F., Forleo V., Muccini F. & Riguzzi F. (2012) - The tectonic puzzle of the Messina area (Southern Italy): Insights from new seismic reflection data. Scientific Reports, 2, 970, Doi: 10.1038/srep00970.

Dumas B. & Raffy J. (2004). Late Pleistocene tectonic activity deduced from uplifted marine terraces in Calabria, facing the Strait of Messina. Quaternaria Nova, 8, 79-99.

Dumas B., Gueremy P., Lhenaff R. & Raffy J. (1982) - Le soulèvement quaternaire de la Calabre méridionale. Rev Géol. Dyn. Géogr. Phys., 23, 27-40.

Dumas B., Gueremy P., Lhenaff R. & Raffy J. (1987) - Rates of uplift as shown by raised Quaternary shorelines in Southern Calabria (Italy). Zeitschrift Geomorphologie N.F., 63, 119-132.

Faccenna C., Funiciello F., Giardini D. & Lucente P. (2001) - Episodic back-arc extensionduring restricted mantle convection in the Central Mediterranean. Earth Planet.Sci. Lett. 187, 105–116.

Faccenna C., Piromallo C., Crespo-Blanc A., Jolivet L. & Rossetti F. (2004) - Lateral slabdeformation and the origin of the Western Mediterranean arcs. Tectonics, 23, http://dx.doi.org/10.1029/2002TC001488.

Favalli M., Karatson D., Mazzuoli R., Pareschi M.T. & Ventura G. (2005) - Volcanic geomorphology and tectonics of the Aeolian Archipelago (Southern Italy) based on integrated DEM data. Bull. Volcanol. 68, 157–170.

Fazio E., Cirrincione R. & Pezzino A. (2008) - Estimating P-T conditions of Alpine-type metamorphism using multistage garnet in the tectonic windows of the Cardeto area (southern Aspromonte Massif, Calabria). Mineralogy and Petrology, 93, 111-142.

Fazio E., Casini L., Cirrincione R., Massonne H.-J. & Pezzino A. (2012) - P-T estimates for the metamorphic rocks of the Stilo Unit (Aspromonte Massif, Calabria) and correlations with analogue Sardinian Variscan crystalline complexes. Special meeting of French and Italian Geological Societies "Variscan 2012", May-22-23 Sassari, Italy. Geologie de la France, 1, 111-113.

Fazio E., Cirrincione R. & Pezzino A. (2015) - Tectono-metamorphic map of the south-western flank of the Aspromonte Massif (southern Calabria -Italy), Journal of Maps, 11, 1, 85-100.

Ferla P. (2000) - A model of continental crust evolution in the geological history of the Peloritani Mountains (Sicily). Mem. Soc. Geol. It., 55, 87-93.

Ferranti L., Antonioli F., Mauz B., Amorosi A., Dai Pra G., Mastronuzzi G., Monaco C., Orrù P., Pappalardo M., Radtke U., Renda P., Romano P., Sansò P. & Verrubbi V. (2006) - Markers of the last interglacial sea level highstand along the coast of Italy: Tectonic implications. Quaternary Int., 145-146, 30-54.

Ferranti L., Monaco C., Antonioli F., Maschio L., Kershaw S. & Verrubbi V. (2007) - The contribution of regional uplift and coseismic slip to the vertical crustal motion in the Messina Strait, Southern Italy: evidence from raised Late Holocene shorelines. Journal of Geophysical Research, 112, B06401, doi: 10.1029/2006JB004473.

Ferranti L., Monaco C., Antonioli F., Maschio L. & Morelli D. (2008a) – Holocene activity of the Scilla fault, southern Calabria: insights from morpho-structural and marine geophysical data. Tectonophysics, 453, 74-93.

Ferranti L., Monaco C., Morelli D., Tonielli R., Tortorici L. & Badalini M. (2008b) – Morphostructural setting and active faults in the Messina Strait: new evidence from marine geological data. Rendiconti online Soc. Geol. It., 1, Note Brevi, 219-221.

DOI: 10.3301/GFT.2017.03

Ferranti L., Mazzella M.E., Monaco C., Morelli D. & Santoro E. (2009) - Active transpression within the frontal zone of the Southern Apennines in northern Calabria by integration of geomorphologic, structural, and marine geophysical data. Rendiconti online Soc. Geol. It., 5, 97-99.

Festa V., Messina A., Paglionico A., Piccarreta G. & Rottura A. (2004) - Pre-Triassic history recorded in the Calabria-Peloritani segment of the Alpine chain, southern Italy. An overview. Periodico di Mineralogia, 73 (2), 57-71.

Festa V., Prosser G., Caggianelli A., Grande A., Langone A., & Mele D. (2016) – The application of the vorticity analysis to the Palmi shear zone: new insights for the Alpine evolution of the Calabria-Peloritani terrane (Southern Italy). Geological Journal, 51, 670-681.

Fiannacca P., Williams I.S., Cirrincione R. & Pezzino A. (2008) - Crustal Contributions to Late Hercynian Peraluminous Magmatism in the Southern Calabria Peloritani Orogen, Southern Italy: Petrogenetic Inferences and the Gondwana Connection. Journal of Petrology, 49, 1897-1514.

Fiannacca P., Cirrincione R., Bonanno F. & Carciotto M. (2015) Source-inherited compositional diversity in granite batholiths: The geochemical message of Late Paleozoic intrusive magmatism in central Calabria (southern Italy). Lithos, 236-237, 123-140.

Firth C., Stewart I., McGuire W.M., Kershaw S. & Vita-Finzi C. (1996) - Coastal elevation changes in eastern Sicily: implications for volcano instability at Mount Etna. In: McGuire, W.M., Jones, A.P., Neuberg, J. (Eds.), Volcano Instability on the Earth and Other Planets. Geol. Soc. London, Spec. Publ., 110, 153–167,

Frepoli A., G. Selvaggi C. Chiarabba. & Amato A. (1996) - State of stress in the southern Tyrrhenian Subduction Zone from fault-plane solutions, Geophys. J. Int., 125, 879–891, doi:10.1111/j.1365-246X.1996.tb06031.x.

Gasparini C., Iannaccone G. & Scarpa R. (1985) - Fault-plane solutions and seismicity of the Italian Peninsula. Tectonophysics, 117, 59-78.

Ghisetti F. (1981) - Upper Pliocene-Pleistocene uplift rates as indicators of neotectonic pattern: an example from southern Calabria (Italy), Z. Geomorphol., 40, 93–118.

Ghisetti, F., Vezzani, L. (1982) Different styles of deformation in the calabrian arc (Southern Italy): Implications for a seismotectonic zoning Tectonophysics, 85 (3-4), pp. 149-165.

Ghisetti F. (1984) - Recent deformations and the seismogenic source in the Messina Strait (southern Italy). Tectonophysic, 109, 191-208.

Ghisetti F. (1992) - Fault parameters in the Messina Strait (southern Italy) and relations with the seismogenic source. Tectonophysics, 210, 117-133.

Goes S., Giardini D. Jenny S., Hollenstein C., Kahle H.G. & Geiger, A. (2004) - A recent tectonic reorganization in the south-central Mewditerranean. Earth Planet. Sci. Lett., 226, 335-345.

Graessner T. & Schenk V. (1999) - Low-pressure metamorphism of Palaeozoic pelites in the Aspromonte, southern Calabria: constraints for the thermal evolution in the Calabrian crustal cross-section during the Variscan orogeny. J. Metam. Geol., 17(2), 157-172.

Graessner T., Schenck V., Brocker M. & Mezger K. (2000) - Geochronological constraints on timing of granitoid magmatism, metamorphism and post-metamorphic cooling in the Hercynian crustal cross-section of Calabria. J. Metam. Geol., 18, 409-421.

Guarnieri P. (2006) - Plio-Quaternary segmentation of the south Tyrrhenian forearc basin, Int. J. Earth Sci. (Geol. Rundsch.), 95, 107–118.

Gvirtzman Z. & Nur A. (1999) - The formation of Mount Etna as the consequence of slab rollback. Nature, 401, 782-785.

DOI: 10.3301/GFT.2017.03

Hollenstein C., Kahle H.G., Geiger A., Jenny S., Goes S. & Giardini D. (2003) New GPS - constraints on the Africa-Eurasia plate boundary zone in southern Italy, Geophys. Res. Lett., 30(18), 1935, doi:10.1029/2003GL017554.

Jacques E., Monaco C., Tapponnier P., Tortorici L. & Winter T. (2001) - Faulting and earthquake triggering during the 1783 Calabria seismic sequence. Geophys. J. Int., 147, 499-516.

Lajoie K.R. (1986) - Coastal tectonics. In: Geophysics Studies Committee, Commission Physical Sciences, Mathematics and Resources, Active Tectonics. NationalAcademy Press, Washington, pp. 95–124.

Lambeck K., Antonioli F., Purcell A. & Silenzi S. (2004) - Sea level change along the Italian coast for the past 10,000 yrs. Quaternary Science Reviews, 23, 1567-1598.

Lambeck K., Antonioli F., Anzidei M., Ferranti L., Leoni G., Scicchitano G. & Silenzi S. (2011) - Sea level change along the Italian coast during the Holocene projections for the future. Quat. Int. 232, 250–257.

Lanzafame G. & Bousquet J.C. (1997) The Maltese escarpment and its extension fromMt. Etna to the Aeolian Islands (Sicily): importance and evolution of a lithospherediscontinuity. Acta Vulcanol. 9, 113–120.

Lavecchia G., Ferrarini F., De Nardis R., Visini F. & Barbano M.S. (2007) - Active thrusting as a possible seismogenic source in Sicily (Southern Italy): Some insights from integrated structural–kinematic and seismological data. Tectonophysics, 445, 145-167.

Locardi E. & Nicolich R. (1988) - Geodinamica del Tirreno e dell'Appennino centro-meridionale: la nuova carta della Moho. Mem. Soc. Geol. It. 41, 121–140.

Loperfido A. (1909) - Livellazione geometrica di precisione eseguita dall'I.G.M. sulla costa orientale della Sicilia, da Messina a Catania, a Gesso ed a Faro Peloro e sulla costa occidentale della Calabria da Gioia Tauro a Melito di Porto Salvo, in Relazione della Commissione Reale incaricata di designare le zone più adatte per la ricostruzione degli abitati colpiti dal terremoto del 28 dicembre 1908 o da altri precedenti, pp.131–156, Accademia Nazionale dei Lincei, Roma.

Marrett, R.A., & Allmendinger, R.W. (1990) - Kinematic analysis of fault-slip data: Journal of Structural Geology, v. 12, p. 973–986.

Mattia M., Palano M., Bruno V., Cannavò F., Bonaccorso A. & Gresta S. (2008) - Tectonic features of the Lipari–Vulcano complex (Aeolian Archipelago, Italy) from10 years (1996–2006) of GPS data. Terra Nova 20, 370–377.

Mattia M., Bruno V., Cannavò F. & Palano M. (2012) - Evidences of a contractional pattern along the northern rim of the Hyblean Plateau (Sicily, Italy) from GPS data, Geol. Acta, 10, 1–9, doi:10.1344/105000001705.

Mazzoli S. & Helman M. (1994) - Neogene patterns of relative motion for Africa–Europe: some implications for recent central Mediterranean tectonics. Geol. Rund., 83, 464-468.

Mazzuoli R., Tortorici L.& Ventura G. (1995) - Oblique rifting in Salina, Lipari and Vulcano islands (Aeolian Islands, Southern Tyrrhenian Sea, Italy). Terra Nova7, 444–452.

Micheletti F., Barbey P., Fornelli A., Piccarreta G. & Deloule E. (2007) - Latest Precambrian to Early Cambrian U–Pb zircon ages of augen gneisses from Calabria (Italy), with inference to the Alboran microplate in the evolution of the peri-Gondwana terranes. Inter. Jour. Earth Sc., 96, 843-860.

Michelini A., Lomax A., Nardi A., Rossi A., Palombo B. & Bono, A. (2005) - A modern re-examination of the locations of the 1905 Calabria and the 1908 Messina Strait earthquakes. Geophys. Res. Abstracts, 7, 07909, SRef-ID: 1607-7962/gra/EGU05-A-07909.

DOI: 10.3301/GFT.2017.03

Miyauchi T., Dai Pra G. & Sylos Labini S. (1994) - Geochronology of Pleistocene marineterraces and regional tectonics in the Tyrrhenian coast of South Calabria, Italy. Il Quaternario 7(1), 17–34.

Monaco C., Mazzoli S. & Tortorici L. (1996a) - Active thrust tectonics in western Sicily (Southern Italy): the 1968 Belice earthquake sequence. Terra Nova, 8, 372-381.

Monaco C., Tortorici L., Nicolich R., Cernobori L. & Costa M. (1996b) - From collisional to rifted basins: an example from the southern Calabrian Arc (Italy). Tectonophysics, 266, 233-249.

Monaco C. & Tortorici L. (2000) - Active faulting in the Calabrian Arc and eastern Sicily. J. Geodynamics, 29, 407-424.

Monaco C., Bianca M., Catalano S., De Guidi G. & Tortorici L. (2002) – Sudden change in the Late Quaternary tectonic regime in eastern Sicily: evidences from geological and geomorphological features. Boll. Soc. Geol. It., Volume speciale n.1, 901-913.

Monaco C. & Tortorici L. (2007) - Active faulting and related tsunami in eastern Sicily and south-western Calabria. Bollettino di Geofisica Teorica e Applicata, 48 (2), 163-184.

Monaco C., Barreca G., Di Stefano A. (2017) - Quaternary marine terraces and fault activity in the northern mainland sectors of the Messina Straits (southern Italy). Italian Journal of Geosciences, 136 (3), 337-346, doi:10.3301/IJG.2016.10.

Montenat C., Barrier P. & Ott d'Estevou P. (1991) - Some aspects of the recent tectonics in the Strait of Messina, Italy. Tectonophysics, 194, 203-215.

Morelli D., Cuppari A., Colizza E. & Fanucci F. (2011) - Geomorphic setting and geohazard related features along the Ionian Calabrian margin between Capo Spartivento and Capo Rizzuto (Italy). Mar. Geophys. Res. 32, 139-149.

Mulargia F. & Boschi E. (1983) - The 1908 Messina earthquake and related seismicity. Prc. Int. School Phys. E. Fermi, Earthquakes: observation, theory and interpretation, 493-518.

Neri G., Barberi G., Oliva G. & Orecchio B. (2004) - Tectonic stress and seismogenic faulting in the area of the 1908 Messina earthquake, south Italy, Geophys. Res. Lett., 31, L10602, doi:10.1029/2004GL019742.

Neri G., Barberi G., Oliva G. & Orecchio B. (2005) - Spatial variation of seismogenic stress orientations in Sicily, South Italy. Physics of the Earth and Planetary Interiors, 148, 175-191.

Neri G., Marotta A.M., Orecchio B., Presti D., Totaro C., Barzaghi R. & Borghi A. (2012) - How lithospheric subduction changes along the Calabrian Arc in southern Italy: geophysical evidences, Int. J. Earth Sci. (Geol. Rundsch.), 101(7), 1949–1969.

Nicolich R., Laigle M., Hirn A., Cernobori L. & Gallard J. (2000) - Crustal structure ofthe Ionian margin of Sicily: Etna volcano in the frame of regional evolution.Tectonophysics 329, 121–139.

Ortolano G., Cirrincione R. & Pezzino A. (2005) - PT evolution of Alpine metamorphism in the southern Aspromonte Massif (Calabria - Italy). Schweizer Mineralogische und Petrographische Mitteilungen, 85, 31-56.

Ortolano G., Cirrincione R., Pezzino A. & Puliatti, G. (2013) - Geo-Petro-Structural study of the Palmi shear zone: Kinematic and rheological implications. Rendiconti Online Societa Geologica Italiana, 29, 126-129.

Ortolano G., Cirrincione R., Pezzino A., Tripodi V. & Zappalà L. (2015) - Petro-structural geology of the Eastern Aspromonte Massif crystalline basement (southern Italy-Calabria): an example of interoperable geo-data management from thin section – to field scale. Journal of Maps, 11(1), 181-200.

DOI: 10.3301/GFT.2017.03

Palano M., Ferranti L., Monaco C., Mattia M., Aloisi M., Bruno V., Cannavò F. & Siligato G. (2012) - GPS velocity and strain fields in Sicily and southern Calabria, Italy: updated geodetic constraints on tectonic block interaction in the central Mediterranean. J. Geophys. Res. 117, B07401, http://dx.doi.org/10.1029/2012JB009254.

Patacca, E., Sartori, R., Scandone, P. (1993) Tyrrhenian Basin and Apennines. Kinematic evolution and related dynamic constraints Recent evolution and seismicity of the Mediterranean region, 161-171.

Patacca E., Sartori R., Scandone P. (1990). Tyrrhenian Basin and Apenninic Arcs: kinematic relations since late Tortonian times. Mem. Soc. Geol. It., 45, 425-451

Pepe F., Bertotti G. & Cloething S. (2004) - Tectono-stratigraphic modelling of the North Sicily continental margin (southern Tyrrhenian Sea), Tectonophysics, 384(1–4), 257–273, doi:10.1016/j.tecto.2004.04.002.

Pezzino A., (1982) - Confronti petrografici e strutturali tra i basamenti metamorfici delle unità inferiori dei Monti Peloritani (Sicilia). Periodico di Mineralogia, 1, 35-50.

Pezzino A., Pannucci S., Puglisi G., Atzori P., Ioppolo S. & Lo Giudice A. (1990) - Geometry and metamorphic environment of the contact between the Aspromonte - Peloritani Unit (Upper Unit) and Madonna dei Polsi Unit (Lower Unit) in the central Aspromonte area (Calabria). Boll. Soc. Geol. It., 109, 455-469.

Pezzino A., Angi G., Cirrincione R., De Vuono E., Fazio E., Fiannacca P., Lo Giudice A., Ortolano G. & Punturo R. (2008) - Alpine metamorphism in the Aspromonte Massif: implications for a new framework for the southern sector of the Calabria-Peloritani Orogen (Italy). Inter. Geol. Review, 50, 423-441.

Pirazzoli P.A., Mastronuzzi G., Saliège J.F. and Sansò P.; 1997: Late Holocene emergence in Calabria, Italy. Marine Geology, 141, 61-70.

Piromallo C. & Morelli A. (2003) - P wave tomography of the mantle under the Alpine-Mediterranean area, J. Geophys. Res., 108(B2), 2065, doi:10.1029/2002JB001757.

Polonia A., Torelli L., Mussoni P., Gasperini L., Artoni A. & Klaeschen, D. (2011) - The Calabrian Arc subduction complex in the Ionian Sea: regional architecture, active deformation and seismic hazard: Tectonics, v. 30, TC5018, doi:10.1029/2010TC002821.

Polonia A., Torelli L., Gasperini L. & Mussoni P. (2012) - Active faults and historical earthquakes in the Messina Strait area (Ionian Sea), Nat. Hazards Earth Syst. Sci., 12, 2311-2328, doi:10.5194/nhess-12-2311-2012.

Pondrelli S., Morelli A. & Ekström G. (2004) - European-Mediterranean Regional Centroid Moment Tensor catalog: solutions for years 2001 and 2002. Phys. Earth Planet. Int., 145, 127–147 .

Pondrelli S., Salimbeni S., Ekström G., Morelli A., Gasperini P. & Vannucci G. (2006) - The Italian CMT dataset from 1977 to the present, Phys. Earth Planet. Inter., 159, 286–303, doi:10.1016/j.pepi.2006.07.008.

Prosser G., Caggianelli A., Rottura A. & Del Moro A. (2003) - Strain localisation driven by marble layers: the Palmi shear zone (Calabria–Peloritani terrane, Southern Italy). GeoActa, 2, 35–46.

Ridente R., Martorelli E., Bosman A. & Chiocci F.L. (2014) - High-resolution morpho-bathymetric imaging of the Messina Strait (Southern Italy). New insights on the 1908 earthquake and tsunami. Geomorphology, 208, 149-159.

Rosenbaum G. & Lister G.S. (2004) - Neogene and Quaternary rollbac evolution of the Tyrrhenian Sea, the Apennines and the Sicilian Maghrebides, Tectonics, 23, TC1013, doi:10.1029/2003TC001518.

DOI: 10.3301/GFT.2017.03

Rottura A., Bargossi G. M., Caironi V., Del Moro A., Maccarrone E., Macera P., Paglionico A., Petrini R., Piccareta G. & Poli G. (1990) – Petrogenesis of contrasting Hercynian granitoids from the Calabrian Arc, Southern Italy. Lithos, 24, 97-119.

Rust D. & Kershaw S. (2000) - Holocene tectonic uplift patterns in northeastern Sicily: evidence from marine notches in coastal outcrops. Marine Geology, 167, 105-126.

Scarfì L., Langer H. & Scaltrito A. (2009) - Seismicity, seismotectonics and crustal velocity structure of the Messina Strait (Italy), Phys. Earth Planet. Inter., 177, 65–78, doi:10.1016/j.pepi.2009.07.010.

Scicchitano G., Monaco C. & Tortorici L. (2007) - Large boulder deposits by tsunami waves along the Ionian coast of south-eastern Sicily. Marine Geology, 238, 75-91.

Scicchitano G., Antonioli F., Castagnino Berlinghieri E.F., Dutton A. & Monaco C. (2008) - Submerged archaeological sites along the Ionian Coast of south-eastern Sicily and implications for the Holocene relative sea level change. Quaternary Research, 70, 26-39.

Scicchitano G., Spampinato C., Ferranti L., Antonioli F., Monaco C., Capano M. & Lubritto C. (2011a) - Uplifted Holocene shorelines at Capo Milazzo (NE Sicily, Italy): evidence of co-seismic and steady-state deformation. Quaternary International, 232, 201-213, doi: 10.1016/j-quaint.2010.06.028.

Scicchitano G., Lo Presti V., Spampinato C., Gasparo Morticelli M., Antonioli F., Auriemma R., Ferranti L. & Monaco C. (2011b) - Millstones as indicators of relative sea-level changes in northern Sicily and southern Calabria coastlines, Italy. Quaternary International, 232, 92-104, doi: 10.1016/j-quaint.2010.08.019.

Schick R. (1977) - Eine seismotektonische Bearbeitung des Erdbebens von Messina im Jahre 1908. Geol. Jahrb., 11, 3-74.

Selli R., Colantoni P., Fabbri A., Rossi S., Borsetti A.M. and Gallignani P. (1979) - Marine geological investigation on the Messina Strait and its approaches. Giornale di Geologia, 42 (2), 1-70.

Serpelloni E., Bürgmann R., Anzidei M., Baldi P., Mastrolembo Ventura B. & Boschi E. (2010) - Strain accumulation across the Messina Strait and kinematics of Sicily and Calabria from GPS data and dislocation modeling. Earth and Planetary Science Letters, 298, 1–14.

Spampinato C., Costa B., Di Stefano A., Monaco C. & Scicchitano G. (2011) - The contribution of tectonics to relative sea-level change during the Holocene in coastal south-eastern Sicily: new data from boreholes. Quaternary International, 232, 214-227, doi: 10.1016/j-quaint.2010.06.025.

Spampinato C.R., Scicchitano G., Ferranti L. & Monaco C. (2012) – Raised Holocene paleo-shorelines along the Capo Schisò coast, Taormina: new evidence of recent co-seismic deformation in northeastern Sicily (Italy). Journal of Geodynamics, 55, 18-31, . doi:10.1016/j.jog.2011.11.007.

Spampinato C.R., Ferranti L., Monaco C., Scicchitano G. & Antonioli F. (2014) - Holocene coastal uplift and coseismic deformation at Capo Vaticano (western Calabria). J. of Geodynamics, 82, 178-193, Doi:10.1016/j.jog.2014.03.003.

Stewart I.S., Cundy A., Kershaw S. & Firth C. (1997) - Holocene coastal uplift in the Taormina area, northeastern Sicily: implications for the southern prolongation of the Calabrian seismogenic belt. J. Geodynamics, 24, 37-50.

Tinti S. & Armigliato A. (2001) - Impact of large tsunamis in the Messina Strait, Italy: The case of the 28 December 1908 tsunami. In: Hebenstreit, G.T. (Ed.), Tsunami Research at the End of a Critical Decade. Kluwer, Dordrecht, pp. 139-162.

DOI: 10.3301/GFT.2017.03

Tortorici L., Monaco C., Tansi C. & Cocina O. (1995) - Recent and active tectonics in the Calabrian Arc (Southern Italy). Tectonophysics, 243, 37-49.

Tripodi V., Muto F. & Critelli S. (2013) - Structural style and tectono-stratigraphic evolution of the Neogene–Quaternary Siderno Basin, southern Calabrian Arc, Italy, International Geology Review, 55, 4,468-481.

Valensise G. & Pantosti D. (1992) - A 125 Kyr-long geological record of seismic source repeatability: the Messina Strait (southern Italy) and the 1908 earthquake (Ms 71/2). Terra Nova, 4, 472-483.

Waelbroeck C., Labeyrie L., Michel E., Duplessy J.C., Mcmanus J.F., Lambeck K., Balbon E. & Labracherie M. (2002) - Sea-level and deep water temperature changes derived from benthic foraminifera isotopic records. Quatern. Sci. Rev., 21, 295–305.

Westaway R. (1992) - Seismic moment summation for historical earthquakes in Italy: tectonic implications. J. Geophys. Res., 97, 15437-15464.

Westaway R. (1993) - Quaternary uplift of Southern Italy. J. Geophys. Res., 98, 21741- 21772.

Williams I.S., Fiannacca P., Cirrincione & Pezzino A. (2012) - Peri-Gondwanan origin and early geodynamic history of NE Sicily: A zircon tale from the basement of the Peloritani Mountains. Gondwana Research, 22, 855-865.

Wortel M.J.R. & Spakman W. (2000) - Subduction and slab detachment in the Mediterranean-Carpathian region. Science, 290, 1910-1917.

DOI: 10.3301/GFT.2017.03